Martin O'Malley, *Governor*
Anthony G. Brown, *Lt. Governor*

SHA State Highway Administration
Maryland Department of Transportation

John D. Porcari, *Secretary*
Neil J. Pedersen, *Administrator*

STATE HIGHWAY ADMINISTRATION

RESEARCH REPORT

Development of an Integrated Algorithm for Variable Speed Limit Control and Dynamic Merge Control

Gang-Len Chang, and K.P. Kang
Department of Civil Engineering
The University of Maryland, College Park

Project number MD-08-SP508B4F
FINAL REPORT

July 2008

Technical Report Documentation Page

1. Report No.	2. Government Accession No.	3. Recipient's Catalog No.
MD-08-SP508B4F		

4. Title and Subtitle	5. Report Date
Development of an Integrated Algorithm for Variable Speed Limit Control and Dynamic Merge Control	**July 2008**
	6. Performing Organization Code

7. Author/s	8. Performing Organization Report No.
K.P. Kang and Gang-Len Chang	

9. Performing Organization Name and Address	10. Work Unit No. (TRAIS)
University of Maryland **Department of Civil and Environmental Engineering** **College Park Maryland** **College Park MD 20742**	11. Contract or Grant No.

12. Sponsoring Organization Name and Address	13. Type of Report and Period Covered
Maryland State Highway Administration **Office of Policy & Research** **707 North Calvert Street** **Baltimore MD 21202**	**Final Report**
	14. Sponsoring Agency Code

15. Supplementary Notes

16. Abstract

To improve traffic mobility and safety in highway work zones, this study has focused mainly on developing advanced merge and speed control strategies, including both their individual and integrated control algorithms. Based on the deficiencies and limitations of existing work zone control operations, this research has made contributions mainly on the following four regards:(1) understanding traffic flow characteristics under work zone traffic conditions with empirical data and identifying their interrelations; (2) developing an operational model for computing the optimal set of thresholds for DLM and its implementation algorithm; (3) Proposing an optimal speed limit control model that can maximize the throughput of a lane-closure highway segment with a set of dynamically adjusted speed limits; and (4) constructing an integrated operational algorithm to take the advantage of the strengths of DLM and VSL controls. The simulation results have demonstrated that the developed DLM and VSL controls have better performance in terms of traffic mobility and safety than their existing controls based on static approaches, and also shown that the proposed integrated control of the DLM and VSL control has more promising properties than each individual control.

17. Key Words	18. Distribution Statement: No restrictions		
Dynamic merge control, variable speed control, work zone	**This document is available from the Research Division upon request**.		
19. Security Classification (of this report)	20. Security Classification (of this page)	21. No. Of Pages	22. Price
None	**None**	**120**	

Form DOT F 1700.7 (8-72) Reproduction of form and completed page is authorized.

Table of Contents

List of Tables

List of Figures

CHAPTER 1 . INTRODUCTION

1.1 Background

Performing work-zone activities in highway segments is one of the main contributors to traffic delay and safety, as the capacity reduction due to the lane closure operations often cause drivers to perform complex lane-changing and merging maneuvers which in turn incur excessive queue or a high speed variance over the upstream segment of a work zone (see Figure 1.1.1). To contend with this imperative issue, transportation professionals have proposed a variety of work-zone control devices and strategies over the past two decades. Most of such efforts, however, have been focused mainly on traffic safety such as speed reduction and smooth merging operations, but not on delay minimization or throughput maximization.

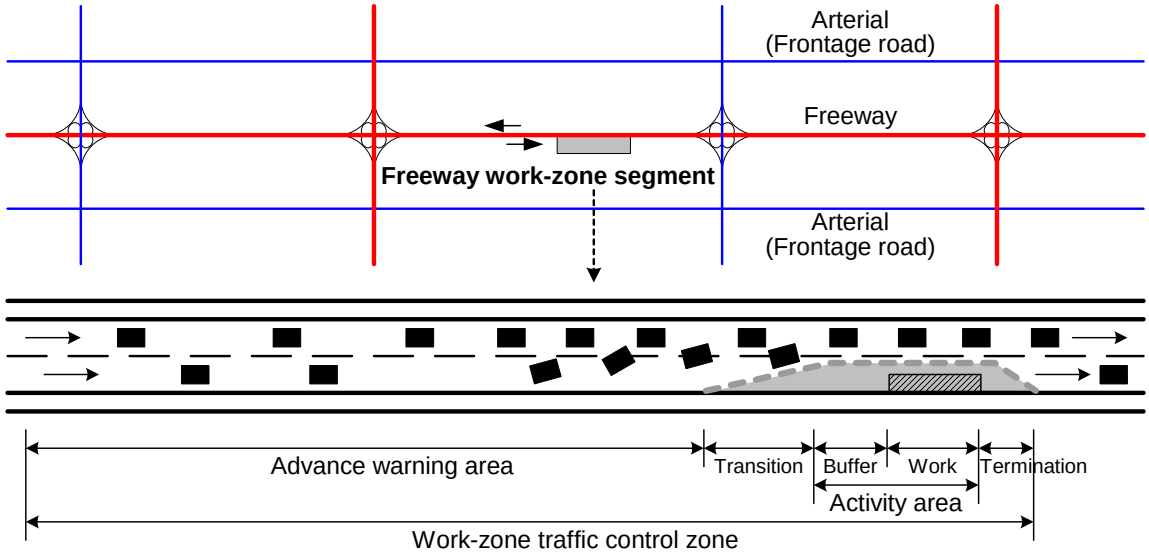

Figure 1.1.1 Illustration of a typical highway work-zone segment

In view of the increasing congestion in most urban networks and the significant delay incurred by frequent work-zone operations, existing safety-oriented control strategies are certainly no longer sufficient to provide the desirable level of operational efficiency. Hence, how to concurrently minimize the work-zone delay and the resulting incidents has emerged as one of the priority issues for traffic professionals.

Most existing work-zone control strategies belong to either of the following two categories: merge and speed controls. The former is used to direct drivers to effectively use the capacity of the closed and open lanes by displaying a proper merging message at several predetermined locations prior to the merging point, while the latter is designed to minimize the shockwave impacts due to the lane-closure operations by regulating the speed of approaching vehicles.

Since the lane-closure activities at highway work zones are always accompanied by mandatory lane-changing and merging maneuvers of traffic between the open and closed lanes, how to properly implement the merge control so as to improve traffic safety and efficiency is a very critical issue. Operational guidelines for selecting the best static merge control strategy to the encountered traffic conditions, however, are not available in both the literature and practices. Some recent developments on the dynamic merge control (McCoy et al., 1999; FHWA, 2004; Datta et al., 2004; Taavola et al., 2004; Chang, Kang, 2005) intend to address the need for implementing different merging controls under different work-zone types and volume levels. The criteria for dynamically implementing the most appropriate merge control in response to the time-varying traffic conditions yet remain to be developed by the traffic community.

As for existing speed control strategies, their common focus is to improve traffic safety with reduced average speed and speed variance across all travel lanes to facilitate approaching vehicles in merging operations. Most available speed control strategies are static in nature, and mainly to post the regulatory speed limits at upstream segments of a highway work-zone. Thus, this static speed limit control is designed for safety improvement under uncongested traffic conditions, rather than maximizing the operational efficiency (e.g., work-zone throughput or average speed) or minimizing the average delay. In recent years, transportation researchers have proposed the use of the variable speed limit (VSL) controls (TRB, 1998; Lyles et al., 2004; Park, Yadlapati, 2003; and Lee et al., 2004) for the work-zone operations. The main control objective of those VSL controls is to determine the appropriate traffic flow speed from the safety perspective under various volume and environmental conditions, but not for operational efficiency such as to maximize the throughput or to minimize the average vehicle delay.

In brief, to ensure both safety and efficiency at highway work zones, most responsible highway agencies face the following critical issues:

- What are the control objectives and criteria of selecting merge control strategy, based on the detected traffic conditions?
- How to implement the most appropriate merge strategy in a timely manner in response to the time-varying traffic conditions?
- When and how to implement the VSL control?
- What control strategy should be used for dynamically computing the set of optimal speeds for each of those work-zone upstream segments?
- How to integrate dynamic merge control with VSL to maximize the work-zone throughput and the operational safety?

1.2 Research Objectives and Scope

This research, proposed in response to the aforementioned critical issues, intends to pursue the following principal objectives:

- Understand traffic flow properties under congested work-zone conditions;

- Develop an advanced dynamic merge control system and its operation algorithm that can integrate the strengths of the static early and late merge controls and can best use the roadway capacity;
- Model an optimal variable speed control system and its operation algorithm based on the evolution of dynamic traffic states and macroscopic traffic characteristics that can maximize the total work-zone throughput and improve the overall traffic safety; and
- Integrate the developed DLM and VSL control strategies to maximize their effectiveness in contending with work-zone congestion.

1.3 Organization of report

Figure 1.3.1 illustrates the principal tasks and organization of this study. A brief description of each chapter is presented next.

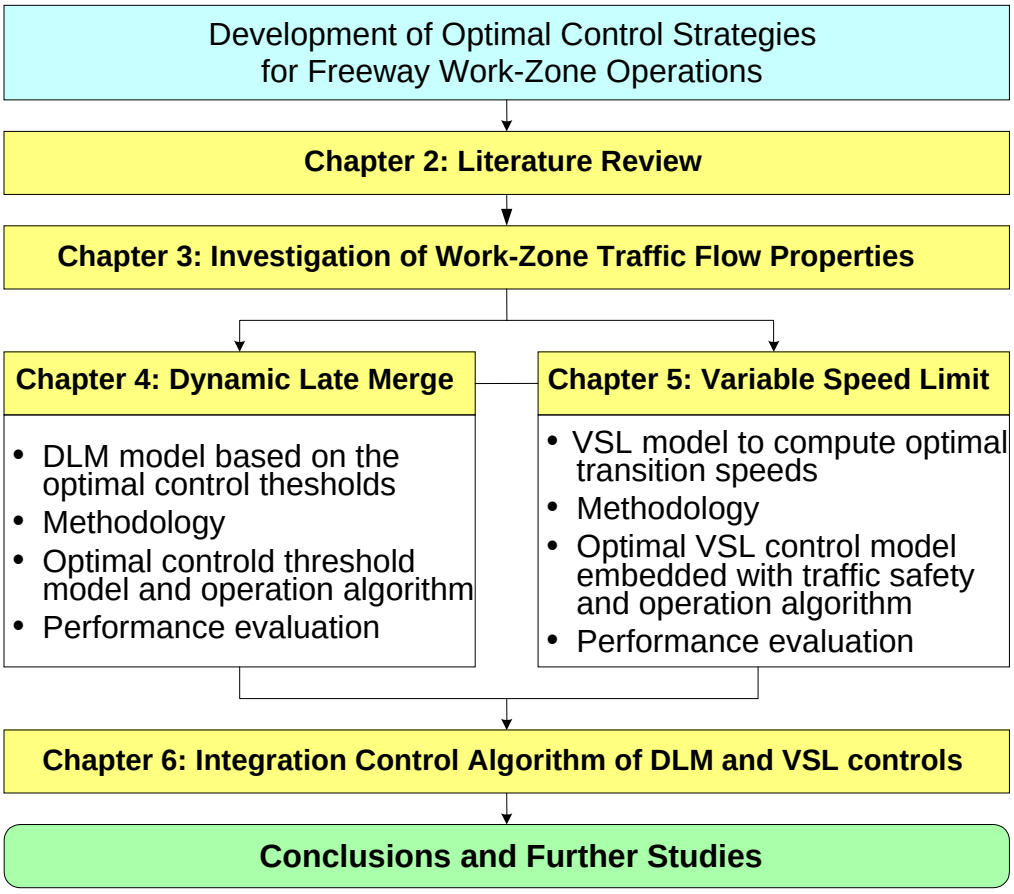

Figure 1.3.1 Organization of this study

Literature Review – To specify the key issues related to highway work-zone control strategies, Chapter 2 presents an extensive literature review of existing merge and speed control methods for highway work-zone operations. The static control strategies are

reviewed mainly on those issues associated with the system configurations for the target work-zone operations, and the dynamic control strategies are focused primarily on the operational algorithms. The strengths and deficiencies of each control approach are also addressed along with their reported performance levels and potential enhancements.

Investigating Macroscopic Traffic Flow Properties in Highway Work Zones – Chapter 3 is focused on analyzing traffic flow characteristics under congested work-zone traffic conditions, and developing empirical models for further operational strategies in highway work zones. To facilitate the investigation of flow-density relations, this study has employed the Extended Kalman Filtering method to estimate the density data under congested traffic conditions. The estimation results have been evaluated with an in-depth calibrated simulation data to ensure their accuracy. Through an extensive statistical analysis and test, this chapter concludes with a set of empirical relationships between the flow and density at highway work zones under various traffic conditions.

Development of an Advanced Dynamic Late Merge (DLM) Control Model and Operation Algorithm – Chapter 4 presents an advanced DLM control model and its operation algorithm, based on a set of the optimized control thresholds. The core of this chapter is to formulate an optimization model that can generate the optimal control thresholds for dynamically selecting the most effective type of merge control, and can best use the capacity of both the open and closed lanes. The proposed optimization model has taken into account the complex interactions between vehicles in the open and closed lanes, and the available sensor information for traffic state monitoring and merging decision makings. This chapter has also presented extensive evaluation results with respect to the proposed DLM model using the optimal dynamic thresholds and the selected measures of effectiveness.

Development of Variable Speed Limits (VSL) Control Model and Operation Algorithm – Chapter 5 reports the development process for the optimal VSL control model that intends for use in improving both the operational efficiency and traffic safety, based on the evolution of dynamic traffic states and macroscopic traffic characteristics. For on-line applications, some non-linear traffic flow relations are approximated with linear functions but updated continuously from on-line detector data. To reflect the need of improving traffic safety, a set of speed boundaries is given as model constraints. Moreover, the normal deceleration rate is used in determining the length of each subsegment. This will ensure that drivers can reduce their speeds at an acceptable braking rate in response to those displayed VSL signs. The proposed VSL optimization model has been evaluated with a simulated system, and the evaluation results are also reported in this chapter.

Integrated Control Algorithm of the DLM and VSL Control Strategies – Chapter 6 focuses on exploring the potential of an integrated control algorithm with DLM and VSL control strategies in work-zone operations, and on comparing its effectiveness with that of each individual control. The core logic of an integrated control is to facilitate the

merging maneuvers and minimize potential vehicle collisions with the VSL during the DLM operation period, so as to maximize their compound effectiveness.

Research Summary and Further studies – Chapter 7 summarizes the results of those completed tasks, and discusses key issues for including investigation of the operational issues of the DLM and VSL controls without sufficient traffic sensors and exploring more advanced controls for contending with missing data and measurement errors.

CHAPTER 2 . LITERATURE REVIEW

2.1 Introduction

This chapter reviews existing strategies in the literature for highway work-zone operations, with an emphasis on two key areas: optimal merge and speed limit controls. The former is used to direct drivers to best use the capacity of the closed and open lanes, depending on the traffic conditions and the distance to the merging point. The latter is designed to minimize the shockwave impacts due to the lane-closure operations. To take advantage of state-of-the-art developments on the merge and speed limit controls, this study has conducted a comprehensive review of related key studies, including their theoretical deficiencies, model formulations, system configuration designs, and potential implementation issues. A summary of review results is presented in the remaining sections.

2.2 Merge controls

Since the lane closure activities at highway work zones are always accompanied by mandatory lane-changing and merging maneuvers between the open and closed lanes, a proper guidance to drivers in order to improve both traffic safety and efficiency is a critical operational issue. In general, one may classify existing merge controls into five categories: NDOR merge, Static Early merge, Dynamic Early merge, Static Late merge, and Dynamic Late merge. Both theoretical developments and field applications of all classified controls are reported in the remaining subsections.

2.2.1 NDOR merge (Nebraska Department of Roads) control

NDOR is a conventional merge control (also called No-merge control), where drivers are advised of the lane closure with signs placed on both sides of the roadway about 1.0 mile and 0.5 mile prior to the work-zone taper. In addition, lane-reduction signs are placed on both sides of the roadway at 1,500 ft ahead of the taper and a flashing-arrow panel is usually placed at the beginning of the taper (see Figure 2.2.1).

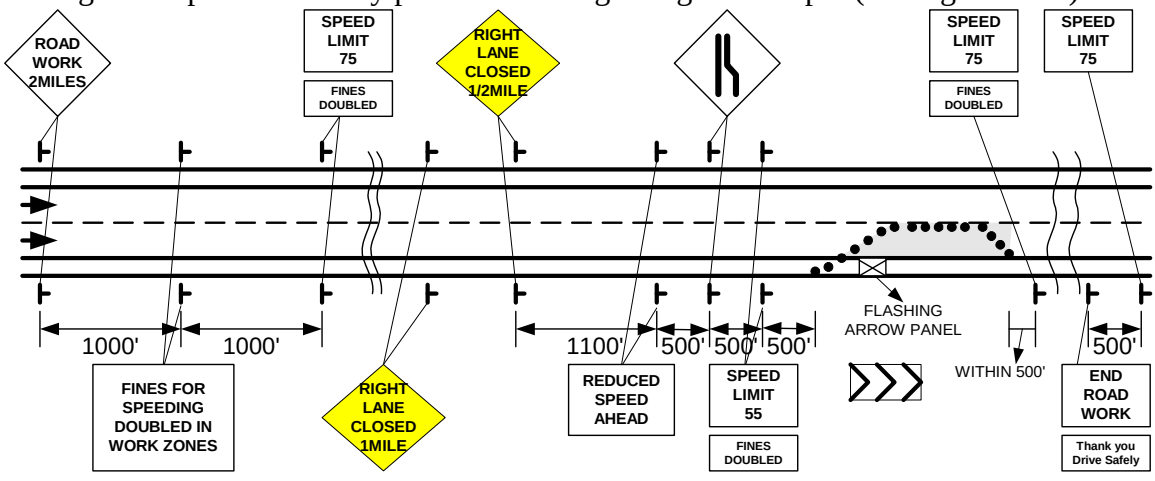

Figure 2.2.1 Configuration of the NDOR merge

A field test (McCoy et al., 1999) has revealed the following conclusions:

- This type of strategy normally works well with respect to the operational efficiency and traffic safety if traffic demand is less than the capacity of the open lane. For example, most conflicts cannot be observed at densities less than 25 vpmpl (vehicles per mile per lane).
- When the demand exceeds that capacity, however, the rapid formation of congestion and the resulting shock waves under such a control strategy may increase the possibilities for rear-end collisions, especially when the congestion extends to the upstream segments.

2.2.2 Static early merge (SEM) control

As illustrated in Figure 2.2.2, this strategy includes the placement of additional lane closure signs at approximately 1.0 mile intervals for several miles in advance of the lane closure location. Such signs are not merge signs (e.g., merge into left/right lane here) but indication of lane closure at the downstream segment (e.g., left/right lane closed 1.0 mile).

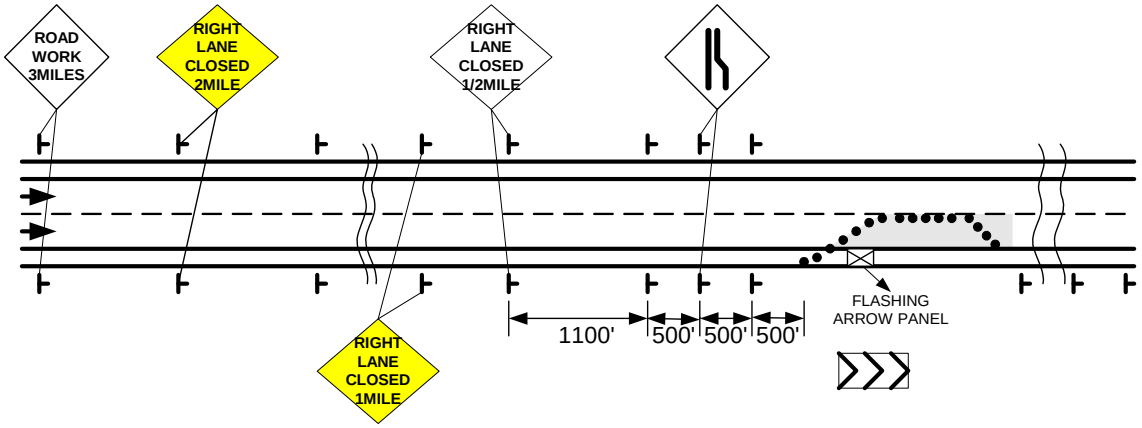

Figure 2.2.2 Configuration of the SEM system

The SEM performance, as reported in the literature (McCoy et al., 1999; McCoy, Pesti, 2001), is summarized below:

- Those early advance-lane-closure signs can increase drivers' awareness of congestion and the lane closure ahead. Such information generally can help drivers to merge into the open lane before slowing down as a result of traffic queues;
- SEM control may reduce rear-end accident potential by alerting drivers of the approaching congestion and queue at the lane closure. The extensive analysis results from simulation (McCoy, Pesti, 2001) found that early merge-control strategies can significantly reduce the frequency of forced merges, especially at a high level of traffic volume; and
- Simulation results (McCoy et al., 1999; McCo, Pesti, 2001) also showed that early merge-control strategies may result in an increase in travel time through the work

zone, because vehicles are more likely to be delayed over a longer distance due to slower vehicles in the upstream of the open lane. This may in turn increase the likelihood that drivers in the open lane will use the closed lane for passing maneuvers, increasing the potential of lane-change related accidents.

2.2.3 Dynamic early merge (DEM) control

As shown in Figs. 2.2.3 and 2.2.4, the DEM system consists of the following key features: dynamic early merge signs (e.g., DO NOT PASS or MERGE RIGHT), activation/deactivation flashing strobes, and traffic sensors at the upstream subsegments, and static early merge signs at the merge point.

When stopped vehicles are detected in the open lane next to a sign, a signal is transmitted to the controller to turn on the flashing strobes on the next upstream sign. When vehicles are moving again, the strobes are turned off. By doing so, the length of the no-passing zone is tailored to the length of congestion.

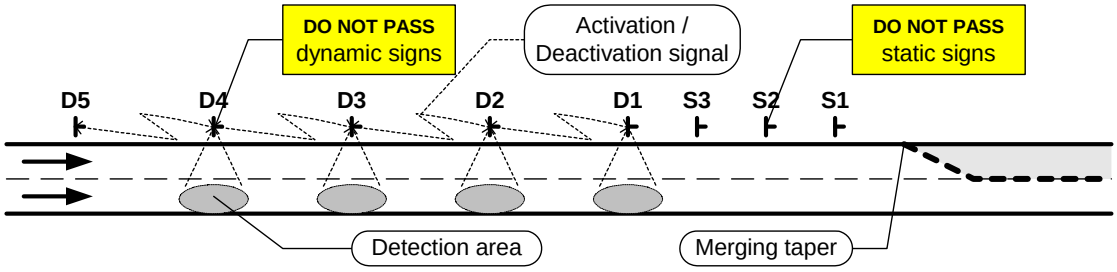

Figure 2.2.3 Configuration of the DEM system (Indiana Dept. of Transportation)

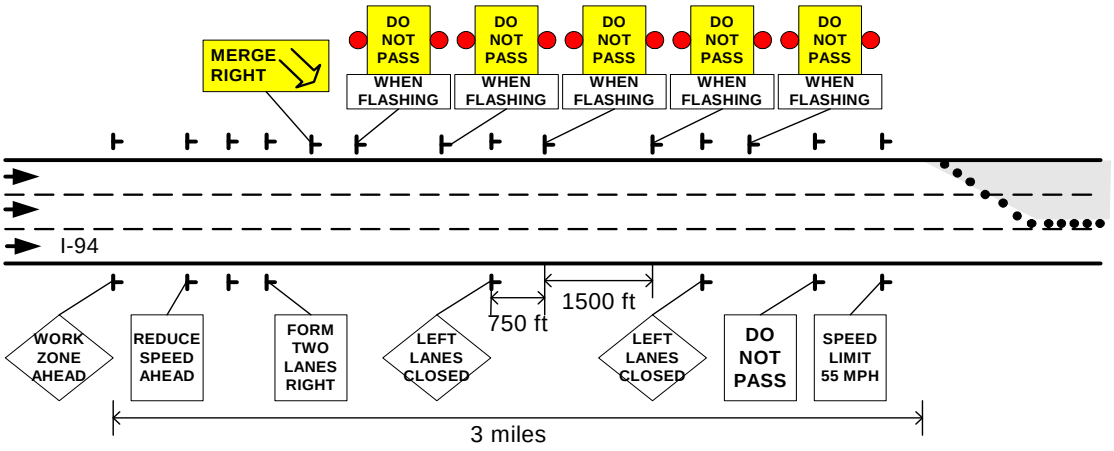

Figure 2.2.4 Configuration of the DEM system (Michigan Dept. of Transportation)

The performance of the DEM system (See Figure 2.2.3) based on the results of field implementation (McCoy et al., 1999; McCoy, Pesti, 2001) is reported below:

- Such a control can smooth the merging operations in advance of the lane closure. In addition, drivers are more likely to merge as suggested, and flows tend to be uniform in the open lane that may result in fewer rear-end accidents;
- The merging operations under DEM take place more uniformly over a much longer distance than those under the NDOR merge; and
- The spacing of the signs for such a system should be designed in a logarithmic format instead of the uniform one in order to account for the speed reduction incurred when traffic approaches the lane closure.

A field implementation at two-lane closure of 3 mainline highway segments (See Figure 2.2.4) has revealed the following findings (FHWA, 2004; Datta et al., 2004):

- The average travel speed increased from approximately 40 mph to 46 mph during the AM peak period and was relatively stable during the PM peak period;
- The average number of stops (per probe vehicle run) decreased from 1.75 to 0.96 during the AM peak period; and
- The average number of aggressive driving maneuvers decreased from 2.88 to 0.55 per time period during the PM peak hours, and was relatively stable during the AM peak period.

2.2.4 Static late merge (SLM) control

As illustrated in Figure 2.2.5, the SLM control is designed to encourage drivers to use either the open or closed lane until they reach the merge point at the lane-closure taper. Such a system is implemented as a means to reduce the conflicts between those drivers who merge into the open lane early and those who remain in the closed lane and merge into the open lane near the front of the queue at the last minute.

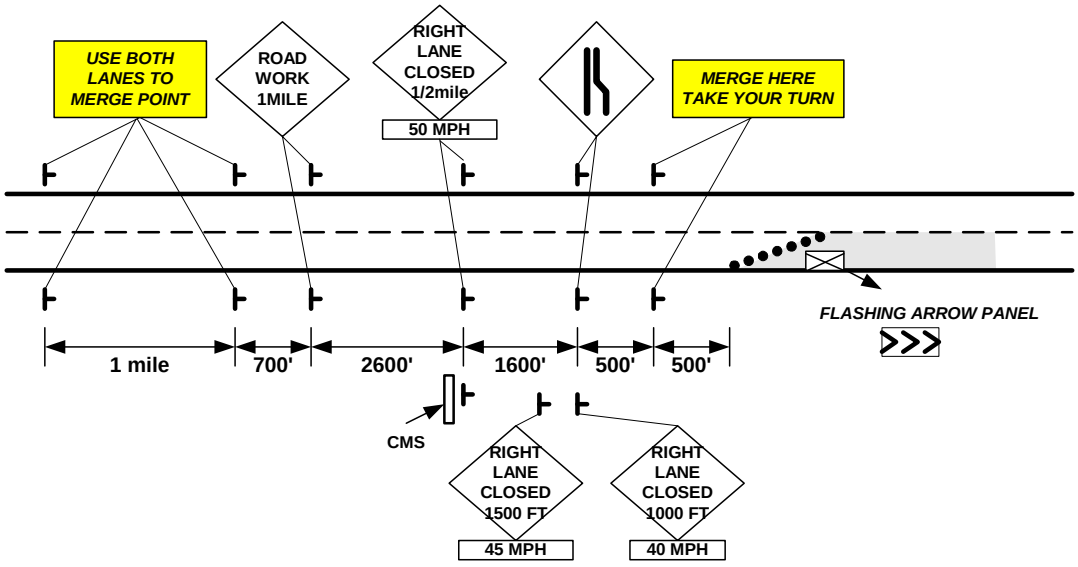

Figure 2.2.5 Configuration of the SLM system

Conceptually, this late merge system is able to address many problems associated with traffic operations in advance of lane closures at rural interstate highway work zones, especially during congested periods. There are two different evaluation results associated with the SLM control.

The field tests by NDOR (Nebraska Dept. of Roads; McCoy et al., 1999; McCoy, Pesti, 2001) have reported the following findings:

- This control method increased the capacity of the merging operations by as much as 15 % in Pennsylvania work zones;
- The lengths of the queues due to congestion can be reduced by approximately 50 %. A decrease in the queue length may reduce the likelihood of extending the congestion pattern beyond the advanced warning signs of the work zone;
- The reduction in queue lengths may in turn reduce the potential of having rear-end accidents as drivers are less likely to be irritated by others passing by them in the closed lane;
- A safety concern has been raised on operating the SLM control during off-peak periods when the total demand is below the capacity of the open lane and traffic speed is high. This is due to the fact that it may be difficult for drivers to decide who has the right-of-way to merge. This may increase the potential for collisions at the merge point; and
- In comparison with the NDOR merge, the SLM system is reported to result in about 75 % reduction in forced merges, and 30 % less lane straddles at highway traffic flow of density (e.g., more than 25 vpmpl). The work-zone throughput was also reported to achieve nearly 20 % increase.

The field tests and simulation experiments by Virginia DOT (Beacher et al., 2005 and Beacher et al. 2005) revealed the following evaluation results different from those reported in the NDOR studies:

- Only the percentage of vehicles in the closed lane increased by a statistically significant margin, with no significant change in the throughput or queue length;
- The difference in performance between those two SLM systems may be partly due to drivers' awareness of the late merge, since the SLM tests in the Nebraska studies were conducted on a freeway in Pennsylvania for several years; and
- The simulation results indicated that the area for the SLM application may be limited to situations where heavy vehicles comprise more than 20 % of the traffic stream.

2.2.5 Dynamic late merge (DLM) control

The basic concept of the DLM control strategy is to detect traffic conditions approaching the work zone in real time, and then to regulate the merging actions (e.g., merging time and locations) of drivers, based on the pre-determined control threshold. For example, when the traffic data were detected to exceed the specified threshold (e.g., congestion level), the DLM control will function similar to the late-merge control and

display their merging messages at proper upstream locations. During the uncongested period, the DLM will be set at the inactive state, and the work zone is operated like the conventional or static early merge control. The DLM control is a relatively new concept to the work zone, and has only very limited implementation practices. The most recent two field tests were conducted at Maryland and Minnesota. Their system configurations and key exploratory findings are reviewed below.

Figs. 2.2.6 to 2.2.7 illustrate the DLM systems implemented in Maryland and Minnesota, respectively. Table 2.3.1 summarizes the deployed configurations, control thresholds, and operational algorithms of those two DLM systems.

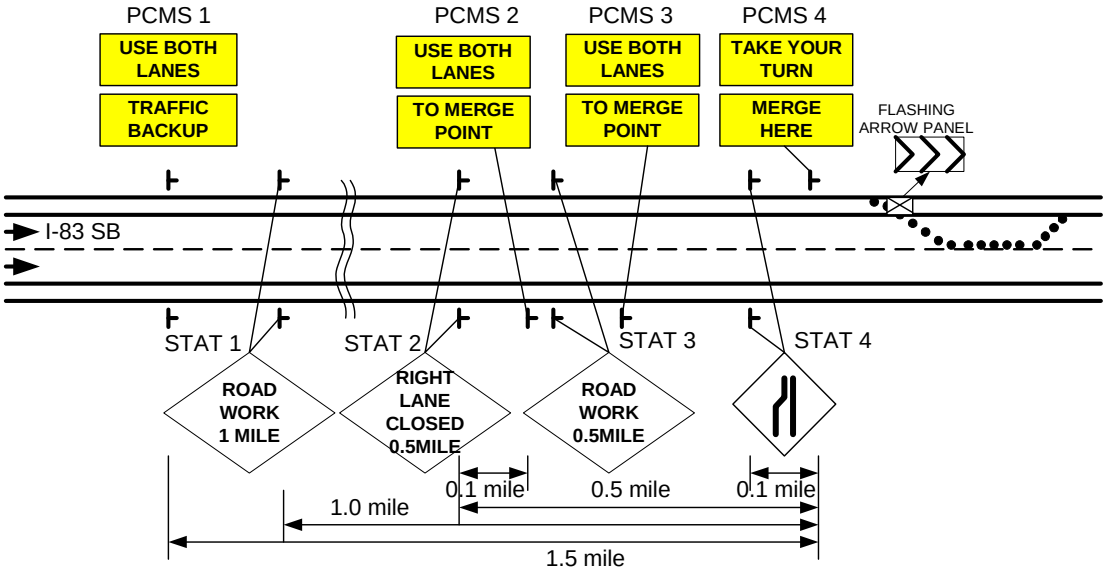

Figure 2.2.6 Configuration of the DLM system (SHA: Maryland State Highway Admin.)

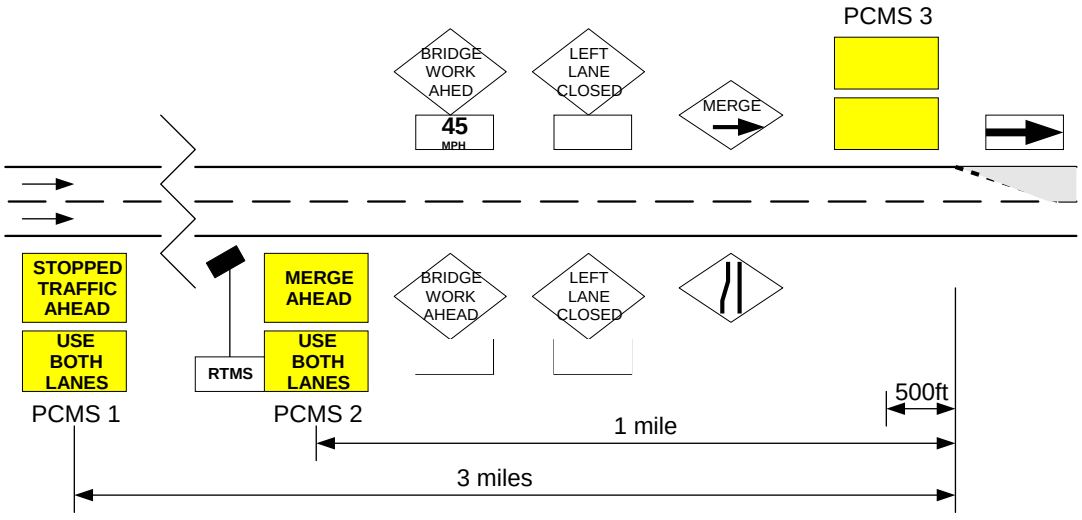

Figure 2.2.7 Configuration of the DLM system (MnDOT: Minnesota Dept. of Transportation)

The DLM system proposed by SHA (Chang, Kang, 2005) has the following key features:

- The first PCMS (Portable Changeable Message Sign) system (i.e., PCMS 1) is located approximately 1.5 miles; the other two (i.e., PCMS 2, and 3) are deployed within 0.5 mile prior to the lane closure; and the final PCMS system (i.e., PCMS 4) is installed at the merge point;
- It deploys traffic sensors (e.g., RTMS: Remote Traffic Microwave Sensor) at the same locations as PCMS 2, 3 and 4, for detecting traffic conditions in real time; and
- It does not separate the PCMS systems (e.g., PCMS 2 and 3) from static warning and merge signs (i.e., STAT 2 and 3), which are similar to those used in the conventional work-zone control to inform the approaching motorists of the lane closure.

Its control thresholds and operational algorithms (IRD Inc., 2003) can be summarized as follows:

- All PCMSs are deactivated if all occupancies are below 5%, and all PCMSs will be activated if any occupancy among the deployed sensors is over 15%. However, note that the PCMS 4 is always active at the merge point.

The other DLM system proposed by MnDOT (Taavola et al., 2004) has been designed as follows:

- The first two PCMS systems (i.e., PCMS 1 and 2) are placed approximately three miles and one mile from the lane closure, respectively. The last third PCMS (i.e., PCMS 3) is placed approximately 500 ft from the beginning of the lane closure taper point;
- A RTMS for monitoring speed and volume data is placed at approximately 1.0 mile (i.e., around PCMS 2) from the lane closure;
- Most main static warning and merge signs are installed between the PCMS 2 and 3; and
- All PCMSs will be activated when speeds near the merge point drop consistently below 30 mph and detectors have detected the continuous flows approaching the work zone. Note that PCMS 3 is always active at the merge point.

The field testing of DLM by Maryland State Highway Administration (SHA) reported the following benefits and deficiencies (Chang, Kang, 2005):

- An increase in the overall throughput;
- A reduction in the maximum queue length;
- A more uniform distribution of volumes between lanes;
- Increasing stop-and-go maneuvers in the work zone; and
- Incurring multiple merging locations on the upstream segment of the work zone.

The DLM system deployed by Mn/DOT, however, is reported to show quite different performance levels (Taavola et al., 2004), where:

- The work-zone throughputs were not increased but rather reduced slightly. During the lane-closure period, the number of vehicles exiting at one-half mile upstream of the taper location increased approximately 40%, indicating that many were willing to use alternative routes to reach their final destinations;
- The maximum queue was shortened by around 35% due to the use of both lanes up to the taper point. Drivers were beginning to utilize the closed lanes, based on the instructions displayed on the PCMS, as the construction period progressed; and
- The instructions of the dynamic late merge system were not followed by drivers, thus resulting in multiple merge locations and unintended stop-and-go traffic conditions.

Note that these two pioneering DLM tests have shed light on the potential effectiveness of such a control operation, and also have identified the following vital issues to be further investigated:

- Selection of an optimal set of thresholds for control: The two DLM systems used only the occupancy for deactivation (e.g., less than 5%) and activation (e.g., more than 15%), or the average speed for deactivation (i.e., more than 30 mph) and activation (i.e., less than 30 mph). Such static control thresholds may not yield the optimal state for properly responding to the work zone traffic dynamics and operations.
- Reliable estimation of the maximum queue length: It should be mentioned that if the actual queue is beyond the first DLM sign, drivers may not know which lane is closed, and vehicles behind them are likely to overtake them via the closed lane. Such maneuvers may increase the potential for rear-end collisions.
- Separation of the PCMS system from conventional merging signs: As shown in Figure 2.2.6, it was observed that the static signs (i.e., STAR 2) still displayed "RIGHT LANE CLOSED 0.5 MILE", while the PCMS displayed "USE BOTH LANES TO MERGE POINT". Most drivers were observed to face a dilemma incurred by the conflicting messages posted on the PCMS and conventional static signs when they were around 0.5 mile in advance of the merging point. Such a dilemma may cause the existence of multiple merging points and increase unnecessary lane-changes, and consequently decrease the DLM performance.
- Inclusion of speed limit signs: Speed control with either a warning sign or other methods should be integrated with the DLM control, as proper traffic flow speeds can smooth lane-changing and merging maneuvers, and prevent motorists from experiencing traffic conflicts such as stop-and-go and spillbacks (Migletz et al., 1999).
- Integration of the DLM with variable speed control for smooth merging operations: The variable speed limit (VSL) control can be the most effective way for maximizing the DLM performance because it can dynamically create a

smooth environment for merging maneuvers by displaying the optimal speed limits based on detected traffic conditions in advance of the work zone (Kang et al., 2004; Lin et al., 2004).

2.2.6 Other supplementary merge devices

In addition to the above primary methods for merging control, highway agencies have also practiced the following merge strategies (Walters, Cooner, 2001; Walters et al., 2000; Pesti et al., 1999):

- Discourage the use of the closed lane with a special pavement surface: An example of such a design is shown in Figure 2.2.8, which is to encourage drivers to merge early onto the open lane, with physical components such as pavement markings, traffic signs, and rumble strips.

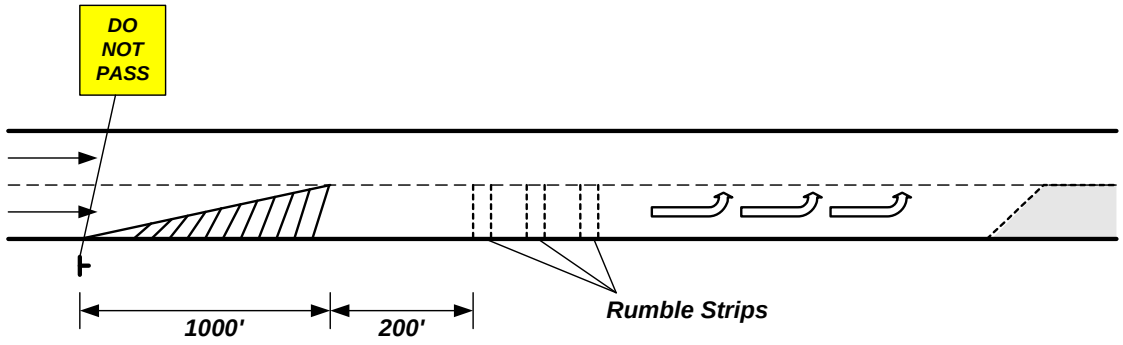

Figure 2.2.8 Discourage the use of the closed lane

- Equal Access Merge: Instead of requiring vehicles on the closed lane to merge into the open lane, this design (as illustrated in Figure 2.2.9) advises vehicles in both lanes to merge alternatively at a designated merging point.

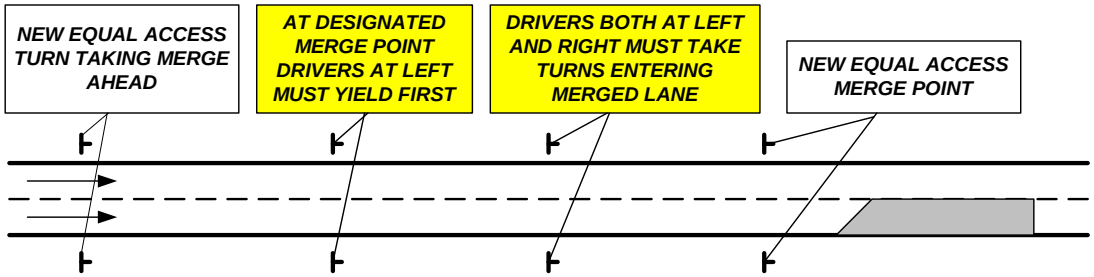

Figure 2.2.9 Configuration of equal access merge

- Always Closing Left Lane: The proposed strategy is to always close the left lane in advance of the median crossovers and lane closures, even if the work is being done in the right lane. This would lead drivers to the right lane when encountering a lane closure. Under such a control, drivers may be better prepared to move onto the open lane further in advance of the work zone.

2.3 Speed controls

As mentioned previously, the primary purpose of the speed control was to reduce average speed and speed variances across the travel lanes, so as to facilitate the approaching vehicles to merge smoothly into the lane closure area (Hall, Wrage, 1997; FHWA, 1994). This section will first review conventional speed limit control posted at work zones, including the speed monitoring displays and speed advisory signs. Recent advances in dynamic variable speed limit control will also be presented subsequently along with some supplementary strategies for enforcing the above speed controls.

2.3.1 Posted speed limit (PSL) control

Under the conventional PSL control, the speed limits are fixed and displayed during the work zone operation. Figure 2.3.1 presents an example of work zone under the PSL control (Stidger, 2003; FHWA, 2003).

A research report by the National Cooperative Highway Research Program (NCHRP, 1999; Migletz et al., 1999) studies suggests that the following four main steps are to be taken in determining the posted speed limits for work zone operations:

- Determine the existing speed limit;
- Determine the work zone condition that applies;
- Determine which factors apply to the appropriate condition of the specific site; and
- Select the work zone speed limit reduction.

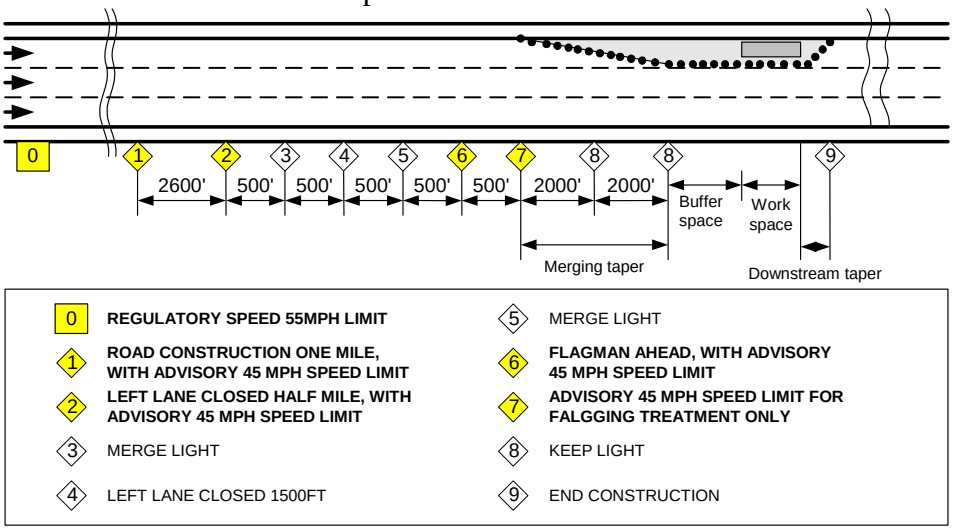

Figure 2.3.1 An example work-zone segment under the PSL control

However, the PSL control based on the above procedures has the following deficiencies:

- These procedures are available only after the work-zone operation schedule is pre-fixed since the results of the first three steps vary with traffic conditions during the operational periods;
- It considers only the average traffic conditions (e.g., average hourly volume) during the work zone operation, which may not be sufficient to respond to the fluctuation of traffic volume during the entire working day; and
- The effectiveness of such speed limits is conditioned on the existence of stable traffic conditions at the work zones.

2.3.2 Speed monitoring display (SMD) and Speed advisory sign (SAS) control

The SMD system measures and displays the speeds of vehicles approaching the work zone. As shown in Figure 2.3.2, the CMS (or PCMS) is designed to warn drivers that they are traveling above the maximum safe speed (e.g., 55 mph). When a speeding vehicle is detected, the CMS will display a message to inform drivers of their speeds and warn them to slow down. On the other hand, the SAS system (see Figure 2.3.3) can display the speed of the downstream traffic to warn drivers of stopped or slow-moving traffic ahead and thereby enable them to reduce their speeds and avoid rear-end crashes.

Some before-and-after field studies (Pesti, 2005; Bowie et al., 2004; Pesti, McCoy, 2001; McCoy et al., 1995) of such system indicate that:

- Both systems are effective in reducing the average speed of vehicles approaching the work zones. For instance, the SMD system did reduce the mean speed of traffic by about 5 mph, and the frequency of drivers exceeding the advisory 55 mph speed limit by as much as 40 %.

Figure 2.3.2 Speed monitoring display

Figure 2.3.3 Speed advisory sign

However, it should be noted that:

- Both systems are focused mainly on improving traffic safety (e.g., speed reduction, and potential accidents), based on the PSL control;
- The effectiveness of both systems is conditioned on its selection of a proper value to reflect the traffic conditions. Otherwise, drivers will be reluctant to follow the speed limits advice if the posted speed threshold is significantly different from real traffic conditions when congestion is building; and
- As illustrated in Figure 2.3.4, most SMD systems are integrated with the PSL control in the work-zone operations, and in most cases, all posted speed limits over the upstream segment are identical (e.g., 55 mph).

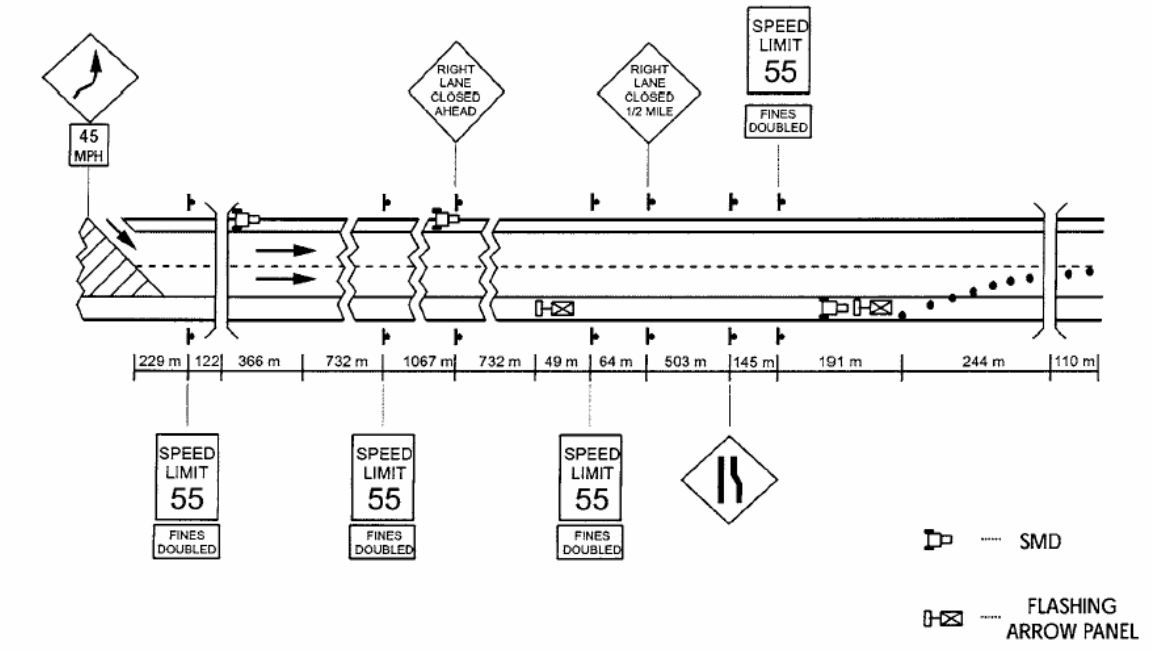

Figure 2.3.4 An example of a work-zone segment controlled by PSL and SMD

2.3.3 Variable speed limit (VSL) control

To effectively respond to traffic conditions and also to increase the compliance rate of drivers, traffic professionals in recent years have experimented variable speed limit (VSL) control in place of the conventional posted speed limit operations in highway work zones (TRB, 1998).

Despite the potential effectiveness of using VSL for highway operations, most existing studies or practices have focused mainly on its impacts on safety related issues. For example, Coleman et al. (1996) reported the use of automated speed management in Australia, which is a fog warning and speed advisory system installed south of Sydney. In the same study, they also introduced a control system which uses a variable speed limit sign to display the current speed limit under construction. Pili-Sihvola and Taskula (1996) introduced a VSL control to warn drivers of black ice and other hazards in Finland. Smulders (1992) and Hoogen and Smulders (1996) stated that the goal of Dutch

speed limit system installed on frequently congested interchanges was not to reduce average speeds but mainly to narrow the speed dispersion. A similar system in United Kingdom described by Wilkie (1997) was designed to minimize the stop-and-go conditions during heavy traffic congestion. Sumner and Andrews (1990) have also reported a variable speed limit system (VSLS) in the state of New Mexico, which was intended to be flexible in response to various environmental conditions. It should be noted that those VSL systems have been applied in highway segments plagued by the bad weathers and recurrent congestions rather than work-zone operations.

Recently, FHWA have solicited field tests of VSL systems in highway work zones. Two preliminary algorithms used in FHWA's VSL projects are summarized below.

i. VSL control during work-zone operations

Lyles et al. (2004) implemented a VSL system on the I-96 work zones, and evaluated its impacts on traffic flow and safety. They concluded that the average speed of motorists appeared to increase, and the travel time seemed to decrease but unlikely to be noticed by the average travelers. Both the average speed and occupancy were used as the control thresholds for displaying the set of speed limits (see Table 2.3.1). The following rules have been employed in their study:

- It was required that the speed limits no higher than 50 mph be posted near some ramp locations; and
- The maximum speed limit in the active work zone was never allowed to be higher than 60 mph, although the trailer at the end of the work zone was permitted to go as high as 70 mph.
-

Table 2.3.1 A set of predetermined speed limits and their occupancy and speed thresholds

Thresholds	Speed limit profiles (unit: mph)		
	Profile #1	Profile #2	Profile #3
Low occupancy – 0 %	50	60	70
High occupancy – 90 %	40	40	40
Mid. occupancy rules – 0 % < Occupancy < 90 %			
Ave. speed < 40 mph	40	40	40
40 mph ≤ Ave. speed < 43 mph	45	45	45
43 mph ≤ Ave. speed < 48 mph	50	50	50
48 mph ≤ Ave. speed < 53 mph	50	55	55
53 mph ≤ Ave. speed < 58 mph	50	60	60
58 mph ≤ Ave. speed < 63 mph	50	60	65
63 mph ≤ Ave. speed < 68 mph	50	60	70
Ave. speed ≥68 mph	50	60	70

The VSL control algorithm implemented by Lyles et al. (2004), however, suffers the following deficiencies:

- The pre-determined control thresholds are static in nature and cannot best respond to the dynamic evolution of traffic conditions; and

- Those displayed speed limit profiles, based on the set of detected average speeds, do not have any theoretical and/or systematic relations with the control objectives such as improving traffic flow and safety.

ii. VSL control under laboratory analyses

Park and Yadlapati (2004) and Lee et al. (2004) conducted simulation experiments to evaluate their VSL strategies using VISSIM and PARAMICS, respectively.

The operational algorithm proposed by Park and Yadlapati has the following features:

- If there is a decrease in the safety indicator (i.e., Minimum Safety Distance Equation, MSDE, see Eqn. 2.3.1) with an unchanged volume or a decrease in volume, the speed distribution of the previous cycle is continued;
- If MSDE continues to decrease without an increase in volume for the next consecutive cycle, the VSL speed is then lowered by 5 mph; and
- If there is an increase in MSDE with accompanying a decrease in volume, or if MSDE continues to decrease without a decrease in volume for two consecutive cycles, the speed posted at the VSL is increased by 5mph.

$$MSDE = \mathbf{1.47} * (V_L * h - V_F * PRT) + \left(\frac{V_L^2 - V_F^2}{\mathbf{30}(f \pm g)} \right) \quad (2.3.1)$$

where,

V_L is velocity of the lead vehicle (unit: mph),

V_F is velocity of the following vehicle (unit: mph),

PRT is perception and reaction time of the following vehicle in seconds,

f and g are friction and grade factors, respectively, and

h is time headway (unit: second).

The latter VSL system (Lee et al., 2004) is operated by the following logic and evaluated with the safety criterion (i.e., average cross-sectional covariance of volume difference between the upstream and downstream of a target location, COVV, see Eqn. 2.3.2):

- If average speed ≤ 60 km/hr, the speed limit is set at 50 km/hr;
- If average speed > 60 km/hr and ≤ 70 km/hr, the speed limit is set at 60 km/hr;
- If average speed > 70 km/hr and ≤ 80 km/hr, the speed limit is set at 70 km/hr;
- Otherwise, i.e., if average speed > 80 km/hr, the speed limit is set at 80 km/hr.

$$COVV = \frac{\mathbf{1}}{n-\mathbf{1}} \sum \left| \mathrm{cov}(V_i - V_{i+\mathbf{1}}) \right| = \frac{\mathbf{1}}{n-\mathbf{1}} \sum_{i=\mathbf{1}}^{n-\mathbf{1}} \sum_{t=t^*-\Delta t}^{t^*} \left[(\Delta v_i(t) - \bar{\Delta v}_{i+\mathbf{1}})(\Delta v_{i+\mathbf{1}}(t) - \bar{\Delta v}_{i+\mathbf{1}}) \right] \quad (2.3.2)$$

where,

n is the number of lanes,

V_i is time series of $\Delta v_i(t)$ during Δt,

t^* is actual time of crash occurrence,
Δt is observation time slice duration (seconds),
$\Delta v_i(t)$ is volume difference between upstream and downstream of location on lane i at time interval t, and
$\overline{\Delta v_i}$ is average volume difference on lane i during Δt.

Based on experimental simulation results, the former study concluded that their proposed VSL logic outperformed the base case (e.g., PSL control) with respect to the safety (MSDE) and mobility (travel time and throughputs) indicators. The latter one also reported similar results using a new crash precursor as the safety criterion (COVV). However, both two operational algorithms still have not overcome the following critical problems:

- Their control thresholds (i.e., MSDE and volume, and average speed, respectively) are still focused on traffic safety, other than the operational efficiency; and
- Their speed limits are determined with a preset increment (e.g., ± 5 mph and ± 10 mph, respectively), without considering their relations to traffic flows between the detected speeds.

2.3.4 Other supplementary strategies

The following strategies play supplementary roles in enhancing the existing PSL control by using additional merge, speed limit signs, or narrow lane width prior to the lane closure.

- Iowa Weave: This strategy forces vehicles to perform the merge maneuvers between the open and closed lanes, based on the instructions shown in Figure 2.3.5. The evaluation report of some field studies (Walters, Cooner, 2001; Walters et al., 2000; McCoy et al., 1999) found that the Iowa Weave can be effective in reducing traffic flow speeds to work zones. For example, more than 50 % of sample vehicles traveled below the posted 30 mph work-zone speed limit, but less than 20 % of drivers were observed to comply with the speed limit when the Iowa Weave was not in place.

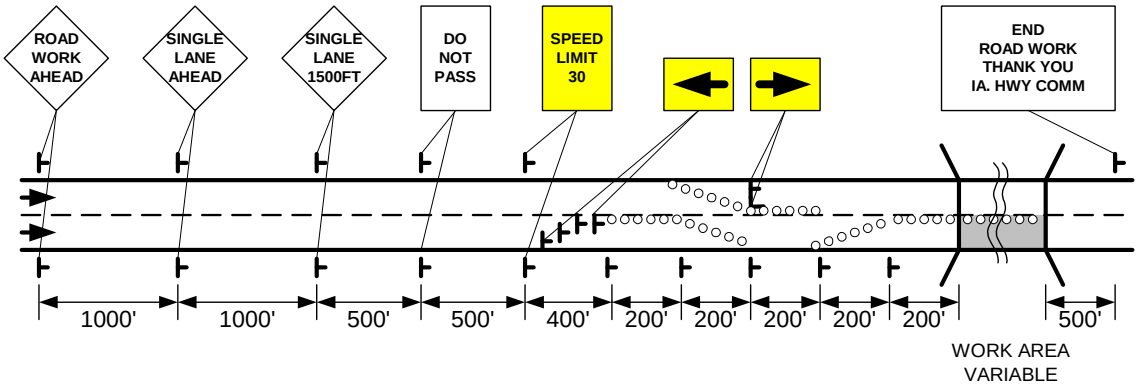

Figure 2.3.5 Configuration of Iowa weave

- Longer Speed Zone Transition: Under the PSL control in work zones, the proposed idea (McCoy et al., 1999) is to replace the 75 mph regulatory speed limit sign with the 65 mph sign, when a 55 mph is used as the PSL sign (see Figure 2.3.6). This would provide a longer and smoother speed transition between the 75 mph and 55 mph speed limit zones.

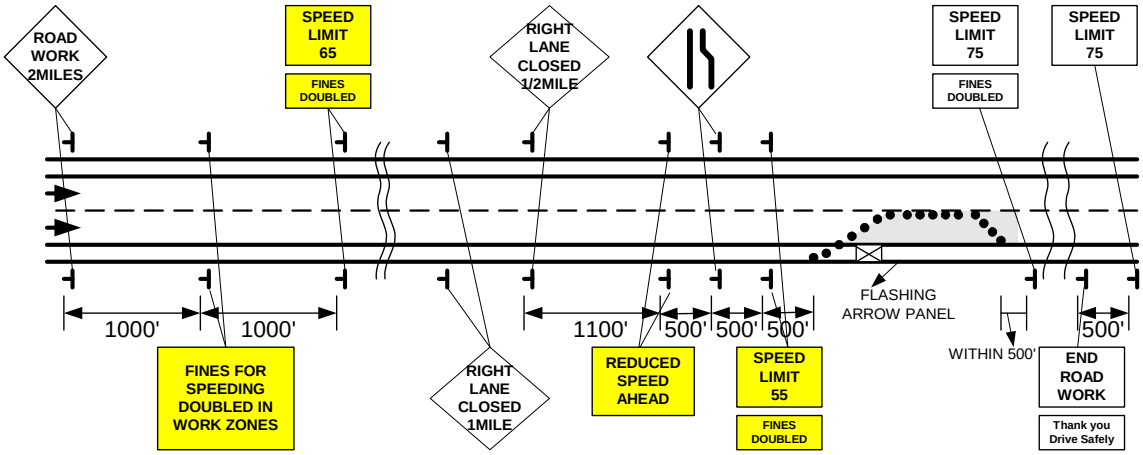

Figure 2.3.6 Configuration of longer speed zone transition

- Narrow Lanes: The key idea of this strategy is to use narrow lanes and pavement markings to slow traffic in advance of the work zone. During the 1998 construction season, the Ohio Department of Transportation experimented this strategy to its work zones (McCoy et al., 1999). Such a strategy has been widely used in European countries (e.g., Germany, the Netherlands, Belgium, Scotland, and France), emphasizing on maintaining the same number of lanes and reducing speeds under work-zone operations. Figure 2.3.7 illustrates an example application of such a strategy (Steinke et al., 2000), and Figure 2.3.8 shows the results reported by German highway agency study (Steinke et al., 2000), which indicates that narrow lanes can effectively slow the speed of traffic flows.

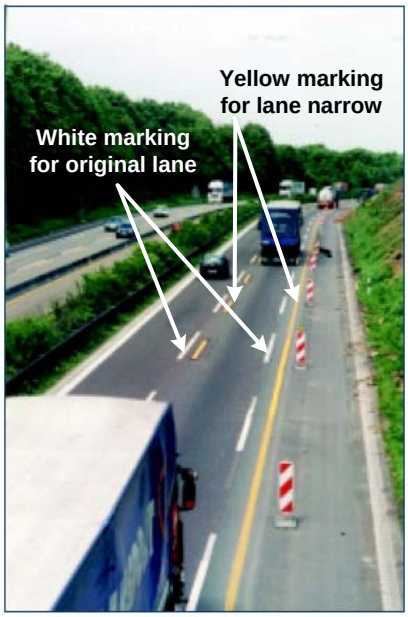

Figure 2.3.7 Lane narrow marked with yellow lines

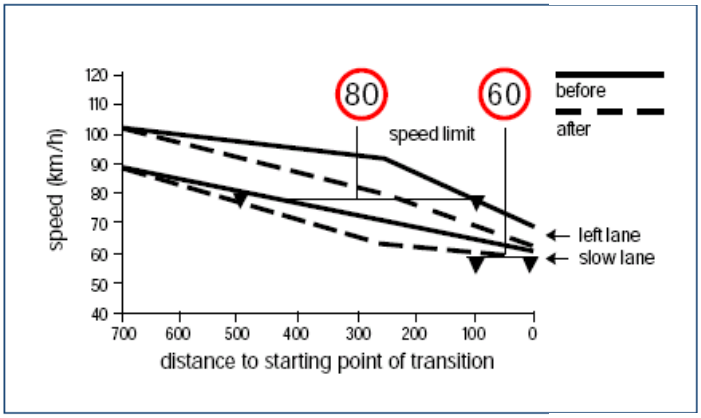

Figure 2.3.8 An Effect of narrow lane on reduced speed

2.4 Closure

This chapter has reviewed two main categories of work zone operational strategies: speed limit and merge controls. Table 2.4.1 summarizes those existing work-zone controls, with respect to their available functions and hardware requirements.

Table 2.4.1 Summary of control strategies for highway work-zone operations

Strategies		Function			Hardware		
		Merge control		Speed control	Real-time display	Communi-cation	Traffic detection
		Early	Late				
Merge Controls	NDOR	**O**					
	SEM	**O**					
	DEM	**O**			**O**	**O**	**O**
	SLM		**O**				
	DLM	**O**	**O**		**O**	**O**	**O**
	Discourage Use of Closed Lane	**O**					
	Equal Excess		**O**				
	Always Close the Left Lane	**O**					
Speed Controls	PSL			**O**			
	SMD / SAS			**O**	**O**	**O**	**O**
	VSL			**O**	**O**	**O**	**O**
	Iowa Weave	**O**					
	Longer Speed Zone Transit.			**O**			
	Narrow Lane			**O**			

The conclusions from the literature review are summarized as follows:

- Except the DLM (and DEM) and VSL controls, most implemented control strategies are based on a static approach, and only a very few studies have addressed the dynamic aspect of such controls;
- Most control strategies are designed mainly to improve traffic safety, but not to improve the operational efficiency such as maximizing the throughput, or minimizing the average delay of vehicles traveling on the entire highway segment plagued by the work-zone incurred traffic queue;
- Despite the potential effectiveness of some limited DLM and VSL systems for highway work-zone operations, their control algorithms have not taken full advantages of available information, and not been able to respond to the time-varying traffic flow patterns and the complex interactions between the open and closed lanes; and
- Since the VSL control has the potential to be effective under a wide range of traffic volume, one can view it as a supplementary control component for any work-zone operation. Thus, to smooth the merging maneuvers and minimize potential collisions during the DLM operations, it is essential to develop a system control process that can integrate the VSL with the DLM so as to maximize the system effectiveness.

CHAPTER 3 . INVESTIGATING MACROSCOPIC TRAFFIC FLOW PROPERTIES IN HIGHWAY WORK ZONES

3.1 Introduction

In review of the literature (Loerger et al., 2001; Bank, 1999), it is clear that most existing traffic flow models were proposed for highway segments without work zone operations. In fact, only very limited field observations on vehicle interactions and traffic flow dynamics in work zones have been conducted by transportation researchers. Hence, how to properly model the impacts of work-zone activities on the traffic flow characteristics remains a challenging issue.

This chapter intends to explore the macroscopic traffic flow relation under work-zone operations with field data. As shown in Figure 3.1.1, description of such data is first presented in Section 3.2. The procedures for estimating density data, along with evaluation methodology are presented in Section 3.3, followed by estimation of the flow-density relations and investigation of their properties in Section 3.4. Potential applications of the calibrated flow-density relation for work-zone control are reported in Section 3.5.

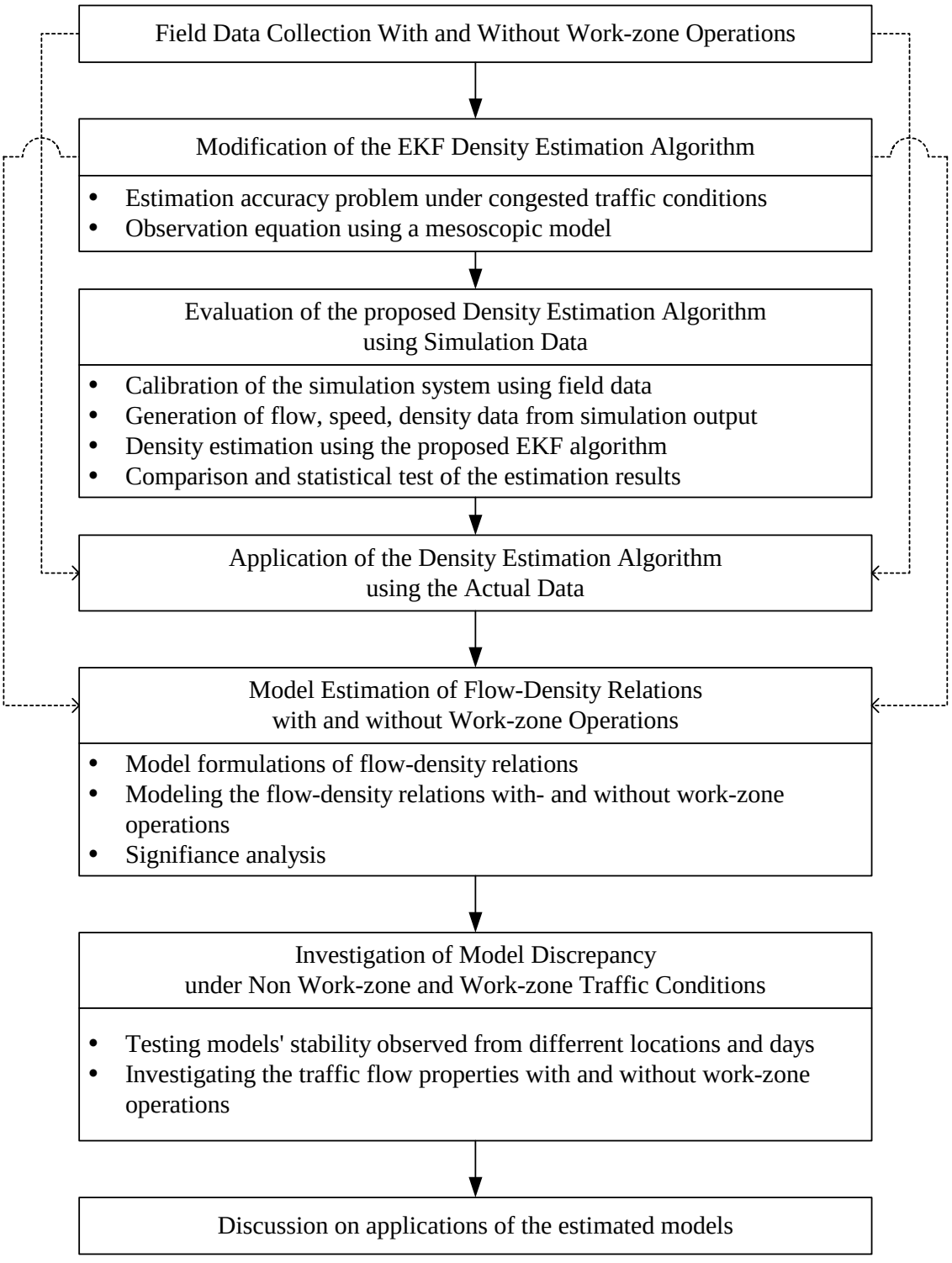

Figure 3.1.1 Flowchart for investigating macroscopic traffic flow properties in highway work zones

3.2 Description of field data collection

As mentioned previously, the traffic flow data were collected from a field study of a dynamic late merge (DLM) system for highway work-zone operations (Chang, Kang, 2005). The target DLM system was deployed prior to the right-lane closure in a work-zone area near the overpass bridge of Cold Bottom road on the I-83 south bound (SB). A graphical illustration of the DLM and work-zone operation is shown in Figure 3.2.1.

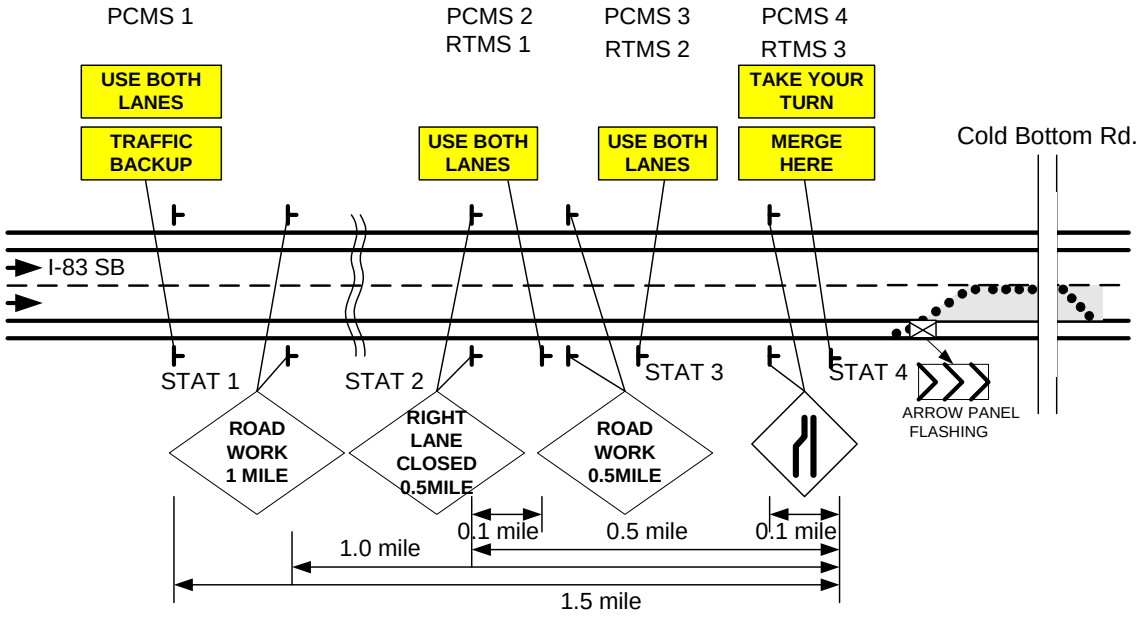

Figure 3.2.1 A Graphical illustration of the DLM and work zone

Although the system was under test for four weeks, only 4 days of work-zone data and 4 days of non-work-zone information have the acceptable quality for use in the analysis. Primarily, data were obtained from RTMS (Remote Traffic Microwave Sensor) traffic sensors that produce the volume, speed, and occupancy for both lanes, at the interval of 2 minutes. A total of three RTMS were installed at the same locations of PCMS 2, 3, and 4 (see Figure 3.2.1).

Table 3.2.1 summarizes the data collected for investigating the traffic flow characteristics with and without work-zone operations.

Table 3.2.1 Summary of field data information

Traffic conditions	Dates (2003)	Collection periods	Data items	Locations
No work zone operation	10/29, 10/30, 11/04, 11/05	4:00am to 10:00am	Volume Speed Occupancy	Upstream point (PCMS 2) Middle point (PCMS 3) Merge point (PCMS 4)
Work zone operation	10/22, 10/23, 11/07, 11/10	8:00am to 14:00pm		

The entire traffic flow patterns over 24 hours have been divided into the following three distinctive periods;

- Period-1: 06:00am to 08:00am, where traffic volume is near its capacity;
- Period-2: 09:00am to 11:00, which includes congested traffic condition caused by the lane-close work-zone operation; and
- Period-3: All time periods other than Period-1 and Period-2, which include normal traffic conditions.

Figures 3.2.2 and 3.2.3 present the traffic flow patterns with and without work-zone operations, respectively. Figure 3.2.2 shows a significantly high level of traffic volume during Period-1, while Figure 3.2.3 exhibits the congested flows during Period-2 and Period-1.

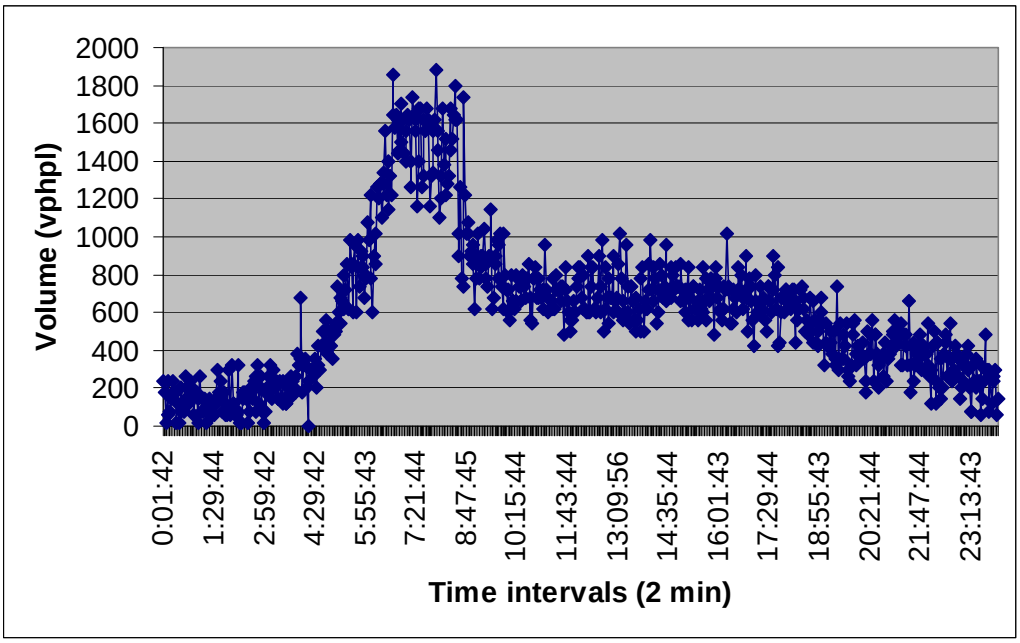

Figure 3.2.2 Traffic flow patterns without work-zone operations

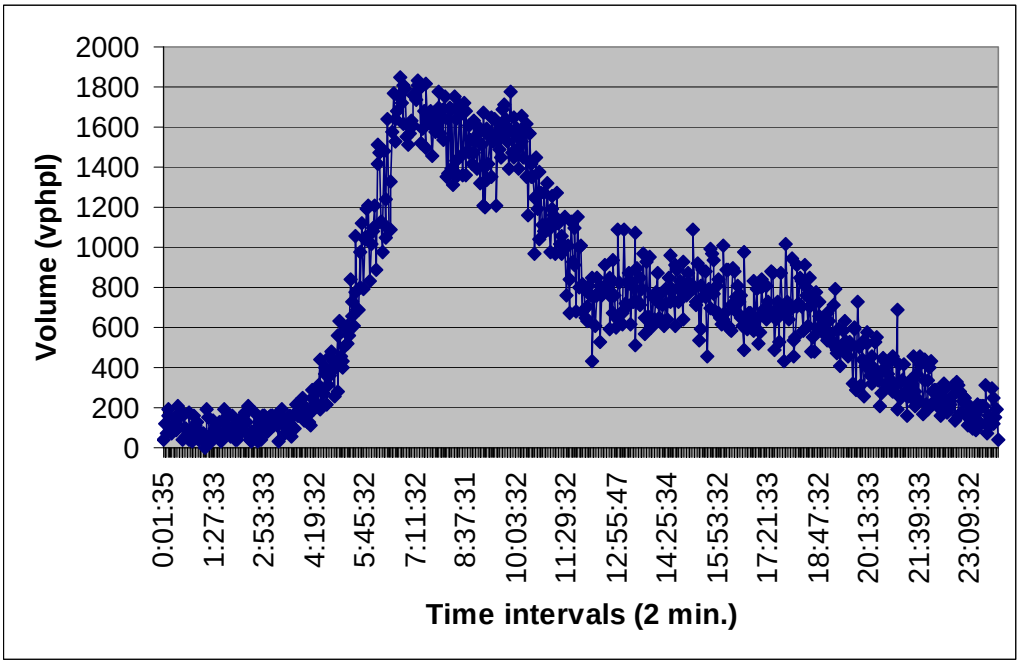

Figure 3.2.3 Traffic flow patterns under work-zone operations

3.3 Density estimation from the field data

As is well recognized, density is one of the key traffic flow factors affecting a driver's choice of speed and is an indicator of traffic conditions (Kang et al., 2004). In fact, the relation between the flow and density is an important barometer for measuring the traffic quality (Wu, 2002).

Despite the critical role of the density data, such information cannot actually be obtained directly from the field survey. Instead, most applications tend to choose the available occupancy data in place of the density data based on the assumption that the relationship between occupancy and density is known and stable (Hall et al., 1993; Hall et al., 1992; Bank, 1989; Persaud, Hurdle, 1988). However, such an assumption is unrealistic under the lane-closed and congested work-zone operations. Thus, it is essential that a model for estimating the density under highway work-zone operations be developed for serving as the input of control operations.

3.3.1 Procedures for the density estimation

To provide a reliable estimate of the density, it is desirable to use the actual traffic data (e.g., volume and speed) obtained from the sensors, since such information can reflect the traffic states under the given density. With respect to the estimation method, the Extended Kalman Filtering (EKF) has been reported in the literature as one of the most effective methods for density estimation under uncongested highway segment without work-zone operations (Gazis, Liu, 2003; Gazis, 2002).

However, under congested traffic conditions, the EKF method with any macroscopic models cannot fully capture the complex interactions between vehicles, and generally yield a high level of estimation errors (Gazis, 2002). Thus, this study intends to incorporate a mesoscopic model to the existing EKF algorithm (Gazis, Liu, 2003), and employ a revised algorithm for estimating the congested work-zone traffic condition.

3.3.2 Mesoscopic prediction model for the speed-density relation

The mesoscopic traffic flow relation employed in the EKF estimation procedures is based on the model proposed by Berg et al. (Berg et al., 2000; Berg, Woods, 1999; Berg and Woods, 1999) and a deterministic optimal velocity model presented by Bando et al. (1995).

To capture the unique queue dynamics incurred near a work zone, as shown in Eqn. 3.3.1, this study incorporates the impact of shock wave on the upstream segments of a highway work zone in the existing mesoscopic model (Berg et al., 2000; Berg, Woods, 1999; Adeli, Ghosh-Dastidar, 2004). That is,

$$\frac{\partial u}{\partial t} + u\frac{\partial u}{\partial x} = \frac{\mathbf{1}}{\pi}\left[\omega \cdot (U(d) - u) + \phi \cdot \frac{\partial U(d)}{\partial d}\left(\frac{\mathbf{1}}{\mathbf{2}d}\frac{\partial d}{\partial x} + \frac{\mathbf{1}}{\mathbf{6}d^2}\frac{\partial^2 d}{\partial x^2} - \frac{\mathbf{1}}{\mathbf{2}d^3}\left(\frac{\partial d}{\partial x}\right)^2\right)\right] + \theta \cdot \frac{\partial Q}{\partial d} \quad (3.3.1)$$

where,

u, d and Q: average speed, mean density, and average flow rate, respectively, at time t and location x;

$U(d)$: optimal speed function, which determines a driver's preferred safe speed;

π : reaction time (e.g., less than 1 min.) of drivers to the work-zone operations;

ω and ϕ: adjustment factors to control the traffic flow fluctuation due to the reduced number of available lane(s), and contribution to the higher order terms, respectively; and

θ : Weight factor for the speed of the shock wave.

The last term in Eqn. (3.3.1) indicates the speed of the shock wave, at which discontinuities in traffic flow states (e.g., the growth of a queue upstream of the lane closure) travel through the stream, depends on the flows and densities existing on each subsegment.

Due to the nonlinear property of Eqn. (3.3.1), one needs to approximate it based on the discrete temporal and spatial structure. Since there is no entry and exit ramp in the target highway work-zone segment, the density evolution in subsegment *i* can be expressed by the following state equation, based on the traffic flow conservation law.

$$d_i(k) = d_i(k-1) + \frac{T}{l_i \cdot n_i}\left[q_{i+1}(k) - q_i(k)\right] \tag{3.3.2}$$

where, $q_i(k) = \alpha_i \cdot Q_{i+1}(k) + \left[1 - \alpha_i\right] \cdot Q_i(k)$ (3.3.3)

and, α_i is the transition flow weight factor which can be calibrated with field measurements.

Thus, using Eqns. (3.3.2) and (3.3.3), Eqn. (3.3.1) can be approximated as follows.

$$\begin{aligned} u_i(k+1) = {} & u_i(k) + \omega \cdot \frac{1}{\pi}\left[U(d_i(k)) - u_i(k)\right] + u_i(k) \cdot \frac{T}{l_i}\left[u_{i+1}(k) - u_i(k)\right] \\ & + \phi \cdot \frac{T}{\pi}\left[\frac{U(d_{i-1}(k)) - U(d_i(k))}{d_{i-1}(k) - d_i(k)}\right] \cdot \left[\begin{array}{l} \dfrac{1}{2d_i(k)} \dfrac{d_{i-1}(k) - d_i(k)}{l_i} \\ -\dfrac{1}{2d_i(k)^3}\left(\dfrac{d_{i-1}(k) - d_i(k)}{l_i}\right)^2 \\ +\dfrac{1}{6d_i(k)^2} \dfrac{d_{i-1}(k) - 2d_i(k) + d_{i+1}(k)}{2l_i^{\,2}} \end{array}\right] \\ & + \theta \cdot \left[\frac{Q_{i-1}(k) - Q_i(k)}{d_{i-1}(k) - d_i(k)}\right] \end{aligned} \tag{3.3.4}$$

where, the optimal velocity function $U(d(k))$ also needs to be approximated with the following approximation equation (Berg, Woods, 1999).

$$U(d_i(k)) = \tanh\left[\begin{array}{l} \dfrac{1}{d_i(k)} - \dfrac{1}{2d_i(k)^3} \dfrac{d_{i-1}(k) - d_i(k)}{l_i} \\ -\dfrac{1}{6d_i(k)^4} \dfrac{d_{i-1}(k) - 2d_i(k) + d_{i+1}(k)}{2i_i^2} \\ +\dfrac{1}{2d_i(k)^5}\left(\dfrac{d_{i-1}(k) - d_i(k)}{l_i}\right)^2 - 2 \end{array}\right] - \tanh(-2) \tag{3.3.5}$$

3.3.3 Estimation procedures

Figure 3.3.1 illustrates the location of sensors used in the DLM operations (see Figure 3.2.1).

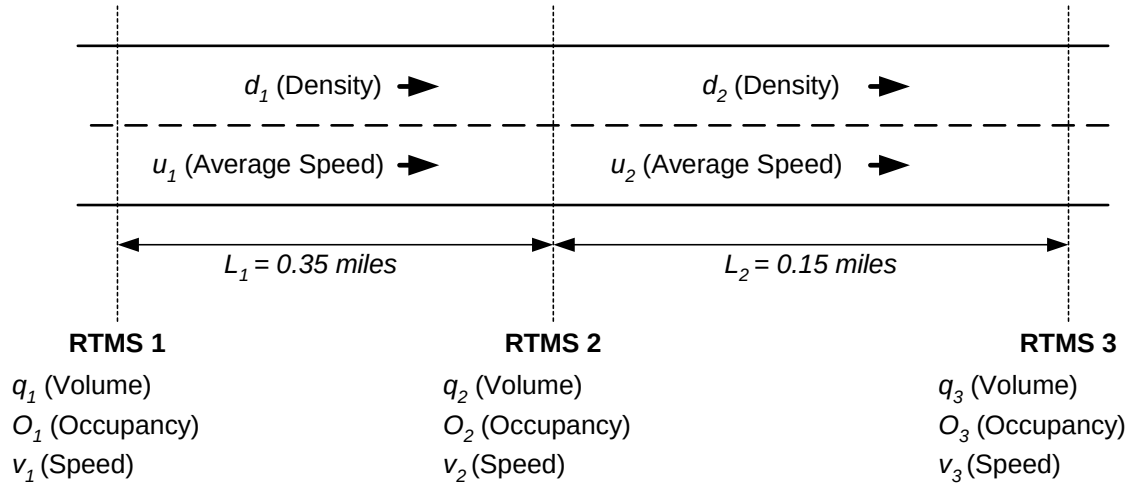

Figure 3.3.1 A schematic plot showing two subsegments of the target freeway work zone

The proposed density estimation procedures with the EKF (Gazis, Liu, 2003) are based on the two new state variable estimates, one from the 'State Eqn. 3.3.2', and the other from an "Observation Eqn. 3.3.4". These two equations and their relations are described as follows: where $k\,(=\mathbf{0}, \mathbf{1}, \mathbf{2}, \cdots)$ denotes a time index (e.g., 2 min.), and so $k=0$ corresponds to a starting time.

Step-1: Initialization

- Set $k=0$
- Initialize the state variables and the covariance matrix

$$d_0 = \bar{d}_0 = E\{y_0\}$$

$$P_0 = \sum{}_0 = \mathrm{cov}[y_0; y_0] = E\{(y_0 - \bar{y}_0)(y_0 - \bar{y}_0)'\}$$

Step-2: Prediction ($k+1\,|\,k$)

- Set $k=1$
- Calculate an observed value for the density, d_k, using Eqns. (3.3.6) and (3.3.7)

$$u_i(k) = h[d_i(k)] = b\exp\left\{-\frac{1}{2}[(d_i(k)/l_i)/a]^2\right\} + \theta_i(k) \qquad (3.3.6)$$

$$u_i(k) = \lambda \cdot v_{i+1}(k) + (1-\lambda)\cdot v_i(k) \qquad (3.3.7)$$

- Predict the state vector, $\bar{d}(k+1\,|\,k)$, using Eqn. (3.3.8) and the covariance matrix

$$\bar{d}_i(k+1\,|\,k) = f_k\left[\bar{d}_i(k)\right] = d_i(k) + \frac{T}{l_i \cdot n_i}\left[q_{i+1}(k) - q_i(k)\right] \qquad (3.3.8)$$

$$P(k+1\,|\,k) = F(k)\cdot P(k\,|\,k)\cdot F(k)^T + \phi(k)\,,$$

where $F(k) = \dfrac{\partial f[\cdot]}{\partial \bar{d}(k)}$ and $\phi_k = \delta_{k,j} \cdot E\left\{\bar{\varepsilon}_j \bar{\varepsilon}_k^T\right\}$ and the symbol $\delta_{j,j}$ is the Kronecker delta. The estimating error for the state variables at the *j*-th step is $\bar{\varepsilon}_j = (\varepsilon_{j,1}, \cdots, \varepsilon_{j,N})^T$.

- Predict the observation vector $u_i(k+1)$, using Eqn. (3.3.4) based on the above predicted $\bar{d}_i(k+1)$.

Step-3: Compute the Kalman gain matrix

- $G(k+1) = P(k+1 \mid k) \cdot H(k+1)^T \left[H(k+1) \cdot P(k+1 \mid k) \cdot H(k+1)^T + \psi(k+1)\right]^{-1}$
  where $H(k+1) = \dfrac{\partial h[\cdot]}{\partial \bar{d}(k)}$ and $\psi(k+1) = \delta(k+1 \mid j) \cdot E\left\{\bar{\varepsilon}_{v,j} \bar{\varepsilon}_{v,k+1}^T\right\}$. The speed measurement error at the *k*-th step is $\bar{\varepsilon}_{v,k} = (\varepsilon_{v,1}, \cdots, \varepsilon_{v,N})^T$

Step-4: Estimation ($k+1 \mid k+1$)

- Update the state vector and its covariance matrix
- $\bar{d}_i(k+1 \mid k+1) = \bar{d}_i(k+1 \mid k) + G(k+1) \cdot \left[\bar{u}_i(k+1) - h_{k+1}\left[\bar{d}_i(k+1 \mid k)\right] \right]$
- $P(k+1 \mid k+1) = P(k+1, k) - G(k+1) \cdot H(k+1) \cdot P(k+1 \mid k)$

Step-5: Iterations

- Go to Step-2 and iterate the algorithm when the updated real time information is available.

3.3.4 Evaluation of the proposed estimation procedures

To evaluate the effectiveness of the proposed procedures for density estimation, this study has developed the following experimental method. In addition, the evaluation tasks are performed with two sets of density data obtained from the simulation and estimation methods. The procedures are summarized below.

- Step-1: Simulate the two target freeway segments (see Figure 3.2.1) with and without work-zone operations with CORSIM, and calibrate those simulation systems with actual field data;
- Step-2: Collect the traffic flow data (e.g., speed, flow, and density) at a time interval of 5 min. from the simulation outputs;
- Step-3: Apply the proposed estimation procedures to estimate the density data using volume and speed information from the simulation results; and
- Step-4: Compare the density data obtained from the simulation results with that estimated with the proposed procedures.

A detailed description of Step-1 and Step-4 is presented below.

i. Step-1: Simulation and Calibration

Traffic data used for calibrating the target simulated highway segment are the volumes, vehicle types (e.g., passenger car and truck), and speed information at a time interval of 5 min., which are obtained from the three locations (upstream, middle, and merge points) shown in Figure 3.3.1 (i.e., RTMS 1, 2, and 3, respectively) under non-work-zone and work-zone operations. Based on the actual work-zone configurations (see Figure 3.2.1), one can build up the two simulation systems with and without work-zone operations, and then adjust the simulation parameters to ensure that their output volume, vehicle types (e.g., passenger car and truck), and speed are consistent with those in the field data.

Table 3.3.1 shows the calibration results for the simulated highway segment without work-zone operations. The locations for data measurement are same as those of sensors shown in Figure 3.2.1. Figure 3.3.2 compares the actual downstream volume data with those obtained from the simulation before and after calibration.

Table 3.3.1 Calibration result from the simulated highway under non work-zone operations

Traffic conditions		Actual data	Simulation results	
			Before calibration	After calibration
Upstream volume (2 lanes)		1747 vphpl	1740 vphpl	1742 vphpl
Heavy truck percentage		12 %	12 %	12 %
Middle point*	Average speed	58.0 mph	57.0 mph	56.1 mph
	Volume	1709 vphpl	1740 vphpl	1700 vphpl
Merge point*	Average speed	43.0 mph	56.0 mph	42.3 mph
	Volume	1617 vphpl	1728 vphpl	1605 vphpl

(*) Note: Their locations are same as those under work-zone operations (see Figure 3.2.1. and Table 3.2.1)

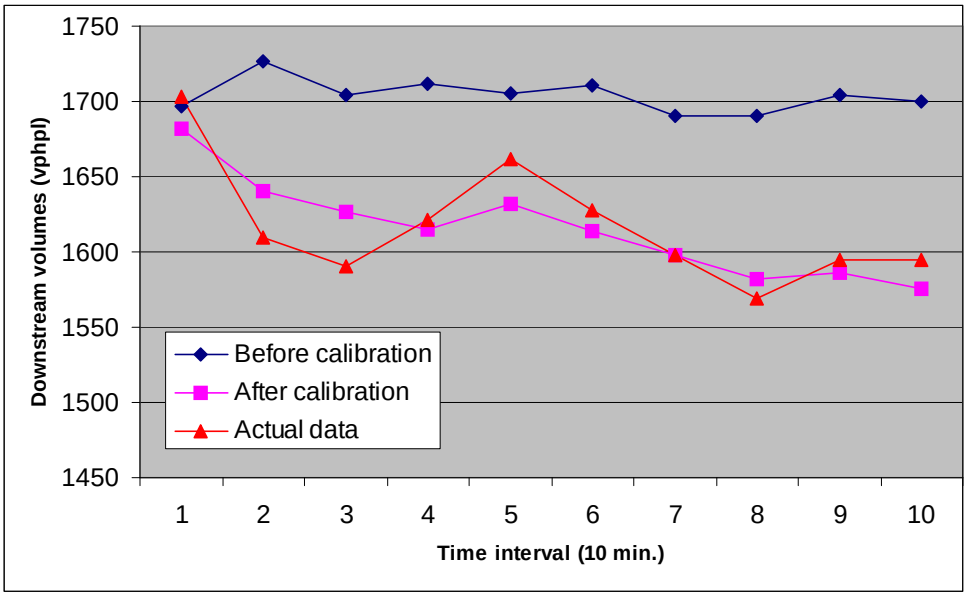

Figure 3.3.2 Comparison of downstream volume data under non work-zone operations

Table 3.3.2 presents the calibration results for the simulated highway work zone, based on the field observed traffic information. Figure 3.3.3 indicates that the calibrated simulation data reliably reflect the actual work-zone traffic conditions around the merge point.

Table 3.3.2 Calibration result from the simulated highway under work-zone operations

Traffic conditions		Actual data	Simulation results	
			Before calibration	After calibration
Upstream volume (2 lanes)		1875 vph	1890 vph	1893 vph
Heavy truck percentage		19 %	19 %	19 %
Middle point *	Average speed	31.0 mph	50.4 mph	34.3 mph
	Volume	1362 vphpl	1406 vphpl	1398 vphpl
Merge point*	Average speed	24.0 mph	46.0 mph	22.6 mph
	Work-zone throughput	1340 vphpl	1380 vphpl	1328 vphpl

(*) Note: Their locations are same as those under work-zone operations (see Figure 3.2.1. and Table 3.2.1)

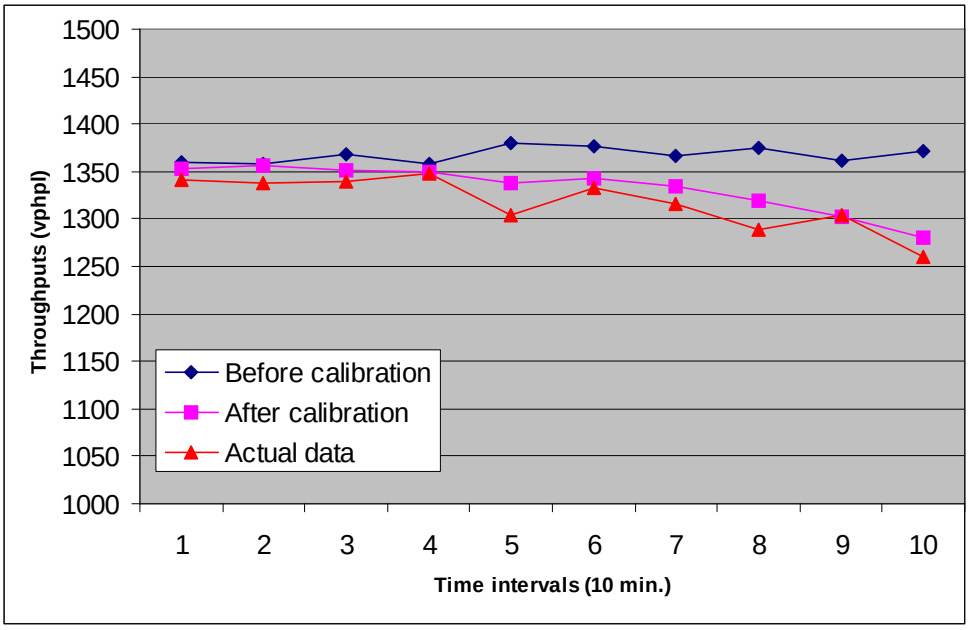

Figure 3.3.3 Comparison of work-zone throughputs under work-zone operations

ii. Step-4: Comparison of the estimated and simulation density data

Based on the above procedures, two kinds ($d_{s,i}$ and $d_{e,i}$) of density data were obtained from the simulation outputs and the proposed estimation algorithm. Figures 3.3.4 and 3.3.5 show comparisons of those two density data under non-work-zone and work-zone operations, respectively. In particular, they indicate that the proposed density estimation procedures well reflect the traffic conditions under either the congested or moderate state.

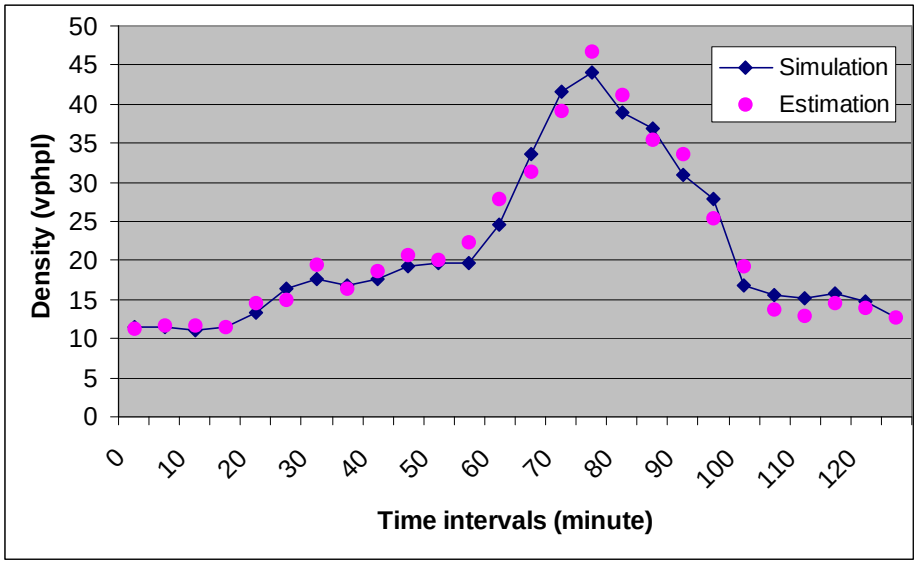

Figure 3.3.4 Comparison of the density data obtained from simulation and estimation under non work-zone operations

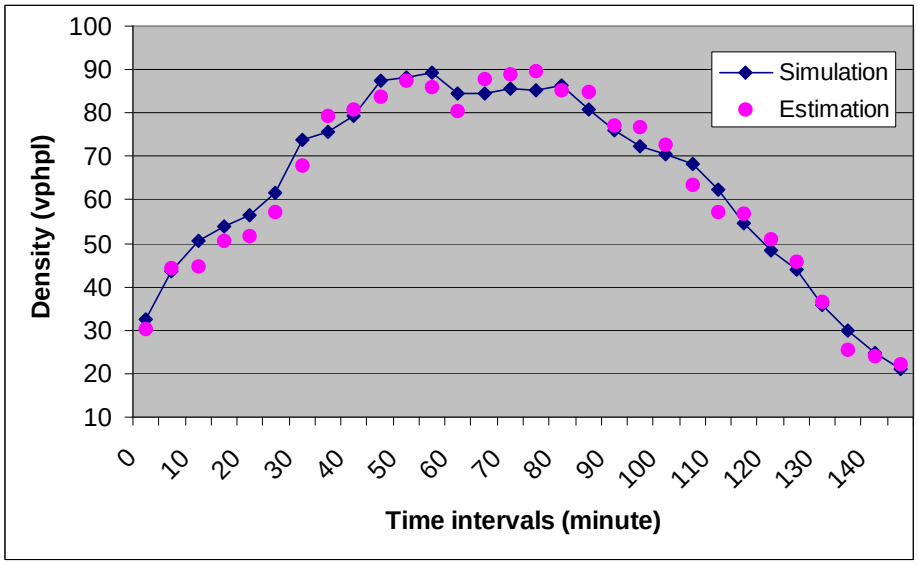

Figure 3.3.5 Comparison of the density data obtained from simulation and estimation under work-zone operations

To compare the density data ($d_{s,i}$ and $d_{e,i}$) statistically, the nonparametric (sign) test has been conducted since one cannot assume the normal distribution over the different time intervals (e.g., the observations over each interval, $i = \mathbf{1}, \cdots, n$). Based on the levels of the density, Table 3.3.3 shows the test results over 3 intervals (e.g., before (heavy) congestion, (heavy) congestion, and after (heavy) congestion). They indicate that

the average values ($\bar{\mu}_2$) of density data obtained from estimation are not different significantly from those ($\bar{\mu}_1$) from simulation over different time intervals. It is proved that the proposed density estimation procedure is available in terms of the accuracy even under the work-zone traffic conditions.

Table 3.3.3 Summary of the nonparametric test

	Intervals based on the levels of density	n	Average density		x	$P*$	Test* ($\alpha = \mathbf{0.05}$)
			$\bar{\mu}_1$	$\bar{\mu}_2$			
Non work-zone condition	Before congestion	8	13.7	13.9	3	0.727	$P > \mathbf{0.05}$ so, H_0 is not rejected.
	Congestion	9	28.8	30.0	2	0.180	
	After congestion	9	20.7	20.2	7	0.981	
Work-zone condition	Before heavy congestion	10	61.5	59.0	7	1.891	
	Heavy Congestion	10	83.3	84.4	4	0.754	
	After heavy congestion	10	45.9	45.1	4	0.754	

Note (*) $H_0 : \bar{\mu}_1 = \bar{\mu}_2$, $H_1 : \bar{\mu}_1 \neq \bar{\mu}_2$

x = binomial random variable (i.e., number of '+' sign in $d_{s,i} - d_{e,i}$ over each interval)

$P = 2P(X \leq x, p = \frac{1}{2}) = 2\sum_{x=0}^{x} b(x;\ n, \frac{1}{2})$ - Cumulative binomial distribution

3.4 Macroscopic traffic flow properties

With the estimated density data, one can plot the relations between flow and density to explore the differences from a macroscopic perspective between those two different traffic conditions. Figures 3.4.1 and 3.4.2 illustrate their relations without and with work-zone operations, respectively. It appears that Figure 3.4.1 is similar to an inverted 'U' relation, a general shape under stationary traffic conditions (Hall et al., 1992; Bank, 1989; Persaud, Hurdle, 1988; Adeli, Ghosh-Dastidar, 2004), while Figure 3.4.2 indicates a more complex shape such as synchronized traffic under non-stationary conditions (Adeli, Ghosh-Dastidar, 2004; Kerner, Rehborn, 1997; Kerner, Rehborn, 1996).

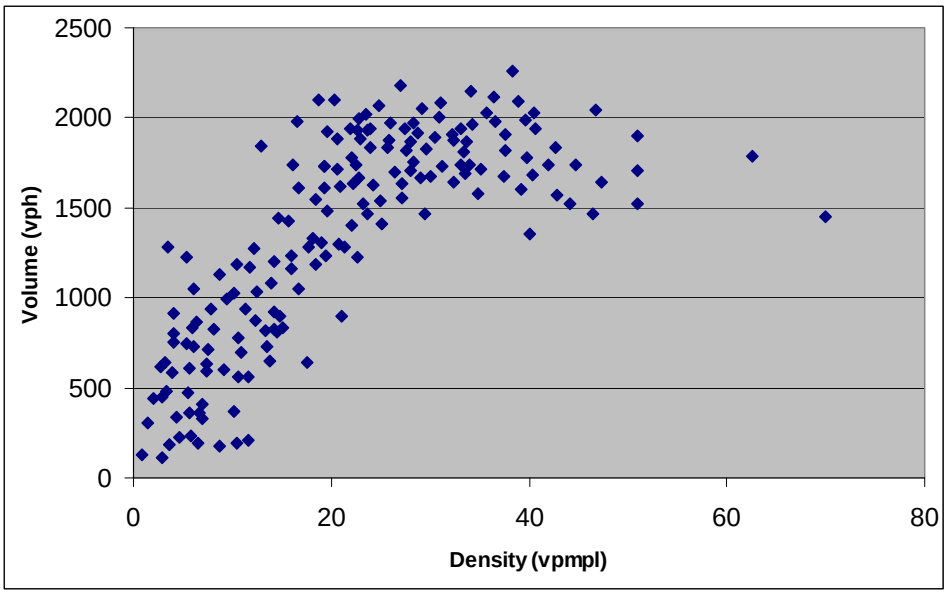

Figure 3.4.1 A relation between flow and density under non work-zone traffic condition (10/29/05)

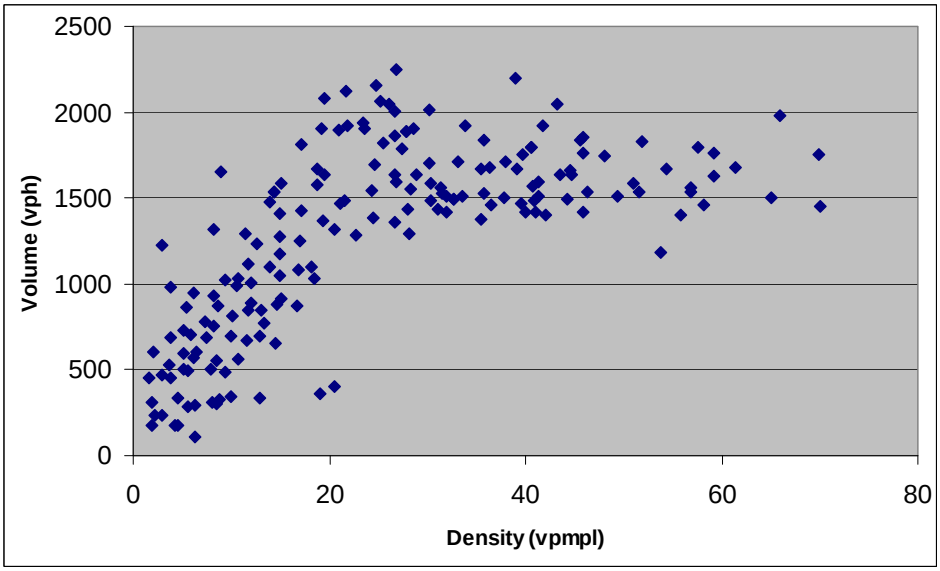

Figure 3.4.2 A relation between flow and density under work-zone traffic condition (11/07/05)

3.4.1 Non-work-zone (stationary) traffic condition

It should again be mentioned that the target work-zone area is a highway segment without ramps and lane-drop to affect the traffic flow capacity. Thus, one can assume that only work-zone activities have some impacts on the traffic condition.

i. Model estimation for the flow and density relation

For the inverted 'U' shape of the flow (q) and density (d), the following expressions have been reported in the literature (Hall et al., 1992; Bank, 1989; Berg et al., 2000).

$$q = a_1 d + a_2 d^2 \tag{3.4.1}$$

$$q = A_1 d + A_2 d^2 + A_3 d^3 + A_4 d^4 \tag{3.4.2}$$

Tables 3.4.1 and 3.4.2 summarize the estimation results of Eqns. (3.4.1) and (3.4.2), respectively, for those 4 days under normal traffic conditions. To investigate traffic flow properties on the upstream subsegments, this study has performed the model estimation for the following two locations: 'Upstream-1' around the 2nd PCMS and 'Upstream-2' around the 4th PCMS (see Figure 3.2.1).

Table 3.4.1 Model estimations using Eqn. (3.4.1) under non work-zone traffic conditions

Dates (2003)		Coefficients (t-values, $t_{0.05} = 1.645$)		Correlation coefficient, R^2
		a_1	a_2	
10/29	Upstream-1	95.06 (39.59)	-1.1759 (-18.00)	0.81
	Upstream-2	113.84 (35.60)	-1.8404 (-19.31)	0.86
10/30	Upstream-1	91.34 (36.15)	-1.1122 (-17.63)	0.87
	Upstream-2	102.67 (32.79)	-1.2857 (-16.85)	0.85
11/04	Upstream-1	104.62 (37.74)	-1.3949 (-19.33)	0.80
	Upstream-2	103.84 (32.51)	-1.3978 (-17.84)	0.80
11/05	Upstream-1	100.14 (36.93)	-1.2899 (-18.06)	0.84
	Upstream-2	94.088 (27.15)	-1.2581 (-13.90)	0.74

Table 3.4.2 Model estimations using Eqn. (3.4.2) under non work-zone traffic conditions

Dates (2003)		Coefficients (t-values, $t_{0.05} = 1.645$)				Correlation coefficient, R^2
		A_1	A_2	A_3	A_4	
10/29	Upstream-1	79.57 (7.13)	0.7632 (0.77)	-0.0644 (-2.42)	0.594e-3 (2.76)	0.84
	Upstream-2	160.77 (11.94)	-6.4292 (-4.01)	0.1261 (2.16)	-0.102e-e (-1.56)	0.88
10/30	Upstream-1	68.25 (5.63)	1.1689 (1.16)	-0.0650 (-2.53)	0.552e-3 (2.73)	0.89
	Upstream-2	149.74 (14.05)	-5.1262 (-5.16)	0.0858 (3.16)	-0.555e-3 (-2.51)	0.87
11/04	Upstream-1	121.85 (10.62)	-2.0151 (-2.02)	-0.605e-2 (-0.23)	0.206e-3 (0.97)	0.83
	Upstream-2	156.33 (12.80)	-5.6881 (-4.89)	0.0979 (2.93)	-0.656e-3 (-2.23)	0.90
11/05	Upstream-1	111.71 (9.19)	-1.6276 (-1.57)	-0.766e-2 (-0.28)	0.177e-3 (0.82)	0.88
	Upstream-2	133.515 (10.2621)	-3.9177 (-3.2537)	0.047747 (1.4035)	-0.189e-3 (0.6405)	0.76

Based on their statistical significance (i.e., t-values and R^2), it seems that all estimated flow-density relations fit the quadratic model structure well. However, Eqn. (3.4.2) with additional parameters do not show any significant improvement on the model's goodness of fit. Since some of the signs and parameters in Eqn. (3.4.2) are also not significant, this study adopts the model estimated with Eqn. (3.4.1) for representing the flow-density relation under normal traffic operations. Figures 3.4.3 and 3.4.4 represent examples of goodness-of-fits for models estimated in the Upstream-1 and Upstream-2 subsegments, respectively, on the day of 10/30/2003.

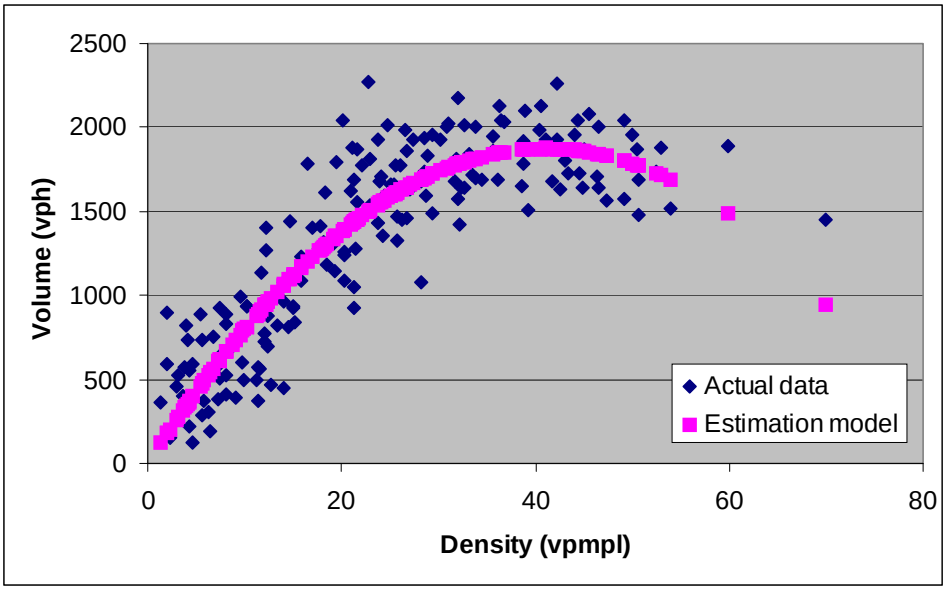

Figure 3.4.3 Goodness-of-fit for the estimation model with the Upstream-1 data (10/30/2003)

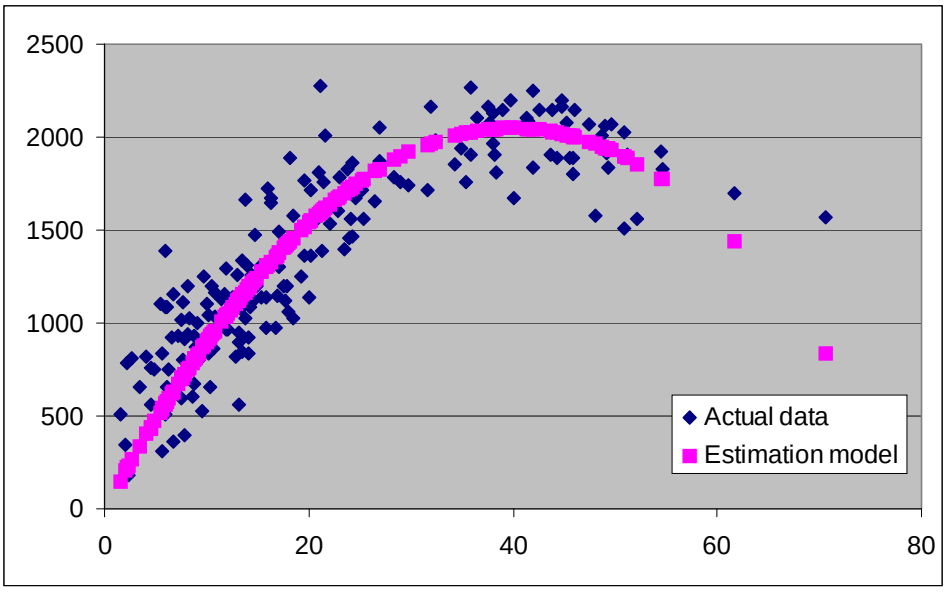

Figure 3.4.4 Goodness-of-fit for the estimation model with the Upstream-2 data (10/30/2003)

ii. Model stability analysis

As shown in Tables 3.4.3 and 3.4.4, those calibrated models with datasets from different days under the Chow-F stability test reveal the following results:

- Most models from the Upstream-2 observations show significant discrepancy among them, but those from the Upstream-1 observations exhibit quite similar parameters (see Table 3.4.3). Such test results may be understandable due to the

fact that although the work zone was not yet under operation, its static warning signs deployed at the shoulder (i.e., around Upstream-1) may have impacts on the approaching drivers and reflect on the day-to-day evolution of traffic conditions;

- The models calibrated from the two upstream subsegments on the same day (see Table 3.4.4), as expected, show the desirable statistical stability under stationary traffic conditions regardless of the locations.

Table 3.4.3 Chow test results from two dates under non work-zone traffic conditions

Dates (2003)		F^*** $v_1 = 2, v_2 = 176 + 176 - 2*2 = 348$		Test results *** ($F_{0.05} = 3.00$)	
Model 1*	Model 2*	Upstream-1	Upstream-2	Upstream-1	Upstream-2
10/29	10/30	0.737	13.219	Accept	Reject
10/29	11/04	2.201	7.144	Accept	Reject
10/29	11/05	1.284	8.775	Accept	Reject
10/30	11/04	2.413	2.237	Accept	Accept
10/30	11/05	0.748	12.551	Accept	Reject
11/04	11/05	4.812	5.081	Reject	Reject

Note: (*) Model 1: $\overline{Y}_1 = \overline{\alpha}_0 + \overline{\alpha}_1 X_1 + \overline{\alpha}_2 X_2$, Model 2: $\overline{Y}_2 = \overline{\beta}_0 + \overline{\beta}_1 X_1 + \overline{\beta}_2 X_2$

Pooled model: $\overline{Y}_p = \overline{a}_0 + \overline{a}_1 X_1 + \overline{a}_2 X_2$

(**) $F^* = \dfrac{\left[\sum e_p^2 - \left(\sum e_1^2 + \sum e_2^3\right)\right]/K}{\left(\sum e_1^2 + \sum e_2^2\right)/(n_1 + n_2 - 2K)}$

(***) $H_0 : \overline{\alpha}_i = \overline{\beta}_i$, $H_1 : \overline{\alpha}_i \neq \overline{\beta}_i$

Table 3.4.4 Chow test results from two subsegments under non work-zone traffic conditions

Dates (2003)		Subsegments	F^* $v_1 = 2, v_2 = 176 + 176 - 2*2 = 348$	Test results ($F_{0.05} = 3.00$)
10/29	Model 1	Upstream-1	0.364	Accept
	Model 2	Upstream-2		
10/30	Model 1	Upstream-1	0.047	Accept
	Model 2	Upstream-2		
11/04	Model 1	Upstream-1	0.684	Accept
	Model 2	Upstream-2		
11/05	Model 1	Upstream-1	1.897	Accept
	Model 2	Upstream-2		

3.4.2 Work-zone (non-stationary) traffic condition

As reported in the literature, the flow-density relation in non-stationary traffic flows has the following distinctive properties:

- Due to the existence of "synchronized traffic (ST)" and its random interferences, it may be difficult to use a simple relation to include all possible states (e.g., free

flow, ST, and traffic jam) (Adeli, Ghosh-Dastidar, 2004; Kerner, Rehborn 1997; Kerner, Rehborn, 1996; Hall F. L., Hall L. M., 1990).

- As reflected in Figure 3.4.2, however, one may assume that the plot between flow and density includes such ST flow patterns (e.g., queue discharge flow) after free flow and before jam states, and its horizontal regime may belong to one of the three subtypes of ST, i.e., both flow and speed remain nearly constant over a long time interval (Adeli, Ghosh-Dastidar, 2004; Kerner Rehborn, 1997).

i. Model estimation for the flow and density relation

Hence, one can explore such relations with the following formulations between flow (q) and density (d).

$$q = b_0 - \exp(b_1 + b_2 d + b_3 d^2 + b_4 d^3) \tag{3.4.3}$$

$$q = b_0\left(1 - \frac{1}{1 + b_1 d}\right) \tag{3.4.4}$$

where b_0 is capacity.

Note that most estimation results using the transformed log function of Eqn. (3.4.3) show that the second parameter, b_2 was not statistically significant. Thus, the following revised formulation, Eqn. (3.4.5), is used in the model estimation.

$$q = b_0 - \exp(b_1 + b_3 d^2 + b_4 d^3) \tag{3.4.5}$$

Table 3.4.5 reports the estimation results based on the data collected from the Upstream-1 and Upstream-2 subsegments over 4 days under work-zone operations. All these 8 models seem to yield reasonably well fit of the flow and density relation.

Table 3.4.5 Model estimations using Eqn. (3.4.5) under work-zone operations

Dates (2003)		Coefficients (t-values, $t_{0.05} = 1.645$)				Correlation coefficient, R^2
		b_0	b_1	b_3	b_4	
10/22	Upstream-1	1662	7.42 (85.83)	-0.549E-2 (-10.26)	0.699E-4 (8.28)	0.85
	Upstream-2	1481	7.30 (242.35)	-0.175E-2 (-13.46)	0.197E-4 (11.30)	0.89
10/23	Upstream-1	1663	7.42 (61.43)	-0.662E-2 (-8.48)	0.800E-4 (6.76)	0.80
	Upstream-2	1402	7.25 (135.83)	-0.235E-2 (-10.33)	0.240E-4 (8.90)	0.88
11/07	Upstream-1	1621	7.39 (47.92)	-0.790E-2 (-5.06)	0.998E-4 (3.73)	0.74
	Upstream-2	1410	7.25 (136.88)	-0.217E-2 (-9.94)	0.236E-4 (8.39)	0.87
11/10	Upstream-1	1610	7.38 (68.49)	-0.670E-2 (-7.14)	0.893E-4 (5.83)	0.83
	Upstream-2	1417	7.25 (181.80)	-0.551E-2 (-11.06)	0.582E-4 (9.23)	0.88

Table 3.4.6 summarizes the model estimation results with the data from the Upstream-1 and Upstream-2 subsegments using Eqn. (3.4.4). Notably, the overall goodness of fit with Eqn. (3.4.4) is not as high as that with Eqn. (3.4.5). Thus, those models estimated with Eqn. (3.4.5) are selected for analyzing traffic flow characteristics under the work-zone operations.

Table 3.4.6 Model estimations using Eqn. (3.4.4) under work-zone operations

Dates (2003)		Coefficients (t-values, $t_{0.05} = 1.645$)		Correlation coefficient, R^2
		b_0	b_1	
10/22	Upstream-1	1802	0.1379 (11.88)	0.76
	Upstream-2	1590	0.1669 (13.46)	0.75
10/23	Upstream-1	1668	0.1437 (9.97)	0.74
	Upstream-2	1450	0.1246 (13.75)	0.75
11/07	Upstream-1	1780	0.1559 (14.71)	0.66
	Upstream-2	1525	0.1468 (17.96)	0.75
11/10	Upstream-1	1809	0.1732 (9.77)	0.72
	Upstream-2	1492	0.1891 (13.45)	0.71

Figures 3.4.5 and 3.4.6 present the relations between the simulated and estimated density-flow at those two subsegments, respectively. Both seem to well reflect the

impacts of synchronized traffic flows on the upstream subsegments prior to the work-zone area.

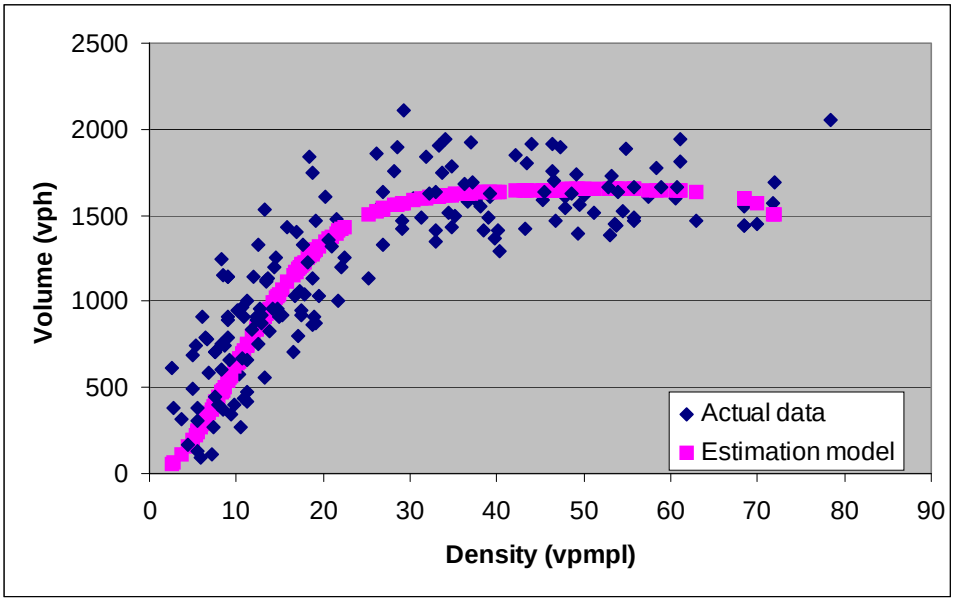

Figure 3.4.5 Goodness-of-fit for the estimation model with the Upstream-1 data (10/22/2003)

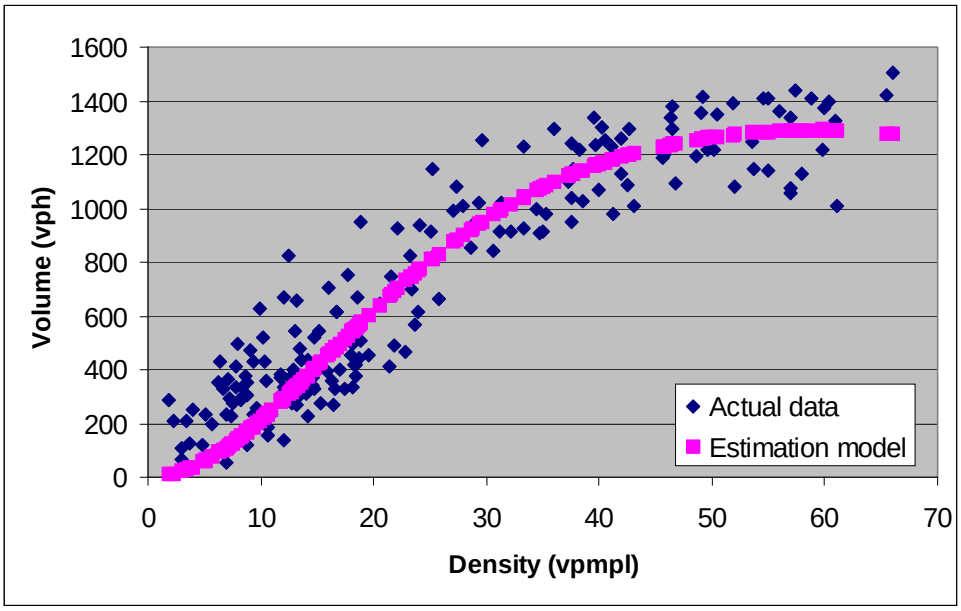

Figure 3.4.6 Goodness-of-fit for the estimation model with the Upstream-2 data (10/22/2003)

ii. Model stability analysis

To ensure the stability of the estimated models, the Chow *F*-test was again implemented to evaluate the following hypotheses:

- The flow – density relation is different significantly on each day, depending on the levels of work-zone traffic conditions; and
- The flow – density relation may also vary with its distance to the work-zone, and the queue discharge flows (e.g., Upstream-1 and Upstream-2).

The statistical results, as reported in Table 3.4.7 and 3.4.8, seem to confirm the above hypotheses that:

- All models from the Upstream-2 observations show differences in their coefficients, but those from the Upstream-1 observations, as expected, exhibit statistically similar results (see Table 3.4.7). This is due to the fact that traffic flow evolutions in the Uptream-2 subsegment shows more fluctuating patterns than those in the Upstream-1 subsegment on the day-to-day evolution of traffic conditions; and
- A comparison of models from the two different subsegments (Table 3.4.8) shows that their parameters are different statistically.

Table 3.4.7 Chow test results from two different dates under work-zone operations

Dates (2003)		F^* $v_1 = 4, v_2 = 180 + 180 - 2*4 = 352$		Test results ($F_{0.05} = 2.37$)	
Model 1	Model 2	Upstream-1	Upstream-2	Upstream-1	Upstream-2
10/29	10/30	2.191	-14.894	Accept	Reject
10/29	11/04	-0.348	-5.884	Accept	Reject
10/29	11/05	8.089	17.722	Reject	Reject
10/30	11/04	-0.770	4.091	Accept	Reject
10/30	11/05	-1.963	-7.684	Accept	Reject
11/04	11/05	26.193	-27.567	Reject	Reject

Table 3.4.8 Chow test results from two subsegments under work-zone operations

Dates (2003)		Subsegments	F^* ($v_1 = 2, v_2 = 180 + 180 - 2*4 = 352$)	Test results ($F_{0.05} = 2.37$)
10/29	Model 1	Upstream-1	48.993	Reject
	Model 2	Upstream-2		
10/30	Model 1	Upstream-1	35.373	Reject
	Model 2	Upstream-2		
11/04	Model 1	Upstream-1	90.942	Reject
	Model 2	Upstream-2		
11/05	Model 1	Upstream-1	53.132	Reject
	Model 2	Upstream-2		

3.5 Conclusions

As mentioned in Section 3.1, most existing models for the congested traffic flow were calibrated with recurrently congested traffic data (e.g., on- and off-ramps and lane-drops), but not under complex work-zone traffic flow conditions.

This chapter has estimated a set of statistical models for the flow-density relation, which serves as a tool for investigating the traffic flow properties under the work-zone operations. Those models can be useful in studying the following issues:

- Estimating the mean density data and predicting its evolution on the upstream subsegments of the work-zone area;
- Evaluating the level of service (LOS) for work-zone traffic quality, since these two parameters can directly reflect the traffic conditions;
- Selecting control thresholds (e.g., maximum traffic flow, the optimal density, and the maximum jam density), when employing the existing static and conventional speed and merge control strategies for work-zone operations; and
- Applying their mathematical forms in solving the optimization control formulation.

In addition, one can conclude that the significant differences in traffic flow characteristics between normal traffic states and work-zone traffic operations should be taken into account in design of advanced highway work-zone operations. More specifically, any proposed work-zone control strategy should reflect the evolution of those traffic properties over the entire segment affected by the work-zone operation. In terms of improving safety and efficiency, the results from this chapter indicate that any control strategy for highway work-zone operations should realistically capture the complex interactions between evolution of traffic queues, the approaching flow rates, merging activities between lanes, and the capacity reduction due to lane-closure operations.

CHAPTER 4 . DEVELOPMENT OF AN ADVNACED DYNAMIC LATE MERGE CONTROL MODEL AND ALGORITHM

4.1 Overview of merge control strategies

Over the past several decades, traffic researchers and engineers have proposed a variety of merge control methods to contend with congestion and safety related issues in highway work zones. For examples, the following merge controls have been implemented or tested in practice: the conventional merge (Walters et al., 2000; McCoy et al., 1999), the static early and late merges (Beacher et al., 2005a; Beacher et al., 2005b; Pesti, 1999), and the dynamic early merge (Datta et al., 2004; Tarko, Venugopal, 2001; Tarko, 1998).

The performance of those control strategies with respect to traffic efficiency and safety, however, remains to be improved, especially in contending with highly fluctuating traffic demand. An extensive review of existing static merge control strategies has revealed the following vital information:

- Static early merge (SEM) controls generally yield the best performance with respect to traffic safety, such as smooth merging operations under the free and moderate traffic conditions, as most vehicles have already merged onto the open lane at the upstream of the merge point;
- Static late merge (SLM) strategies tend to outperform any early merge control in terms of maximizing throughputs and reducing travel time as well as delay, especially under congested traffic conditions;
- The main potential merit of both merge controls lies in their effective use of the available capacities of the open and closed lanes, if some rules for guiding merging actions can be established between drivers in the closed and open lanes; and
- Since SEM and SLM are effective under the “free and moderate” and “congested” traffic conditions, respectively, how to select the optimal thresholds for their implementations has emerged as a critical issue.

To take full advantage of both strategies, traffic researchers have recently proposed a dynamic late merge (DLM) control method (McCoy, Pesti, 2001) that intends to integrate the strengths of those two distinct merge controls, and offers the flexibility to effectively respond to the time-varying traffic demand.

The core concept of the DLM control strategy is to dynamically direct drivers’ merging maneuvers, based on detected traffic conditions and the proper control thresholds. For example, when the traffic data were detected to exceed the specified threshold (i.e., congestion level), the DLM control will function similarly to the SLM control and display their merging messages (e.g., “USE BOTH LANES” / “TO MERGE POINT”) at proper upstream locations (see Figure 4.1.1). During the uncongested period, the DLM will be at the inactive state, and essentially perform like the conventional merge

or SEM control (e.g., “RIGHT/LEFT LANE CLOSED” or “MERGE HERE”) (see Figure 4.1.2).

Figure 4.1.1 Merging behavior prior to the merge point under the congested traffic condition (e.g., SLM)

Figure 4.1.2 Merging behavior prior to the merge point under the non-congested traffic condition (e.g., SEM)

Recently, several states have conducted initial field tests (Chang, Kang, 2005; Taavola et al., 2004) and experimental simulation (Meyer, 2004) to demonstrate the performance of their DLM systems, based on a simple operation algorithm (see Table 4.1.1). Although some DLM systems (Chang, Kang, 2005; Meyer, 2004) seem to

outperform the conventional merge controls, their field experimental operations have revealed the following critical issues to be addressed:

- Despite the clear display of merging messages, most drivers during the field implementation period were not willing to follow the instructions due to a variety of factors; and
- How to select the proper control variables for the DLM operations and determine their appropriate thresholds under the time-varying traffic conditions? (also see Table 4.1.1).

Table 4.1.1 Control thresholds used in the current DLM controls

	Maryland (Chang, Kang, 2005)		Minnesota (Taavola et al., 2004)		Kansas (Meyer, 2004)	
WZ-type	2-1 Type *		2-1 Type		3-1 Type	
Parameter	Occupancy		Speed	Volume	Speed	
Operation	Activation	Deactivation	Activation	Deactivation	Activation	Deactivation
Control threshold	Any sensor > 15%	All sensors < 5%	Sensor < 30mph	not clear	Upstream < 35mph (Lane 2)	Upstream > 40mph (Lane 2)
					Upstream < 46mph (All lanes)	Upstream > 51mph (All lanes)
Field Test	Yes		Yes		with Simulation	

Note (*): 2-1 type means one lane closure of 2 mainline highway segment

In response to those critical issues, this chapter presents a new DLM control model and its operational algorithm, based on the optimal control thresholds. This chapter is organized as follows. The methodology for determining the set of optimal thresholds is presented first, followed by a description of the operation algorithm in Section 4.2. Based on the defined optimal thresholds, the operation process for the proposed DLM control model is developed in Section 4.3. Simulation experiments for evaluating the performance of the proposed control model are reported in Section 4.4. Finally, research results and on-going studies are summarized in Section 4.5.

4.2 Methodology for the DLM control model

Among those critical issues identified in the DLM operations, the study is focused mainly on how to select the control variables and to determine their thresholds in response to traffic flow dynamics.

4.2.1 Investigation on SEM and SLM controls

To assess if the traffic state is suitable for SEM or SLM control, it is essential to examine the operational features of these two merge controls (see Figure 4.2.1 and Table 4.2.1).

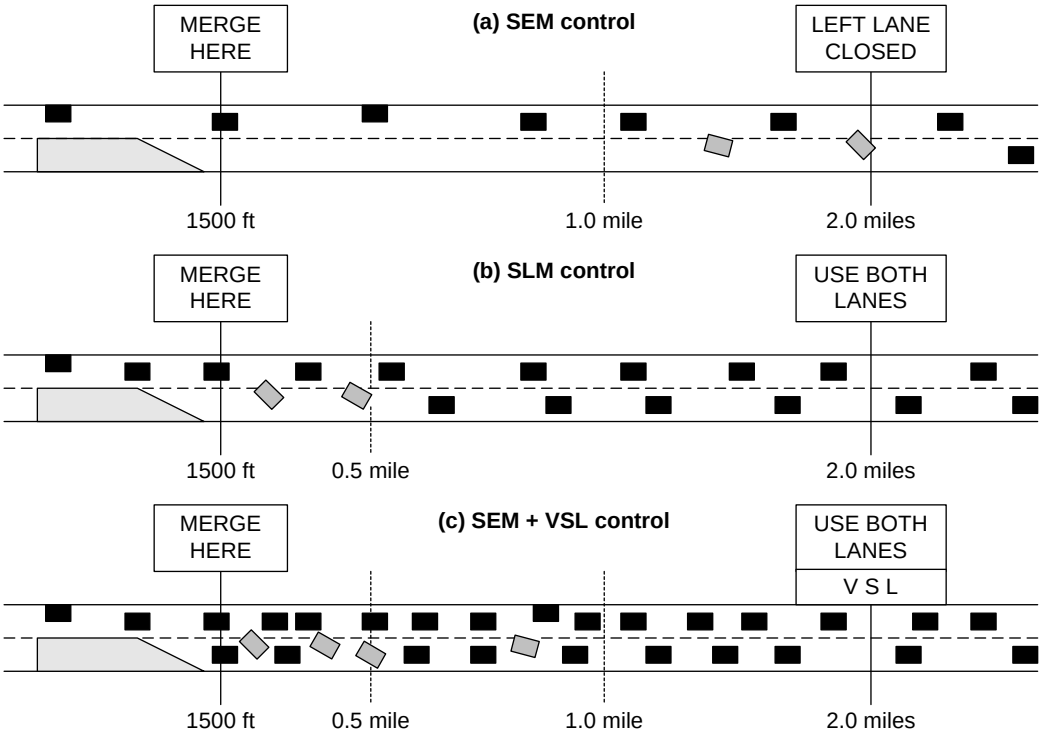

Figure 4.2.1 Illustrations of SEM., SLM, and SLM + α controls

Table 4.2.1 Characteristics of SEM and SLM controls

Merge controls	System operations and traffic conditions
SEM control (see Figure 4.2.1a)	• The purpose is to minimize the speed variations resulted from lane-changing and merging conflicts, by making drivers merge early over the upstream segment, before reaching the merge point. • Drivers should merge into the open lane at the farthest upstream segment (e.g., 2.0 ~ 3.0 miles), and their merging actions should be completed approximately 1.0 mile in advance of the merge point. • It can prevent potential traffic accidents and merging conflicts of speedy drivers between the open and closed lanes at the merge point. • Its effectiveness decreases as the volume increases.
SLM control (see Figure 4.2.1b)	• The purpose is to increase the work-zone throughput by maximizing the use of the closed lane and making drivers merge around the merge point. • Drivers use both lanes until approaching the merge point (e.g., 1000 ~ 1500 ft). • It results in restricted merging maneuvers and a limited merging space (e.g., within 0.5 mile). • The open lane should provide vehicles on the closed lane with a reserved (but, limited) space to merge into the open lane around the merge point. • It can increase the throughputs by alternative merge actions between the open and closed lanes. • As traffic condition becomes heavily congested, the effectiveness of such control will decrease.

SLM+α control (see Figure 4.2.1c)	• The merge control is basically SLM. • Any additional control is needed when the effectiveness of SLM decreases due to continuously increased upstream traffic flows. • It is necessary to reduce the traffic flow rates with the advanced speed control (e.g., VSL: Variable Speed Limit) at the upstream segment.

4.2.2 Concept of the optimal control thresholds

In review of operation characteristics and traffic conditions of SEM and SLM controls, it is clear that each of these two controls has its most applicable traffic conditions. Hence, the best DLM system is to activate one of these two merge controls, based on the optimal control thresholds computed from observed traffic conditions.

Figure 4.2.2 illustrates these two control thresholds (i.e., CT 1 and CT 2), which are the criteria for the system to select the SEM, SLM, or SLM+α control, based on their relation with the detected traffic states. Each of these criteria is briefly discussed below.

- CT 1 should reflect the traffic state that remains at free or moderate flow condition, where drivers on the open lane are nearly unimpeded (e.g., no significant speed changes) to change from the closed to the open lanes when the DLM system activates the SEM control.
- CT 2 should indicate the boundary of the congested traffic state in a work zone, beyond which the open lane cannot provide sufficient merging space for vehicles on the closed lane to merge into the open lane under the DLM operation. Thus, some other control measures such as speed control to the approaching flows will be needed.

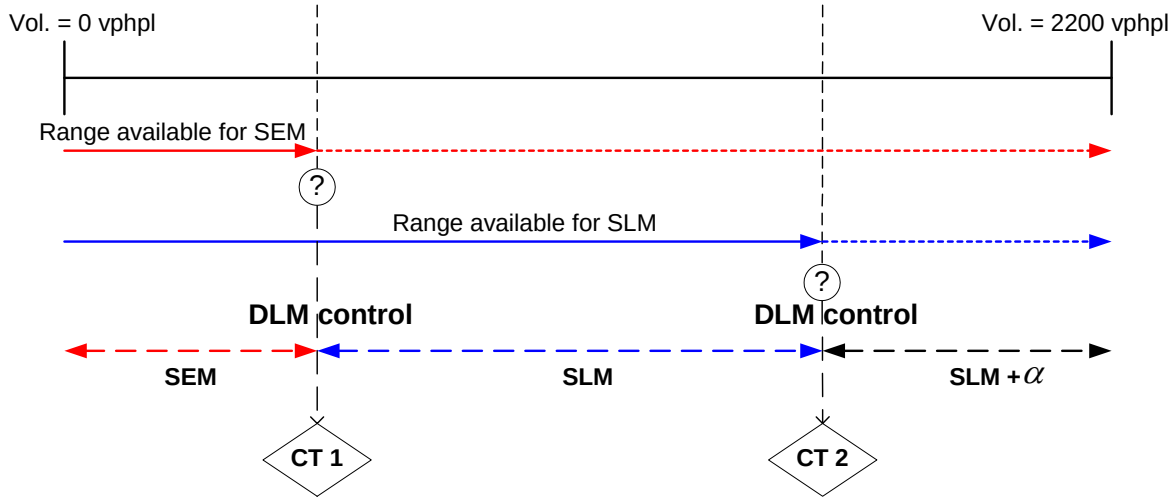

Figure 4.2.2 Concept of the optimal control thresholds (CT 1 and CT 2)

Depending on the time-varying traffic conditions, to maximize the effectiveness of both merge controls (i.e., SEM and SLM), the proposed DLM system should be capable of computing the optimal thresholds (i.e., CT 1 and CT 2). This study selects the maximization of the throughputs as the control objective.

4.2.3 Key variables and parameters

For convenience of model formulation, the presentation hereafter has divided the continuous time duration into discrete intervals and the highway work-zone segment into discrete subsegments. A graphical illustration of key variables reflecting the traffic conditions on each subsegment and open (and closed) lane is shown in Figure 4.2.3, and their definitions are concisely presented in Table 4.2.2.

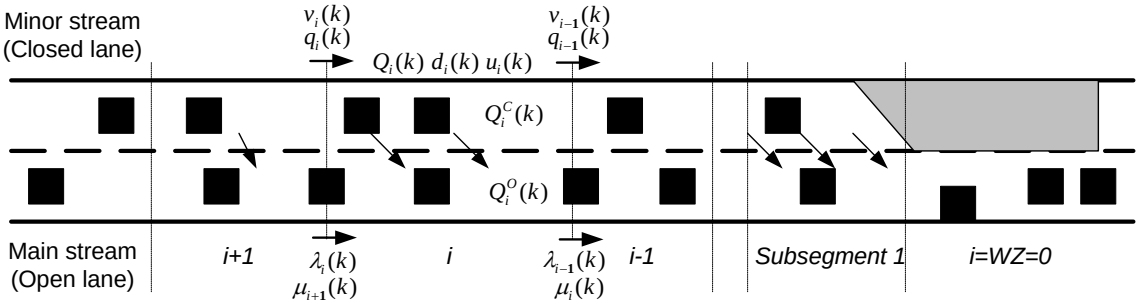

Figure 4.2.3 Traffic variables for the DLM control model under a typical work zone

Table 4.2.2 Definitions of key variables

- Control time interval and subsegment index
  - T : Unit time interval for control operations (e.g., 1 min, 5 min, 10min, etc.)
  - k : Time interval index
  - i : Subsegment index ($i = 1 \cdots N$)
- Network geometric and physical data
  - l_i : Length of subsegment *i* on the open or closed lane
  - n_i : Number of lanes in subsegment *i* on the open or closed lane
- Traffic volumes and speeds
  - $q_i(k)$: Detected traffic volume entering subsegment *i* from subsegment *i+1* during interval *k*
  - $v_i(k)$: Detected speed of $q_i(k)$ in subsegment *i* during interval k
- Model parameters
  - $\omega_i(k)$: Average speed weight factor in subsegment *i* during interval k
  - $\eta_i(k)$: Lane-changing probability in subsegment *i* during interval k

Table 4.2.3 Definitions of key variables (Cont.)

- Decision variables
  - $Q^{O}_{i,MOD}(k)$: Moderate flow rate (MOD) in subsegment i on the open lane during interval k
  - $Q^{C}_{i,OMC}(k)$: Optimal merging capacity (OMC) in subsegment i on the closed lane during interval k
- State variables
  - $d_i(k)$: Mean traffic density in subsegment i on the open or closed lane during interval k
  - $d_i^j(k)$: Jam (maximum) traffic density in subsegment i on the open or closed lane during interval k
  - $u_i(k)$: Mean speed in subsegment i on the open or closed lane during interval k
  - $u_i^f(k)$: Free flow (boundary) speed in subsegment i on the open or closed lane during interval k
  - $Q_i(k)$: Potential flow rate in subsegment i on the open or closed lane during interval k
  - $Q^{O}_{i,MFR}(k)$: Maximum flow rate (MFR) in subsegment i on the open lane during interval k

4.2.4 Optimal control thresholds and DLM operational logic

To capture the interrelations between the proposed control thresholds and actual traffic flow patterns and merge maneuvers, this study has defined one state variable $Q^{O}_{i,MFR}(k)$ and the following two decision variables: $Q^{O}_{i,MOD}(k)$ and $Q^{C}_{i,OMC}(k)$, corresponding respectively to those two control thresholds (i.e., CT 1 and CT 2). A graphical illustration of these variables is shown in Figure 4.2.4, where:

- $Q^{O}_{i,MOD}(k)$ (Moderate flow rate, MOD), which denotes the optimal flow rate on the open lane that can carry flow rates of both lanes and achieve the maximal total throughputs under the moderate traffic state (see Figure 4.2.4a). This variable is defined mainly to make the selection between the SEM and SLM controls.
- $Q^{C}_{i,OMC}(k)$ (Optimal merging capacity, OMC), which is defined as the optimal level of flow rate on the closed lane that can be merged onto the open lane, in order to achieve the maximal work-zone throughput under the congested traffic state (See Figure 4.2.4b). This variable is used mainly to determine if any additional control (e.g., SLM+α) to SLM is needed or not.
- $Q^{O}_{i,MFR}(k)$ (Maximum flow rate, MFR), which reflects the max. number of vehicles that the open lane can accommodate, including those merging from the closed lane, without causing severe queue spillback (See Figure 4.2.4b). This

variable is defined for computing the maximum throughputs over all upstream subsegments.

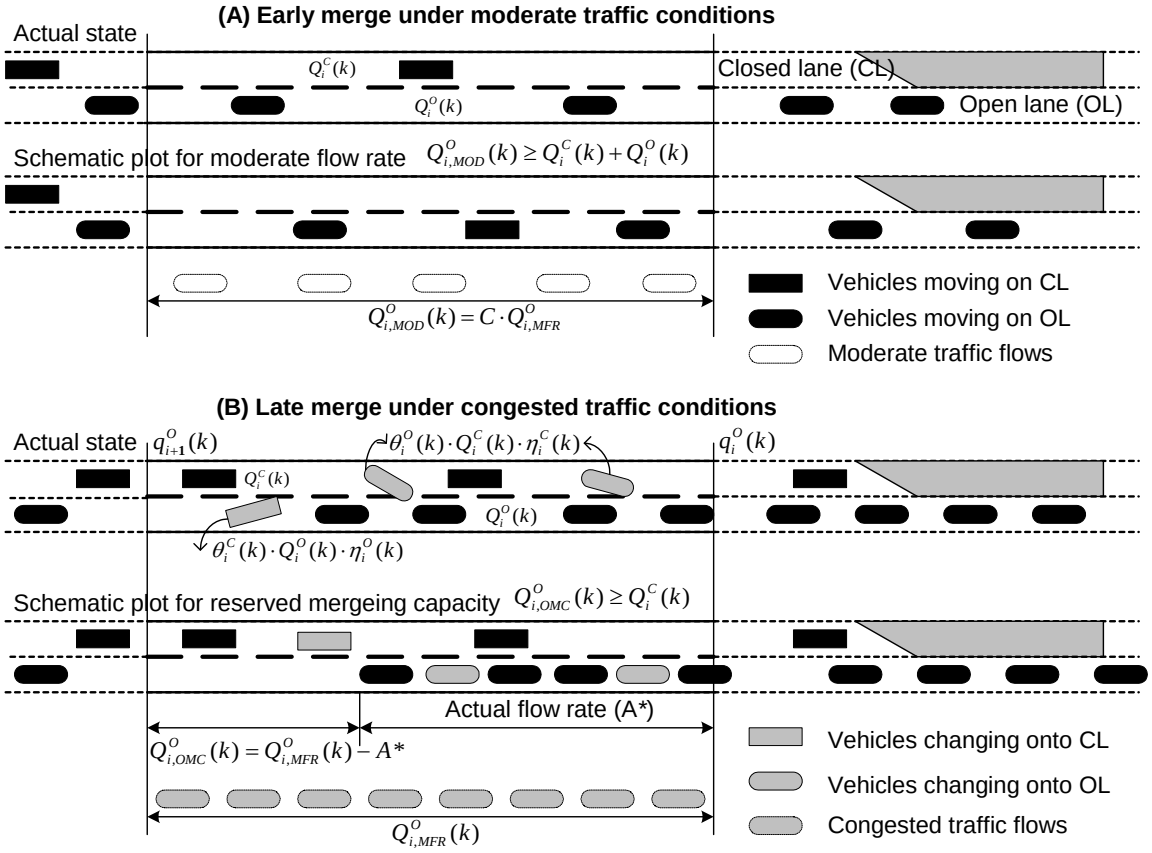

Figure 4.2.4 Illustration of control thresholds

Using the above thresholds, the core logic of the proposed integrated control is summarized below along with the graphical illustration (See Figure 4.2.5):

- As shown in Figure 4.2.5, the traffic conditions under the DLM control model can be divided into three states: Moderate, Congested, and Heavily Congested traffic conditions.
- If the sum of the average flow rates on both lanes at the current traffic state is lower than MOD, $Q_{i,MOD}^O(k)$ on the open lane, then the traffic condition is under the moderate state and one shall activate the proposed DLM model with the early merge (SEM) control mode. Otherwise, it reflects a congested traffic state, and the DLM model should be activated with the late merge (SLM) control mode until OMC, $Q_{i,OMC}^C(k)$ on the closed lane is greater than the average flow rate on the closed lane.
- Under the heavily congested traffic state (i.e., $Q_{i,OMC}^C(k)$ is less than the average flow rate on the closed lane) where the approaching volume has far exceeded the

allowable maximum flow rate on the open lane(s), one shall retain the late merge control mode, but inform the drivers in advance of traffic jam and alert them the need to exercise merging and lane-changing maneuvers. Under such a severe congestion state, one needs to implement the advanced speed control (e.g., VSL control) along with the DLM operation to reduce the approaching vehicles' speeds and flow rates (also see Figure 4.2.1c).

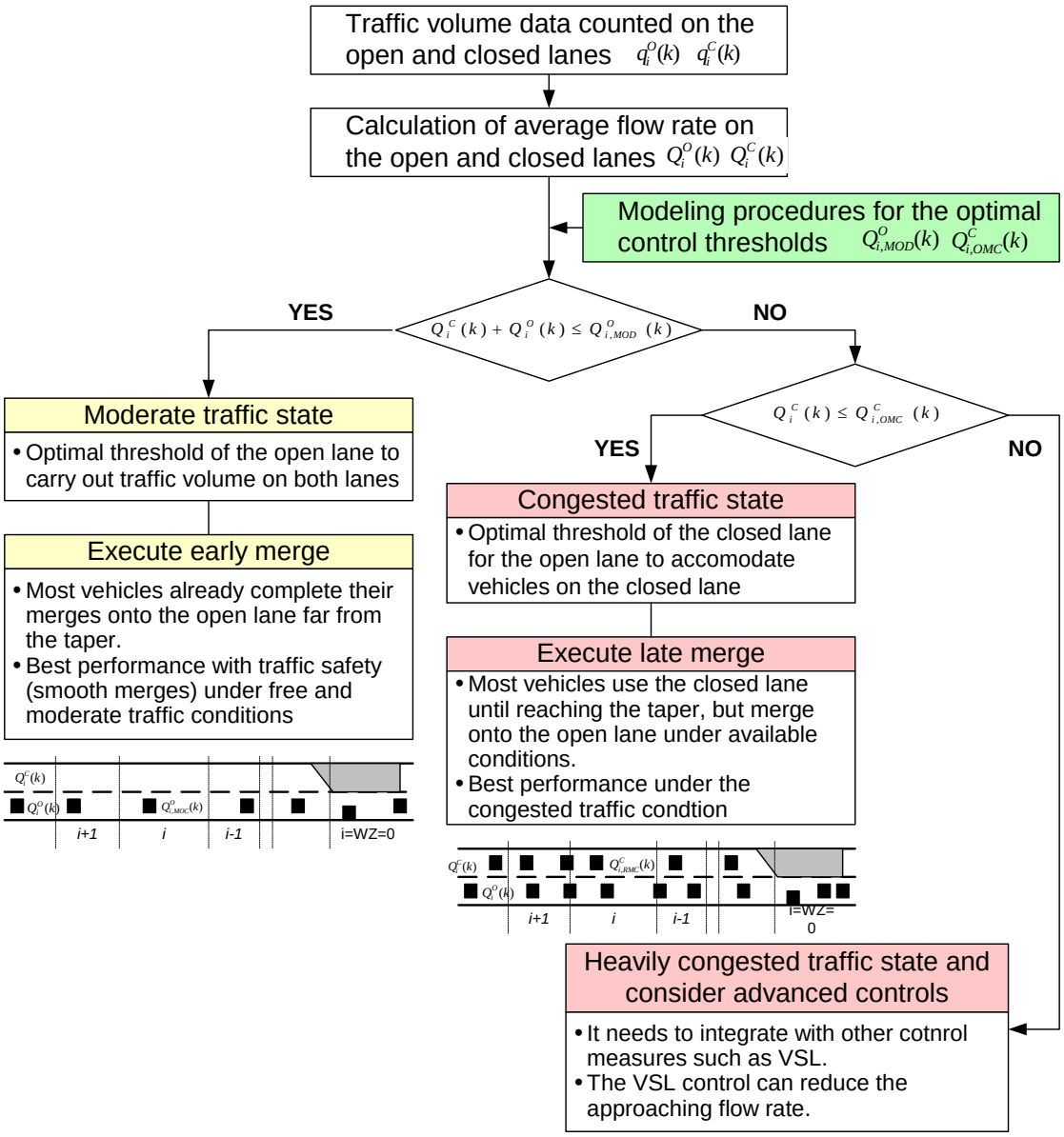

Figure 4.2.5 Methodology for the DLM control algorithm

4.3 Model descriptions for the optimal control thresholds

4.3.1 Model components

Figure 4.3.1 shows the procedures to produce the optimal control thresholds. The solid lines indicate the procedures to calculate the input data and estimate model parameters, and then formulate main equations for the control threshold variables. More specifically,

- With the traffic sensor data (e.g., traffic volume and speed) and the model parameters, the mean density and the average speed are calculated, and used as the system state variables.
- Based on the traffic flow equilibrium relation, the estimated traffic flow state is expressed with the detected volume data and the estimated lane-changing parameters. With the mean density and average speed, the maximum traffic flow rate (MFR) is used to derive the operational relations of the two decision variables (i.e., MOD and OMC).
- Equations for the traffic flow state variable, MFR, MOD, and OMC are employed in the model components (see the dotted box) to ensure that the available capacity of both lanes is optimally used with the computed optimal MOD and OMC.

The remaining subsections are focused mainly on: calculation of input variables from sensor data; estimation of lane-changing parameters, and derivations as well as formulations of the traffic flow state variable, MFR, MOD and OMC.

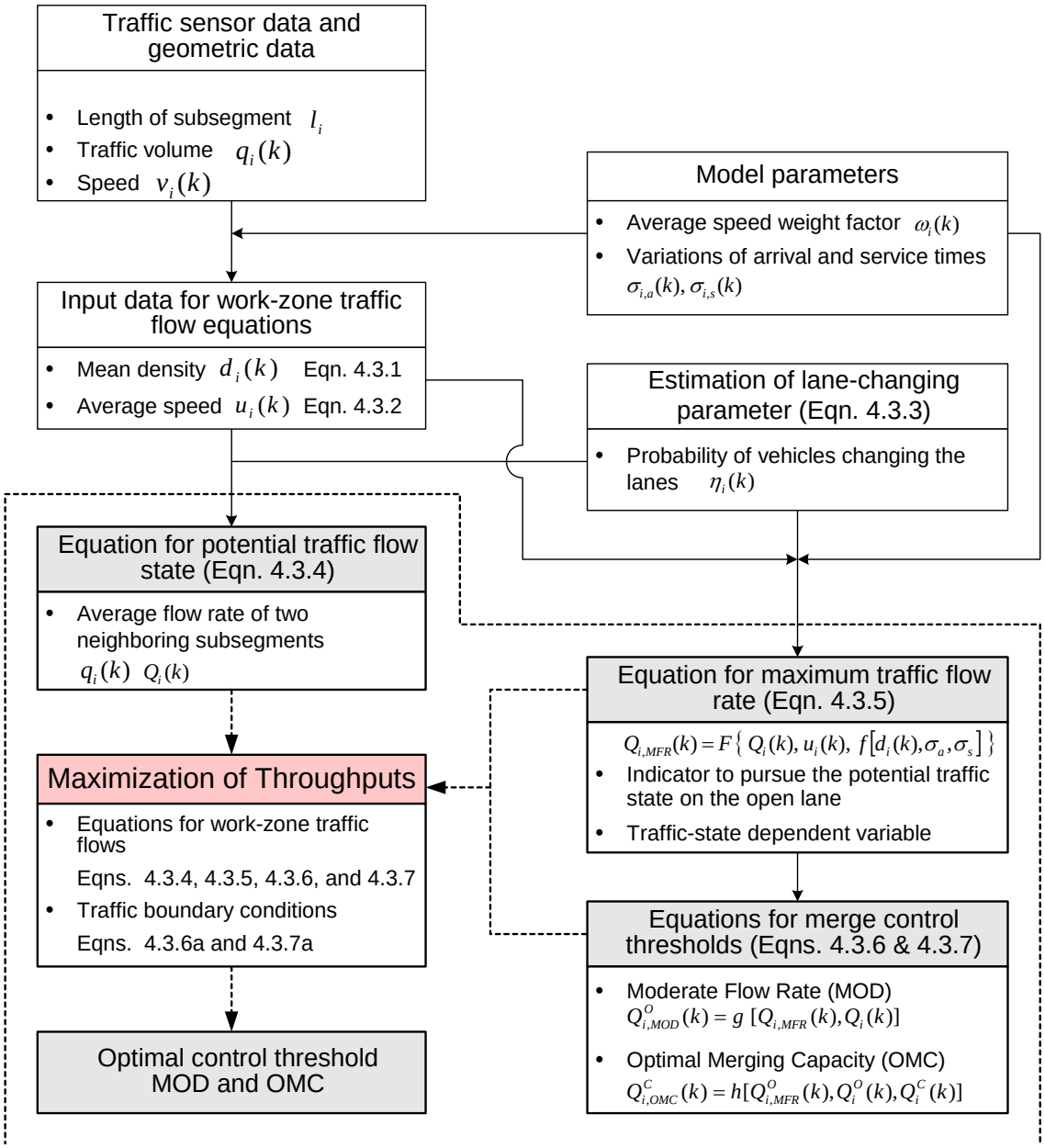

Figure 4.3.1 Modeling procedures for the optimal control thresholds

4.3.2 Calculation of input variables for work-zone traffic flow equations

To estimate the mean density $d_i(k)$, one shall use the conservation law, where the temporal variation of mean density on the open (or closed) lane during each control time interval (T) is determined by the difference between the input and output flows, $q_i(k)$ and $q_{i-1}(k)$ at the boundaries of subsegments on the open (or closed) lane.

$$d_i(k) = d_i(k-\mathbf{1}) + \frac{T}{l_i \cdot n_i}\left[q_i(k) - q_{i-\mathbf{1}}(k)\right] \quad (4.3.1)$$

$$\mathbf{0} \le d_i(k) \le d_i^j \quad (4.3.1a)$$

where, $d_i(k)$ is the mean density in subsegment i, and $q_i(k)$ and $q_{i-\mathbf{1}}(k)$ are transition flow rates in neighboring subsegments i and $i-\mathbf{1}$, during time interval k.

In addition, the average speed $u_i(k)$ can be approximated with the following weighted average of the detected speeds, $v_i(k)$ and $v_{i-\mathbf{1}}(k)$, between neighboring subsegments.

$$u_i(k) = \omega_i(k) \cdot v_i(k) + \left[\mathbf{1} - \omega_i(k)\right] \cdot v_{i-\mathbf{1}}(k) \quad (4.3.2)$$

$$\mathbf{0} \le u_i(k) \le u_i^f \quad (4.3.2a)$$

where, $u_i(k)$ is the average speed in subsegment i during interval *k*, and $\omega_i(k)$ is the average speed weight factor.

4.3.3 Estimation of lane-changing parameter, $\eta_i(k)$

The estimation of lane-changing maneuvers between the open and closed lanes is based on the following assumptions:

- As illustrated in Figure 4.3.2, the work-zone subsegment *i* can be viewed as a basic queuing system (e.g., service station), meaning that during interval k, the detected input and output flows, $q_i(k)$ and $q_{i-1}(k)$, can be viewed, respectively, as average arrival rate $\lambda_i(k)$ and service rate $\mu_i(k)$.
- The actual lane lane-changing decision of drivers is based on the average headway available to change the lane, under the assumption that most drivers are willing to cooperate with the displayed merging message on each location.
- The mandatory lane-changing maneuver is defined as a merging action that occurs when the detected traffic flow on the open lane is served with a shorter headway $\mu_i(k)$ than the minimum headway τ, since τ is the headway allowable for vehicles to move without causing severe queue spillback.
- The mandatory lane-changing maneuver around the merge point does not guarantee a high probability (≈ 1.00) since drivers can't physically merge into the target lane under the heavily congested traffic condition, which results in a traffic queue.

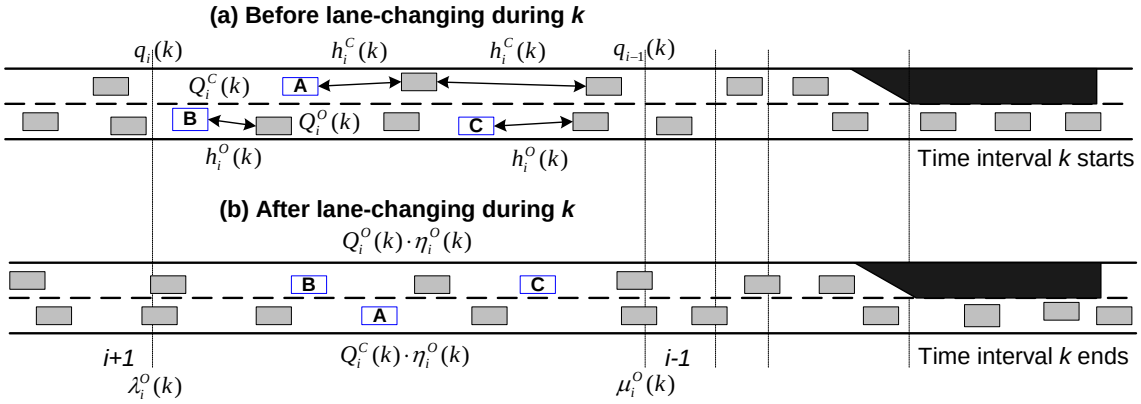

Figure 4.3.2 Actual lane-changing maneuver based on the headway distribution

Under the mandatory lane-changing traffic condition (e.g., $\mu_i(k) \le \tau$) in the work-zone operation, drivers on the current (closed) lane (particularly, around the merge point) will likely try to merge into the target (open) lane (e.g., forced merge) despite the short merge headway t_i^M . Otherwise (e.g., $\mu_i(k) > \tau$), drivers can change the lane with the normal headway t_i^N ($t_i^M < t_i^N$). The former case (e.g., $\mu_i(k) \le \tau$) is based on the Erlang distribution to consider the mandatory lane-changing proportion with the merge headway t_i^M , and the latter case (e.g., $\mu_i(k) > \tau$) is based on the shifted negative exponential distribution to consider the lane-changing proportion with the normal headway t_i^N .

Based on the above assumptions, thus, $\eta_i(k)$ is defined as the lane-changing probability $P[h_i(k)]$, and composed of two functions. Depending on the relation between the current average service rate $\mu_i(k)$ and the minimum headway τ , as expressed in Eqn. (4.3.3), one is a probability which is less than the merge headway t_i^M , and the other is a probability which is greater than the normal headway t_i^N , respectively, in subsegment i during time interval k .

$$\eta_i(k) = P[h_i(k)] = 1 - \left\{1 + \frac{t_i^M}{\mu_i(k)}\right\} \cdot e^{-\frac{t_i^M}{\mu_i(k)}} \qquad for \;\; \mu_i(k) \le \tau$$
$$= e^{-\frac{t_i^N - \tau}{\mu_i(k) - \tau}} \qquad for \;\; \mu_i(k) > \tau \tag{4.3.3}$$

where, $\mu_i(k)$ (i.e., average service rate) is equal to $3600/q_{i-1}(k)$ (see Figure 4.3.2), and τ is the minimum headway. t_i^M and t_i^N are the mandatory merge headway and the normal lane-changing headway, respectively.

4.3.4 Equation for traffic flow equilibrium condition

Since no on- or off- ramp exits in the target work-zone segment, the transition flow between adjacent subsegments is taken as the averaged flow rates of two neighboring subsegments on the open (or closed) lane.

$$q_i(k) = \frac{1}{2}\{Q_i(k)\cdot[1-\eta_i(k)]+Q_{i-1}(k)\} \tag{4.3.4}$$

where, $Q_i(k)$ is the estimated flow rate in subsegment *i* during interval *k*, and $\eta_i(k)$ is the model parameter for estimating the proportion of vehicles changing between the open and closed lanes.

4.3.5 Equation for maximum flow rate (MFR), $Q_{i,MFR}(k)$

As the main potential traffic state variable, MFR indicates the volume level that the open lane can accommodate the vehicles merging from the closed lane without causing severe queue spillback. This variable needs to be estimated with the input variables and detected traffic data.

Based on the assumption of the basic queuing system (see Figure 4.3.2) in the work-zone subsegment i, this study derives MFR from the non-stationary queuing model (i.e., state dependent (SD) G/G/1 model) to reflect the non-equilibrium traffic flow properties under the congested work-zone traffic conditions. Eqn. 4.3.5a represents the influence of the congestion factor $f[d,\sigma_a,\sigma_s]$ on the average speed (u).

$$u = \frac{u_{ideal}^f}{\mathbf{1}+ f[d,\sigma_a,\sigma_s]} \tag{4.3.5a}$$

where, $f[d,\sigma_a,\sigma_s]$ is a function of the mean density (d) and the general distributions of the arrival and service processes (i.e., the expected arrival time $\mathbf{1}/\lambda$ and its standard deviation σ_a, and the expected service time $\mathbf{1}/\mu$ and its standard deviation σ_s, respectively).

To specify the property of $f[d,\sigma_a,\sigma_s]$, Eqn. 4.3.5b (Vandaele et al., 2000; Kraemer, 1976) has been proposed based on the G/G/1 queuing model. This equation indicates that a high variation (e.g., $\beta_a = \sigma_a \cdot u^f \cdot d^j$) or a high density (e.g., d) leads to far lower speeds than the free-flow speed, u_{ideal}^f.

$$\text{If } \beta_a^2 \le \mathbf{1},\ u = \frac{\mathbf{2}\cdot u_{ideal}^f\cdot(d^j-d)}{\mathbf{2}\cdot(d^j-d)+d\cdot(\beta_a^2+\beta_s^2)\cdot\exp\left[\dfrac{-\mathbf{2}\cdot(d^j-d)\cdot(\mathbf{1}-\beta_a^2)^2}{\mathbf{3}\cdot d\cdot(\beta_a^2+\beta_s^2)}\right]}$$

$$\text{If } \beta_a^2 > \mathbf{1},\ u = \frac{\mathbf{2}\cdot u_{ideal}^f\cdot(d^j-d)}{\mathbf{2}\cdot(d^j-d)+d\cdot(\beta_a^2+\beta_s^2)\cdot\exp\left[\dfrac{-(d^j-d)\cdot(\beta_a^2-\mathbf{1})^2}{(d^j+d)\cdot(\beta_a^2+\mathbf{4}\cdot\beta_s^2)}\right]} \tag{4.3.5b}$$

where, β_a and β_s are squared coefficients of variation of arrival and service times, respectively.

Grounded on the G/G/1 concept, the SD G/G/1 queuing model (Vandaele et al., 2000) further assumes that vehicles are served at a rate that depends upon the number of vehicles already on the road. Thus, the delays in the queues under work-zone operations will reduce the ideal free-flow speed (u_{ideal}^{f}) to actual desired flow speed (u_{actual}^{f}). To reflect such a relation, this study employs the following exponential relation between the free-flow speed and the average flow rate (Jain, Smith, 1997).

$$u_{actual}^{f} = u_{ideal}^{f} \cdot (\mathbf{1} - \frac{d}{d^{j}}) \cdot \exp\left[-\frac{a \cdot Q}{Q_{MFR}} \right] \tag{4.3.5c}$$

where:

u_{actual}^{f} is the desired flow speed under the actual traffic condition,

Q is the average flow rate in the system,

Q_{MFR} is the maximum flow rate of the system, and

a is the pressure coefficient for the exponential function (e.g., a = 3, 5, and 7).

Then, MFR, $Q_{i,MFR}(k)$ in subsegment i during interval k, can be derived from the basic relationship, $Q_i(k) = u_i(k) \cdot d_i(k)$, where the average speed $u_i(k)$ is the combination of Eqn. 4.3.5b and Eqn. 4.3.5c based on the SD G/G/1 model. Consequently, Eqn. 4.3.5 means that MFR is the state-dependent variable, defined as the function of the potential flow rate $Q_i(k)$ to ensure the maximum use of the target lane under the detected traffic conditions.

$$Q_{i,MFR}(k) = F\left\{ Q_i(k), u_i(k), f\left[d_i(k), \sigma_a, \sigma_s\right] \right\} \tag{4.3.5}$$

where, $Q_i(k)$ is the potential flow rate and $u_i(k)$ is the average speed in subsegment i during interval k; and $f\left[d, \sigma_a, \sigma_s\right]$ is the influence of congestion on the speed (also see Eqn. 4.3.5b). More specifically,

If $\beta_a^2 \le \mathbf{1}$,

$$Q_{i,MFR}(k) = \frac{a \cdot Q_i(k)}{\ln\left[\dfrac{\mathbf{2} \cdot u_{i,ideal}^{f}(k) \cdot d_i(k) \cdot [d_i^{j}(k) - d_i(k)]}{u_i(k) \cdot \left[\mathbf{2} \cdot [d_i^{j}(k) - d_i(k)] + (\beta_a^2 + \beta_s^2) \cdot d_i(k) \cdot \exp\left[\dfrac{-\mathbf{2} \cdot [d_i^{j}(k) - d_i(k)] \cdot (\mathbf{1} - \beta_a^2)^2}{\mathbf{3} \cdot d_i(k) \cdot (\beta_a^2 + \beta_s^2)} \right] \right]} \right]}$$

If $\beta_a^2 > \mathbf{1}$,

$$Q_{i,MFR}(k) = \frac{a \cdot Q_i(k)}{\ln\left[\dfrac{\mathbf{2} \cdot u_{i,ideal}^{f}(k) \cdot d_i(k) \cdot [d_i^j(k) - d_i(k)]}{u_i(k) \cdot \left[\mathbf{2} \cdot [d_i^j(k) - d_i(k)] + (\beta_a^2 + \beta_s^2) \cdot d_i(k) \cdot \exp\left[\dfrac{-[d_i^j(k) - d_i(k)] \cdot (\beta_a^2 - \mathbf{1})^2}{[d_i^j(k) + d_i(k)] \cdot (\beta_a^2 + \mathbf{4} \cdot \beta_s^2)}\right]\right]}\right]}$$

4.3.6 Equation for moderate flow rate (MOD), $Q_{i,MOD}^{O}(k)$

To implement the early merge control, as indicated in Figure 4.2.4a, it is essential that traffic flows after merges remain at the moderate state but not congested conditions. For example, traffic flow may remain at the free flow speed until it reaches certain level (C) of the maximum flow rate (MFR). This factor should be calibrated (e.g., c = 2/3, 70%, 75%, etc.) to ensure no significant speed change in the range available for the SEM control. Eqn. 4.3.6 is proposed to approximate the "optimal moderate traffic state", defined as $Q_{i,MOD}^{O}(k)$ for the early merge control as follows:

$$\begin{aligned} Q_i^O(k) + Q_i^C(k) \le Q_{i,MOD}^{O}(k) &= g\,[\,Q_{i,MFR}^{O}(k),\, Q_i^O(k)\,] \\ &= C \cdot Q_{i,MFR}^{O}(k) \end{aligned} \tag{4.3.6}$$

where, $Q_i^O(k)$ is the potential flow rate to estimate the maximum flow rate (MFR) $Q_{i,MFR}^{O}$ on the open lane in subsegment i during interval k.

Note that the set of potential flow rates $Q_i(k)$ should be less than $Q_{i,MFR}(k)$.

$$Q_i(k) \le Q_{i,MFR}(k) \tag{4.3.6a}$$

4.3.7 Equation for the optimal merging capacity (OMC), $Q_{i,OMC}^{C}(k)$

When the traffic flow rates on the closed lane reach OMC, one can assume that the available capacity of the closed lane has been optimally used by travelers. As illustrated in Figure 4.2.4b, OMC can be defined as the difference between the maximum flow rate (MFR) and actual traffic flows (A^*) on the open lane. With the measured average flow rate, one can compute A^* by adding the vehicles changing onto the open lane and subtracting the vehicles moving over to the closed lane during interval k. Such a relation is expressed mathematically as follows.

$$\begin{aligned} Q_{i,OMC}^{C}(k) &= h[\,Q_{i,MFR}^{O}(k),\, Q_i^O(k),\, Q_i^C(k)\,] \\ &= Q_{i,MFR}^{O}(k) - \left[q_i^O(k) + q_i^C(k)\right]/2 + Q_i^O(k) \cdot \eta_i^O(k) - Q_i^C(k) \cdot \eta_i^C(k) \end{aligned} \tag{4.3.7}$$

where, the 2nd term is the measured average flow rate; the 3rd term is the actual flow rate moving over the closed lane; and the 4th term denotes the additional flow rate changing onto the open lane. In addition, $\eta_i(k)$ is the model parameter for estimating the proportion of vehicles changing the open or closed lane.

In addition, the following boundary conditions need to be satisfied to keep the reasonable optimal merging capacity $Q_{i,OMC}(k)$ within the maximum flow rate $Q_{i,MFR}(k)$.

$$Q_{i,OMC}(k) \le Q_{i,MFR}(k) \tag{4.3.7a}$$

4.3.8 Model formulation

As indicated previously, the system performance of the proposed DLM control is based on the maximization of the total throughputs over the upstream subsegments, including the work-zone area.

$$Max. \quad \sum_k \left(\sum_i \left[q_{WZ}(k) + Q_i^O(k) + Q_i^C(k) \right] \cdot T \right) \tag{4.3.8}$$

where, $q_{WZ}(k)$ describes the work-zone downstream boundary flows.

Assuming that all the related parameters (i.e., $\omega_i(k)$, $\eta_i(k)$, etc) and traffic data (i.e., $q_i(k)$ and $v_i(k)$) from sensors are available, the proposed DLM control model can be calibrated and executed using the optimal control thresholds to maximize the objective function, subjected to the following dynamic traffic flow constraints and boundary constraints:

- Traffic flow constraints:
  Eqns. 4.3.4, 4.3.5, 4.3.6, and 4.3.7 are the principal system constraints to describe the potential traffic flow rate, MFR, MOD, and OMC, respectively. Eqns. 4.3.1 and 4.3.2 are used in estimating the mean density and average speed, respectively. Eqn 4.3.3 is used in estimating the actual proportion of vehicles changing lanes.

- Boundary constraints:
  Eqns. 4.3.6a to 4.3.7a are the physical constraints to generate the reasonable value of the optimal flow rate, based on the physical relations among OMC, MFR, and the traffic flow rate.

The above model will yield the solutions for the following variables: $Q_{i,}(k)$ (Optimal potential flow rate), $Q_{i,MOD}(k)$ (MOD: Moderate flow rate), and $Q_{i,OMC}(k)$ (OMC: Optimal merging capacity).

4.4 Performance of the DLM control using the optimal control threshold

To simulate the on-line work-zone control with the proposed DLM algorithm (see Figure 4.2.3 in Section 4.2), this study employs CORSIM-RTE (CORridor SIMulation – Rune Time Extension), a program designed to capture the on-line interaction between the execution of the merge control algorithm and the time-varying traffic conditions due to the work-zone operation. Figure 4.4.1 illustrates an example of the target work-zone system for simulation experiments, in which one left lane was closed on a two-lane freeway segment.

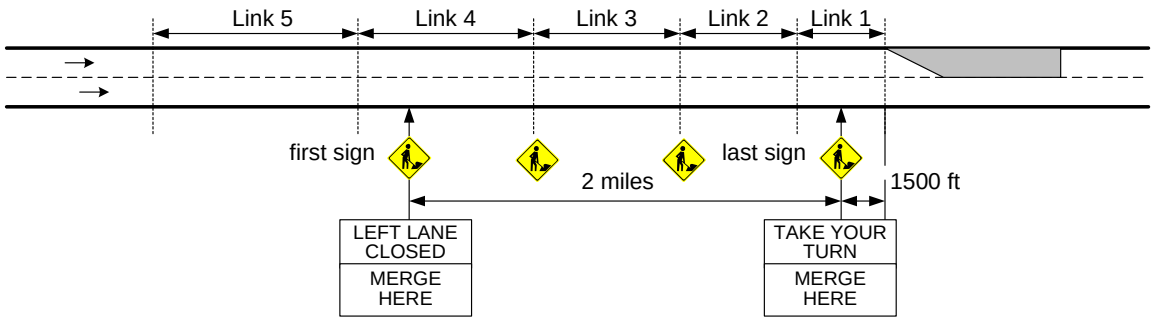

Figure 4.4.1 Configuration of the simulated DLM control system

Under this experiment, it is assumed that drivers are willing to cooperate with the merge messages, where the warning sign for the SLM control is located at 1500 ft prior to the merge point (i.e., Link 1) to guide them to use both lanes continuously until reaching the merge point, and the signs for the SEM control are located at 2.0 miles (i.e., Link 4) and followed locations (i.e., Links 2 to 3) for drivers to merge early onto the upstream open lane before reaching the merge point. Note that the warning sign at Link 1 is always activated for the mandatory merge maneuver.

With respect to the proposed optimal control thresholds (i.e., MOD and OMC), it is difficult to consider OMC in the simulation experiment, because SLM or SLM+α controls are identical in terms of the late merge operations. Thus, this evaluation is focused on the performance of the DLM control between SEM and SLM, using the optimized MOD control threshold.

4.4.1 Checking the traffic state-dependent control threshold

Before evaluation, it should be verified that the proposed MOD properly responds to time-varying traffic conditions.

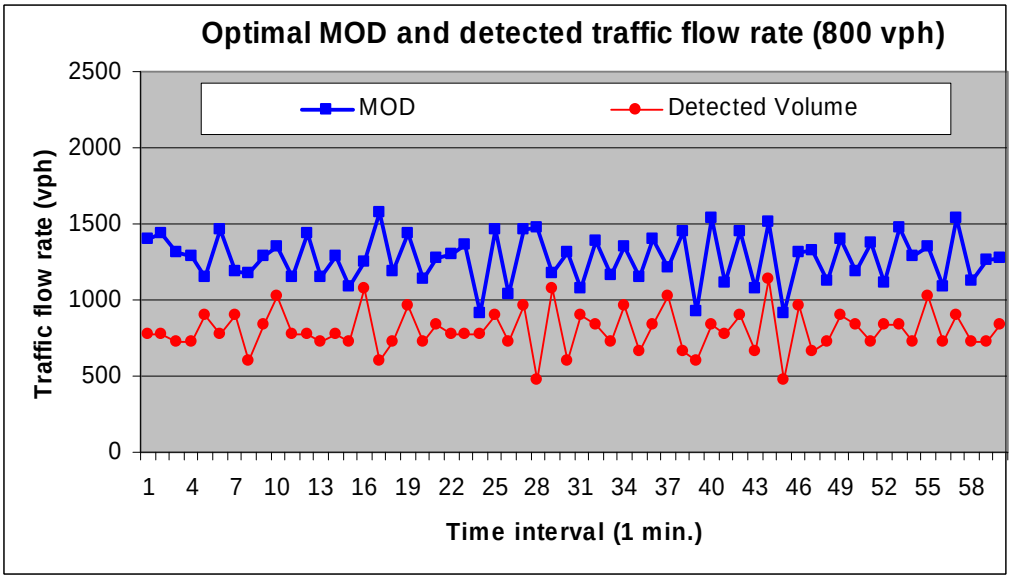

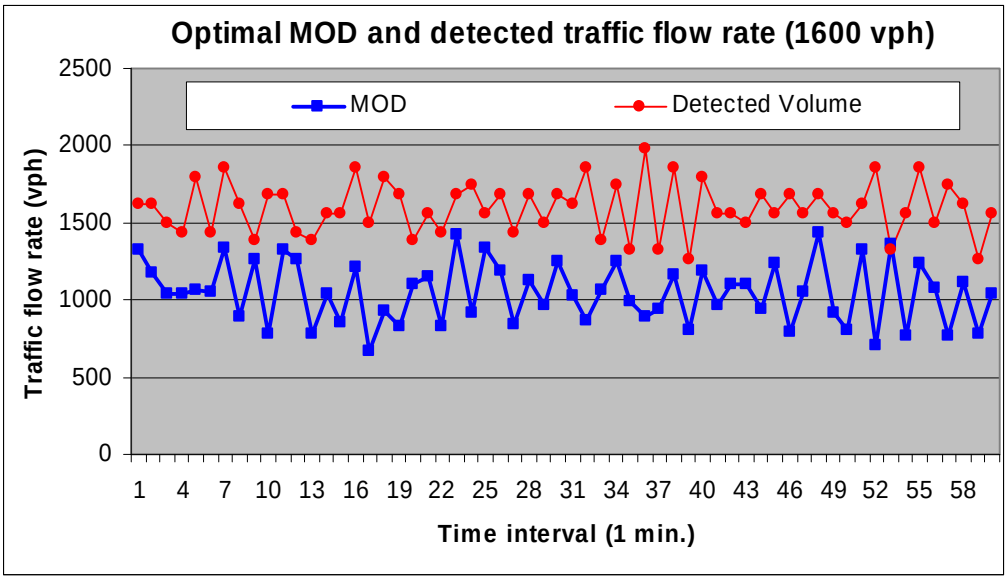

Figure 4.4.2 An example of time-varying optimal control threshold (MOD)

As shown in Figure 4.4.2, for instance, it generates a higher value than the detected traffic flow rate under the free and moderate traffic conditions (e.g., 800 vph), while it produces a lower value than the detected traffic flow rate under the congested traffic condition (e.g., 1600 vph). Consequently, the proposed DLM control will activate the SEM control under the former traffic state and the SLM control under the latter case.

4.4.2 Performance of the optimized time-varying control threshold

To show the optimality of the control threshold (MOD), one can compare the performance (e.g., throughputs) between the new and existing DLM systems with their corresponding control thresholds. As reviewed previously (see Table 4.1.1), most DLM control systems have been tested only with the static control thresholds. For example, the DLM system tested in Mn/DOT simply used 30 mph as a criterion for the system activation and deactivation. To compare the performance of two DLM controls based on the optimal MOD and the static control threshold (i.e., 30 mph), one should design proper levels of traffic volumes suitable for the SEL and SLM controls. Besides, to show their best performances, those conditions need to reflect time-varying traffic states during the simulation period (e.g., 1 hour).

- Figure 4.4.3 compares the merge strategies under the time-varying traffic conditions (e.g., the level of average traffic volume = 2000 vph) between the new and previous DLM controls. Despite the fluctuating traffic condition, the new control executed SEM (mark 'E') during short time periods, and then continued to execute SLM (mark 'L') (see Figure 4.4.3b). However, the previous one (see Figure 4.4.3c) selected the early and late merges alternatively during the whole time period. As the simulation result, the new and previous DLM controls produced 1670 vphpl and 1510 vphpl throughputs, respectively.

- Figure 4.4.4 compares the merge strategies under the other time-varying traffic conditions (e.g., the level of average traffic volume = 2400 vph). The new control (see Figure 4.4.4b) continued to execute SLM until the middle time period, and then SEM and SLM, alternatively, while the previous one (see Figure 4.4.4c) executed SEM during the initial short time period and then continued to execute SLM during the whole time period. In comparison, the new and previous DLM controls produced 1718 vphpl and 1505 vphpl throughputs, respectively.
- These two cases indicate that the proposed DLM control responds well to the time-varying traffic conditions and has best used the functions of SEM and SLM with their optimized control thresholds. However, the previous DLM control with the static control threshold may have limitations in effectively contending with time-varying traffic conditions and result in a decrease of the DLM performance due to the untimely activation of SEM and SLM.

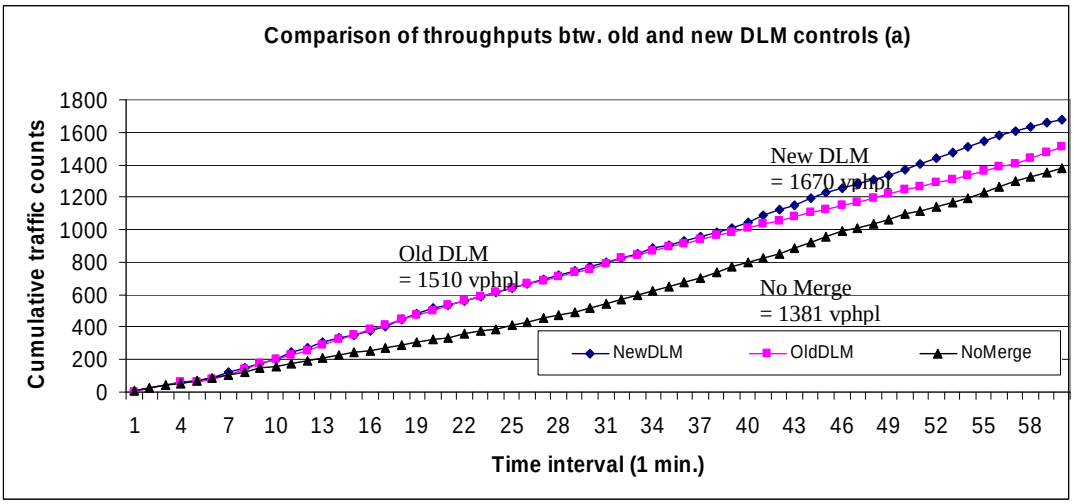

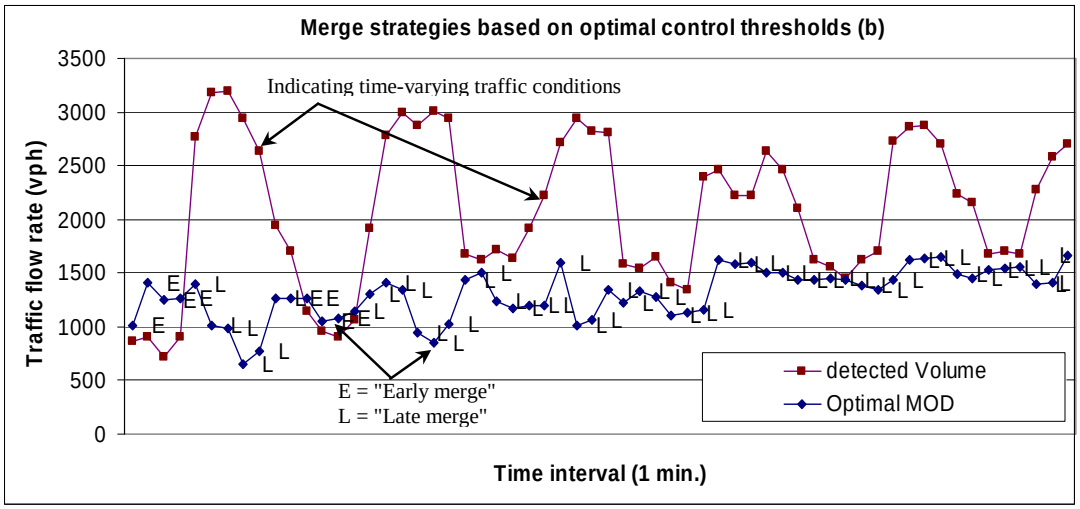

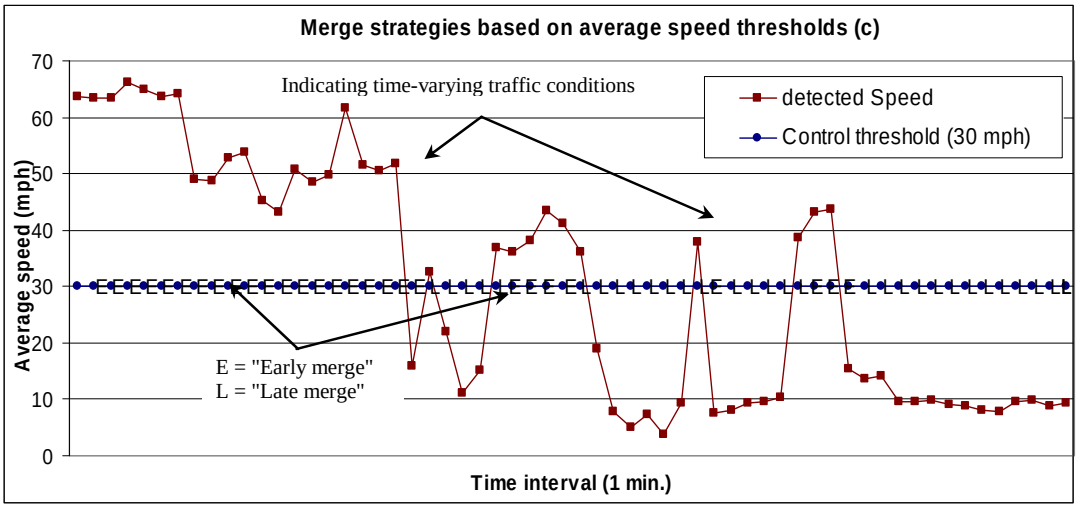

Figure 4.4.3 Comparison of the new and previous DLM controls under time-varying traffic condition (2000 vph)

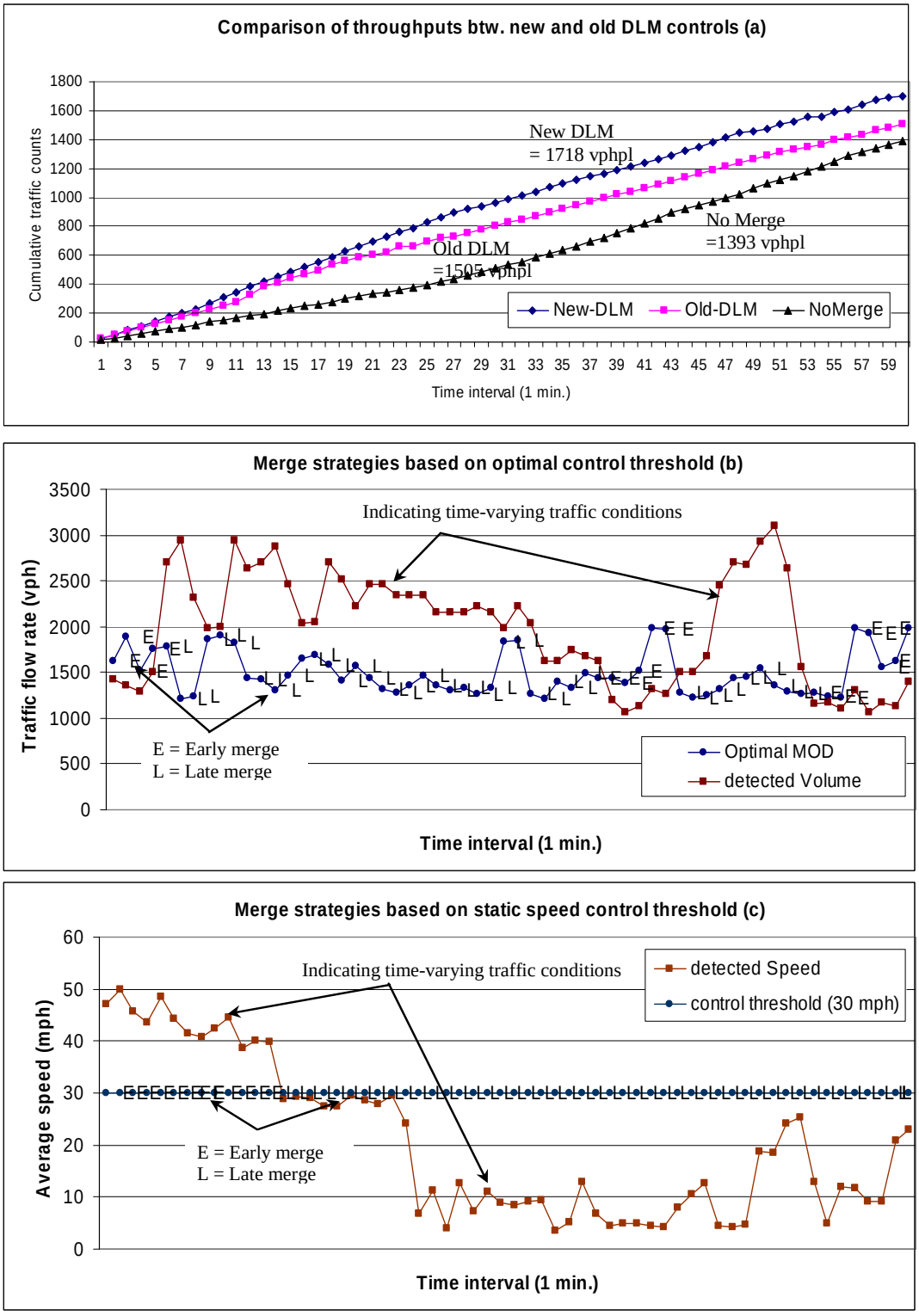

Figure 4.4.4 Comparison of the new and previous DLM controls under time-varying traffic condition (2400 vph)

- Figure 4.4.5 compares the average speeds and their variations between the new and previous DLM controls under the same time-varying traffic conditions (i.e., the level of average traffic volume = 2000 vph).
- It is notable that as indicated in Figure 4.4.5a, the average speed around the merge point under the new DLM control (i.e., Link 1, see Figure 4.4.1) is higher than that under the previous one, which implies that the new control reduced the number of traffic conflicts around the merge point. Figure 4.4.5b also indicates that the merge strategies based on the optimal MOD led to a smooth merge operations, while the previous one resulted in a high speed variation due to the frequently changed merge strategies between SEM and SLM (also see Figure 4.4.3c).

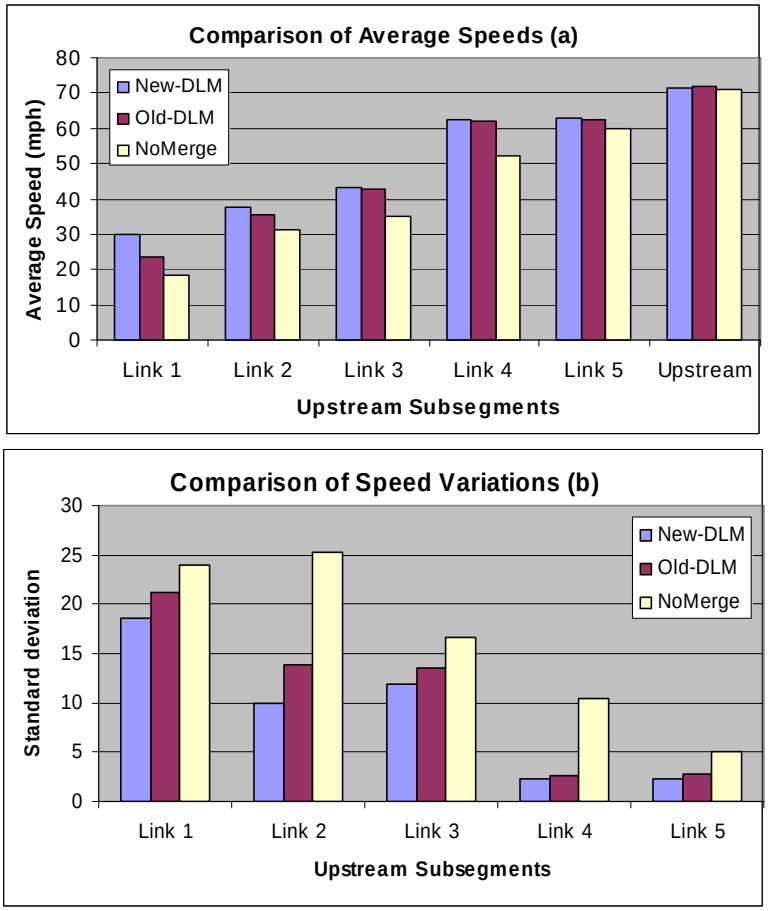

Figure 4.4.5 Comparison of the average speeds and speed variations under time-varying traffic condition (2000 vph)

- Figure 4.4.6 presents the simulation results under other traffic conditions (i.e., the level of average traffic volume = 2400 vph). As indicated in Figure 4.4.6a, the average speed under the new DLM control is overall higher than that under the previous one. In addition, as shown in Figure 4.4.6b, their speed variations are not

significantly different under these two DLM controls, despite the fact that the new DLM frequently changed the merge strategies (also see Figure 4.4.4b).

- This also implies that the changes of merge strategies, based on the proposed optimal control threshold, does not incur the speed changes significantly, which also means that MOD responded timely to the current traffic states on both lanes when vehicles change the lanes according to SEM and SLM..

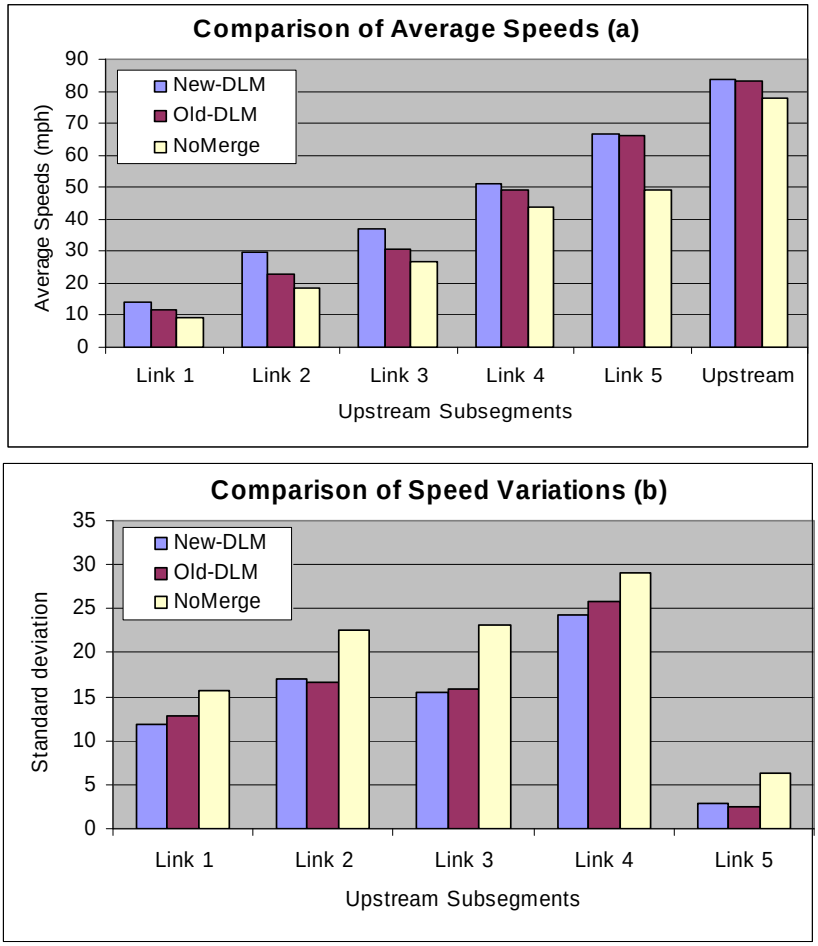

Figure 4.4.6 Comparison of the average speeds and speed variations under time-varying traffic condition (2400 vph)

4.5 Conclusions

This chapter has presented an advanced DLM control design and its operational algorithm for highway work-zone operations, based on the optimal control threshold model. This study is focused on how to select the control variables (e.g., SEM and SLM controls) and to determine their thresholds in response to traffic flow dynamics since each merge control has its most applicable traffic conditions. To achieve this objective, two decision variables (i.e., MOD and OMC) and one potential state variable (MFR) are defined and modeled in capturing interactions between dynamic traffic states and macroscopic traffic flow equations for the DLM control model.

From simulation experiments, the optimal control threshold (e.g., MOD), based on the proposed model (i.e., maximization of the total throughputs), has shown to respond well to time-varying traffic conditions and yielded more work-zone throughputs than the existing DLM control based on the static control threshold. It has also demonstrated that the proposed DLM control results in an increase in the average speed and decrease in the speed variation.

However, the simulation results have indicated that the average speeds under the DLM control may significantly vary due to its more frequent changes of merge strategies between SEM and SLM, especially, in case of more fluctuating traffic conditions. To enforce the performance of the proposed DLM control under the more congested and fluctuating traffic conditions, it is necessary to integrate an advanced speed control strategy such as the variable speed limit (VSL) control to reduce the approaching flow rate and to mitigate the impact of speed variation caused by the frequently changed merging controls.

CHAPTER 5 . DEVELOPMENT OF OPTIMAL VARIABLE SPEED LIMIT CONTROL MODEL AND ITS OPERATION ALGORITHM

5.1 Introduction

Contending with congestion and incidents in highway work zones has long been recognized as one of the priority tasks of most highway agencies. A common practice over the past several decades for work zone operations is to recommend or enforce a reduced speed limit via variable message signs (VMS) which may or may not respond to fluctuations in approaching traffic demand.

However, most speed controls, in practice, are static in nature, mainly to post the regulatory speed limits (referred as PSL) at upstream subsegments of a highway work zone. The common focus of the PSL control is on safety improvement, rather than on maximizing the operational efficiency or minimizing the average delay.

In view of increasing congestion in most urban networks and significant delay incurred by frequent work-zone operations, some researchers and engineers have started the development of a variable speed limit (referred as VSL) control system. Such a control strategy aims to properly respond to time-varying traffic conditions with a dynamically adjusted set of speed control that covers the entire upstream subsegments impacted by the work-zone operations and other emergency cases (e.g., bad weather, recurrent congestions, and environmental conditions).

Most field studies and simulation experiments have reported that properly regulating traffic flow speeds with VSL can indeed reduce the potential risk of rear-end collision in work zones. Table 5.1.1 summarizes the evaluation results of various VSL systems in the literature and Table 5.1.2 also summarizes the configuration and operation algorithm of available VSL systems.

Table 5.1.1 Summary of VSL system evaluations

Country	Purposes	Traffic Efficiency		Traffic Safety	
		Travel time (Speed)	Lane dist. (Occupancy)	Accidents (Headway)	Speed distribution
Australia (Coleman et al. 1996)	To avoid rear-end collisions by displaying a fog warning and speed advisory system.	Increased travel time			Reduced the number of speeders (but, temporary)
Germany (Coleman et al. 1996)	To stabilize traffic flow in congestion and lessen the probability of crashes To inform hazardous environmental conditions			Reduced crash	

Finland (Pili-Sihvola and Taskula 1996)	To increase the fluency of traffic flow by increasing the seasonal speed limit in winter To warn drivers of black ice and other hazards with a variable speed limit system			(Decreased proportion of short headway)	Reduced mean speed and standard deviation of speed
Nether-lands (Smulders 1992 and Hoogen and Smulders 1996)	To narrow speed dispersion in fog and congestion rather than reduce average speed		(Increased average roadway occupancy)	Increased average headway (Reduced percentage of small headway)	Reduced speeds in all lanes, Reduced severity of shock waves
			The differences of volume, speed, and occupancy between and within lanes became smaller and variations also decreased		
England (Wilkie 1997)	To minimize stop-and-go driving during heavy traffic	Increased travel time	More even lane-usage	Decreased accidents (Increased average headways)	
USA (Sumner and Andrew 1990, Lyles et al. 2004, and Park and Yadlapati 2004)	To display variable speed limits and lane-control information in response to congestion ahead				Not changed drivers' average speeds
	To evaluate the effects of VMS and VSL for the adverse conditions	(Reduced mean speed)			Increased speed deviations
	To evaluate the effects of the VSL for the work zone operations	Decreased travel time (Increased average speed)			Little difference of speed variance before or during VSL operation
	To evaluate the proposed VSL control logic that considers safety and mobility measures *	Increased travel time		Better safety measure (MSDE, Min safe distance equation)	
Canada (Lee et al. 2004)	To reduce the difference of the current speed and the speed limit *	Increased travel time		Reduced average total crash potential	

Note (*): Their results are based on simulated traffic conditions (see Table 5.1.2)

Table 5.1.2 Overviews of VSL system configurations and operations

Country	Installed sites	System overviews (Operation algorithms)
Australia (Coleman et al., 1996)	M4 and M5 and tunnels, as well as General Holmes Drive in Sydney (Automated speed management system installed on south of Sydney)	• Variable speed signs are connected to road loops and a visibility detector. • The speed of a vehicle passing a detector is displayed to the next vehicle as an advisory speed • The advisory speed is based on the visibility distance and the speed of the preceding vehicle
Germany (Coleman et al., 1996)	Autobahn between Salzburg and Munich, between Sieburg and Cologne, and near Karlsruhe Autobahn	• VMS displays not only the current speed limit but also its reason (e.g., construction, fog, crash ahead, ice, and high winds)
Finland (Pili-Sihvola , Taskula, 1996)	E18 road in Southeast Finland. The total length of the weather-controlled road is 25km	• The central unit of the road weather information system analyses road conditions and recommends speed limits because sensors detector ice or snow, wet pavement, heavy rain, fog, and high winds. • The speed limits on the motorway section were lowered during adverse road conditions from 62 to 50 mph in winter, and from 75 to 62 mph or 50 mph in summer with depending on conditions. • The system, installed on a section of roadway 9 mi long, includes 36 variable speed limit signs.
Nether-lands	A2 highway between Amsterdam and Utrecht (Dutch speed management system)	• The system covers a 12-mi length of highway with three interchanges, with signs spaced at intervals of about 0.6 mi. • The normal speed limit is 75 mph, but lower limits of 56, 43, or 31 mph are displayed depending on sensed traffic conditions. (Smulders, 1992; Hoogen, Smulders, 1996)
England (Wilkie, 1997)	A 14-mi section of M25 outside of London, which is one of the most congested freeways in England and one of the busiest motorways in Europe	• Loop detectors measure traffic density and speed, speed cameras. • The VMS system reduces the speed limit from 70 to 60 mph, then further to 50 mph when volume thresholds are reduced. • The speed limits are displayed on changeable message signs spaced at 0.6-mi intervals, and are enforced by photo radar. • The system monitors traffic speeds and stationary traffic to slow vehicles down approaching a queue, and has additional logic to stop speed limit settings fluctuation too often.
USA (Sumner, Andrew, 1990; Lyles et al., 2004; Park, Yadlapati,	John C. Lodge freeway in Detroit	• It was an advisory system, not an enforceable system. • It consists of 21 variable speed signs at 1,600-ft intervals, 11 lane control locations at 2,600-ft intervals, and 14 television camera locations at 1,300-ft interval.
	Albuquerque in New Mexico (Variable Speed Limit System, VSLS)	• The VSLS was well designed and was intended to be flexible in its modes of operation and in the environmental conditions it could sense and act upon.

2004)	I-96 in Virginia	• A set of pre-determined speed limit profiles • Speed limits no higher than 50 mph should be posted near some ramp locations. • The maximum speed limit in the active work zone was never allowed to be higher than 60 mph. • The regulatory speed limit was 70 mph when no work zone was present and 50 mph when the VSL system was not deployed.
	Experimental simulation with VISSIM	• Two performance measures, mobility (travel time & throughput) and safety (MSDE: minimum safety distance equation) • If condition changes, the VSL logics determine a new and pre-determined posted speed limit. • It is required to evaluate under the fluctuating traffic conditions.
Canada (Lee et al., 2004)	Experimental simulation with PARAMICS software	• Crash prediction model (COVV: average cross-sectional covariance of volume difference) • When crash potential exceeds the threshold, the control strategy determines a pre-determined posted speed limit. • It is required to calibrate and validate the PARAMICS model using real traffic data.

However, as reviewed in the literature, most existing VSL related systems suffer the following two common limitations in their applications:

- Main control objectives are proposed in response to traffic safety concerns, but not for operational efficiency, such as to maximize the throughput from a work-zone segment or to minimize the average delay for vehicles traveling through the entire highway segment plagued by the work-zone incurred traffic queue; and
- Core control algorithms do not intend to minimize traffic congestion by dynamically setting the optimal speed limits and coordinating them based on their spatial relations.

This chapter presents a dynamic VSL control algorithm for addressing the above objectives. The proposed VSL system has the following distinct features: (*a*) adopting the maximization of work-zone throughput as its control objective which is subjected to some embedded safety related constraints; (*b*) computing a sequence of optimal transition speeds for approaching vehicles, based on dynamic interactions between the work zone traffic flows and those in upstream highway segments; and (*c*) dynamically adjusting the set of displayed optimal speed limits, based on the detected speed distributions and flow rates so as to effectively respond to potential demand variation and non-compliance behavior of some drivers.

This chapter is organized as follows. The key features of the proposed VSL system are briefly described in Section 5.2. A set of equations for dynamic traffic state evolution is presented along with the VSL optimization model in Section 5.3. The operation algorithm for the VSL control is illustrated in Section 5.4. Design of

simulation experiments for evaluating the performance of the proposed algorithm under the real time control environment is reported in Section 5.5. Finally, research results and related future studies to the VSL control are summarized in Section 5.6.

5.2 VSL System Description

The proposed VSL system consists of sensors, variable speed limit signs, variable message signs and a central processing unit to execute control actions. As shown in Figure 5.2.1, variable message signs (VMS) are used to inform drivers of the traffic condition ahead and to display the enforced speed limit based on the VSL control strategies.

Depending on the approaching volume, driver compliance rate, and the resulting congestion, the central processing unit that integrates all system sensors and signs will compute the time-varying optimal speed limit for each VMS dynamically and display it in a timely fashion.

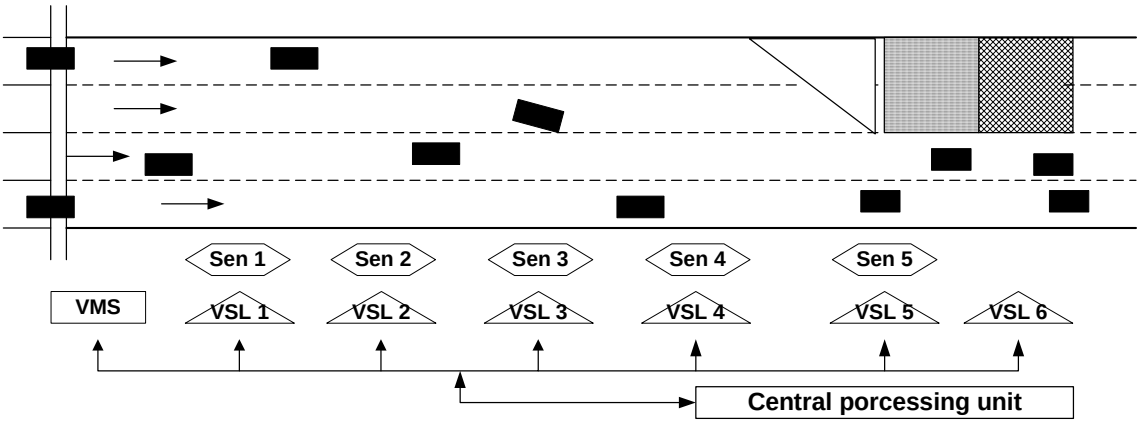

Figure 5.2.1 Configuration of a VSL System

5.3 Methodology for VSL Control Model

Figure 5.3.1 illustrates an example highway work zone where its capacity has been reduced due to lane closure operations. To minimize the potential queue formation ahead of the lane-closure location, one shall first divide the upstream segment of the maximum queue length into a number of segments with each being monitored by a set of sensors, VMS, and VSL signs. The objective of variable speed limit control is thus to maximize the total throughput from the work zone, but subject to some predefined safety constraints.

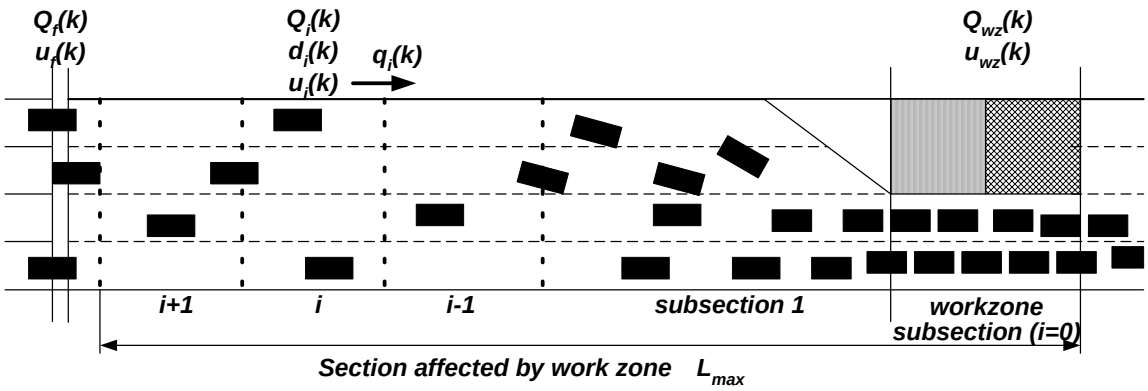

Figure 5.3.1 Traffic flow variables for the VSL control model

To perform an optimal dynamic VSL control, a set of traffic models is needed to capture the complex interactions between traffic state evolution and all control parameters. In particular, those traffic state evolution equations should be mathematically formulated to represent the actual operational constraints. As recognized in many studies (Lyles et al., 2004; Park, Yadlapati, 2004; Lee et al., 2003), traffic density and speed have been taken as state variables, of which the former is a key factor affecting drivers' choice of speed and the VSL system's selection of appropriate speed limits.

The proposed optimal control VSL algorithm for work-zone operations includes the following variables and parameters:

- Control time and subsegment index
  - T : Unit time interval for control operations (e.g., 1 min, 5 min, 10min, etc.)
  - k : Time interval index
  - i : Subsegment index ($i = 1 \cdots N$)
- Network geometric and physical data
  - l_i : Length of subsegment i
  - n_i : Number of lanes in subsegment i
- Traffic volumes
  - $q_i(k)$: Transition flow rate entering subsegment $(i-1)$ from subsegment i during interval k
  - $Q_i(k)$: Average flow rate in subsegment i during interval k
- Model parameters
  - α_i : Transition flow weight factor
  - β_i : Speed-density equation adjustment factor
  - γ_i : Shockwave weight factor

- Control variables
  - $v_i(t)$: Variable speed limit ratio in subsegment i during interval k
- State variables
  - $d_i(k)$: Mean traffic density in subsegment i during interval k
  - $d_i^J(k)$: Jam (maximum) traffic density in subsegment i during interval k
  - $u_i(k)$: Mean speed in subsegment i during interval k
  - $u_i^f(k)$: Free flow (boundary) speed in subsegment i during interval k

With the above variables and parameters, one shall first use the conservation law to approximate the evolution of dynamic density (Chang et al., 1995). The temporal variation of mean density, $d_i(k)$, during each control time interval (*T*) is determined by the difference between the input and output flows, $q_{i+1}(k)$ and $q_i(k)$ at the subsegment boundaries, and can be presented as follows:

$$d_i(k) = d_i(k-1) + \frac{T}{l_i \cdot n_i}[q_{i+1}(k) - q_i(k)] \tag{5.3.1}$$

In addition, the transition flow between adjacent subsegments is taken as a weighted average of two neighboring subsegments flows. That is,

$$q_i(k) = \alpha_i \cdot Q_i(k) + [1-\alpha_i] \cdot Q_{i-1}(k) \tag{5.3.2}$$

where, α_i is the model parameter (i.e., transition flow weight factor) which can be calibrated with field measurements. Wu and Chang (1999) stated in their paper that it should lie within the interval [0.5, 1.0]. For example, Cremer et al. (1989) calibrated it to be 0.95 with field data.

For the average speed, $u_i(k)$, one can also establish its evolution relation with the following properly selected speed-density relation and shockwave formation equations:

$$u_i(k) = u_i(k-1) + \beta_i \cdot \{S[d_i(k-1), v_i(k-1)] - u_i(k-1)\} + \gamma_i \cdot w_i(k-1) \tag{5.3.3}$$

where, the second component describes an adaptation of the average speed to the speed-density characteristics, $S[d_i(k-1), v_i(k-1)]$ as

$$S[d_i(k), v_i(k)] = [u_{i+1}^f(k) \cdot v_i(k)] \cdot \left[1 - \frac{d_i(k)}{d_i^J(k)}\right] \tag{5.3.4}$$

This equation is originally formulated with the Greenshield model and can be modified to account for the linear interaction between $d_i(k)$ and $v_i(k)$; and the third component takes into account the shock wave between downstream (*i-1*) and upstream (*i*), that is,

$$w_i(k) = \frac{[Q_{i-1}(k) - Q_i(k)]}{[d_{i-1}(k) - d_i(k)]} \tag{5.3.5}$$

Model parameters, β_i and γ_i are speed-density equation adjustment factor and shockwave weight factor, respectively. Note that the actual average speed measured from detectors doesn't usually fit with the proposed linear speed-density equation. Thus, based on the difference between the calculated and measured speeds during the previous time interval *(k-1) T*, the average speed needs to be adjusted with β_i during the time interval *kT*. In addition, γ_i is required to include the impact of shockwave on the subsequent upstream subsegments.

With the above formulations, one can construct the control model for highway work-zone operations to optimize the variable speed limit. Although there are several performance measures for highway control, this study has employed the maximization of the total throughput as the main measure of effectiveness (MOE) for the proposed highway work-zone operation system. Thus, one can express the objective function as follows:

$$Max. \qquad \sum_k \left(\sum_i^N \left[q_{wz}(k) + Q_i(k) \right] \cdot T \right) \tag{5.3.6}$$

where $q_{wz}(k) = Q_0(k)$ describing the work zone downstream boundary flow, and $Q_i(k) = u_i(k) \cdot d_i(k)$. The set of constraints for the above objective is shown below:

[Dynamic constraints]
- Equations : (5.3.1) ~ (5.3.5)

[Boundary constraints]
- $0 \le d_i(k) \le d_i^J$: (5.3.7)
- $u_{i-1}^f \le u_{i+1}^f(k) \cdot v_i(k) \le u_{i+1}^f$: (5.3.8)
- $0 \le v_i(k) \le 1$: (5.3.9)

It is noticeable that the speed-density relation in traffic flow is likely to be non-linear. However, due partly to the lack of such a model for work-zone traffic in the literature and partly to the need of efficient on-line operations, the proposed model has approximated speed-density with a linear function, but constantly updated it with the differences between field measured speeds (i.e., from detectors) and the model output, and also adjusted the results with the embedded parameters. With such an algorithm, one can circumvent the need to solve a non-linear formulation which may or may not have a solution, and is certainly not sufficiently fast for real-time operations.

5.4 VSL Control Algorithm

As reviewed in Sections 2.3 and 5.1, it should be mentioned that most VSL control strategies evaluated in the previous studies (Lee et al., 2004; Park, Yadlapati, 2004) changed a set of speed limits based on their pre-determined control thresholds

(e.g., averaged volume and speed), which are static in nature and may not respond timely to surges in traffic conditions. Thus, it is difficult to state that their VSL logic produce the optimal speed limit controls.

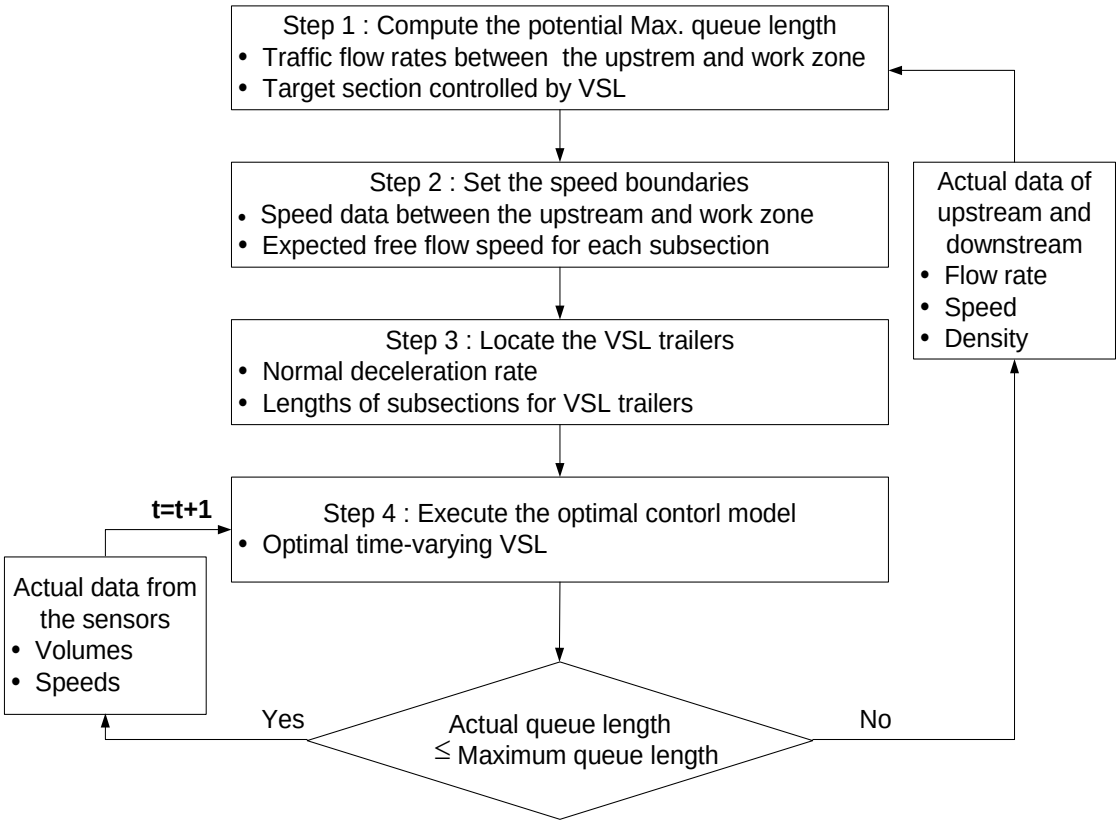

Figure 5.4.1 A Step-by-step description of dynamic algorithm for the VSL control

Figure 5.4.1 presents the principal steps for executing the proposed VSL system, including the interactions between sensors, VSL, and the feedback process. The entire process is designed to ensure that the VSL can always reflect the optimal speed limit and take into account some embedded safety constraints. Primary activities to be performed in each step are summarized below.

Step-1: Compute the potential maximum queue length

The purpose of this step is to approximate the maximum queue length, based on the difference in maximum flow rates (Q_{wz}, Q_f) between the upstream segment and the work zone because the computed queue length will be used as the target segment ($L_{\max}$) controlled by VSL. If the actual traffic queue caused by the work zone operations exceeds the $L_{\max}$, then the target segment should be extended to cover the entire roadway segment potentially impacted by the work zone traffic queue.

Step-2: Set the speed boundaries for VSL control

This step is designed to set a speed boundary (u_i^f) that reflects the free flow speed for each subsegment *i*. This boundary is designed to prevent the optimal speed limit of subsegment *i* from exceeding the boundary of its upstream subsegment (*i+1*). Thus, a set of optimal speed limits based on these boundaries will enable drivers to smoothly adjust their speeds when approaching the work zone. Such speed boundaries will be revised dynamically, based on the detected speed data (i.e., u_f and u_{WZ}).

Step-3: Locate the VSL trailers

The location of each VSL trailer set should be determined on the basis of the average decelerating rate of drivers when they perceive each displayed VSL sign. By using a normal deceleration rate (e.g., *a*=3.3mph/sec, ITE, 1982), the target segment can be divided into *n* subsegments (i.e., x_i) as follows.

$$x_i = u_{i+1}^f \cdot t + \frac{1}{2} a \cdot t^2 \text{ and, } x_i = \frac{(u_{i+1}^f)^2 - (u_i^f)^2}{2a} \tag{5.4.1}$$

This is to ensure that when perceiving the VSL signs, drivers do not experience uncomfortable and unsafe deceleration rate because the normal deceleration rate is calculated with the assumption of taking smooth speed reduction.

Step-4: Execute the optimal control model

Finally, Step 4 is to optimize a set of VSL over all subsegments during each control time interval based on the LP formulations shown in Section 5.3. As mentioned in Step-1, if the actual queue length is longer than the computed maximum queue length, then go to Step-1. Otherwise, the system shall repeat Step-4 with actual data updated from the sensors.

5.5 Model Evaluation with Simulation Experiments

5.5.1 Design of simulated system

The system design for simulation experiments is based on the actual highway work-zone traffic conditions. All system parameters (e.g., rubbernecking factor, car-following sensitivity factor, and desired free-flow speed) need to be calibrated with the real work zone data. The work-zone throughput, based on a total of 93 sites reported in the literatures, is summarized in Table 5.5.1.

Table 5.5.1 Work-zone throughput data measured in previous studies

Type*	Work-zone throughput (vphpl)									Sources
	1000	1100	1200	1300	1400	1500	1600	1700	1800	
2-1		2	5	6	5	7	8	1		Dixon et al. (1996) Krammes et al. (1992) Dudek et al. (1981) Kermode et al. (1970) Jiang(1999)
3-1					3	5				Dudek et al. (1981)
3-2	3	1		4	4	3	1			Krammes et al. (1992) Dudek et al (1981)
4-1		1	1	3	2	5	6	2		Krammes et al. (1992) Dudek et al. (1981) Kermode et al. (1970) Kim et al. (2001)
4-2			4		9	1			1	Krammes et al. (1992) Dudek et al. (1981) Kim et al. (2001)
Sum	93									

Note (*): 2-1 (the number of total lanes – the number of closed lanes)

Although the ranges of some work-zone types are widely scattered because of differences in surveys, one can approximate their distributions of maximum throughput as follows:

- Type 2-1 : 1500 ~ 1600 vphpl
- Type 3-1 : 1400 ~ 1500 vphpl
- Type 3-2 : 1300 ~ 1500 vphpl
- Type 4-1 : 1500 ~ 1600 vphpl
- Type 4-2 : 1200 ~ 1400 vphpl

Figure 5.5.1 illustrates an example work-zone system for simulation experiments, where one lane was closed on a 2-lane highway due to work-zone activities. The maximum link speed limit and the length of work zone area are set to be 65mph and 4000ft, respectively. This simulated system has been simulated for one hour with a microscopic traffic simulation model, CORSIM produced by Federal Highway Administration (FHWA, 2003).

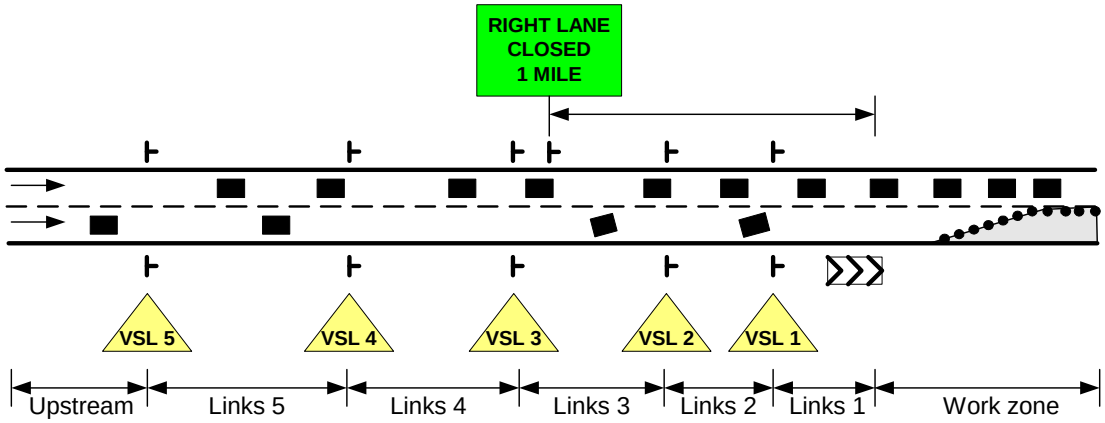

Figure 5.5.1 An example of typical work zone configuration (2lanes-1closed type)

The maximum throughput through the simulated system was then compared with the empirically observed throughput (i.e., 1500 ~ 1600 vphpl) for calibration of simulation model parameters such as rubbernecking factors and car-following factors that reflect driver behavior. A simulated work-zone system can be used in the VSL evaluation only after the completion of its parameter calibration.

5.5.2 Simulation of the on-line control process

To simulate the on-line work zone control with the proposed VSL algorithm, this study employs a CORSIM-RTE (CORridor SIMulation – Run Time Extension), a program designed to capture the on-line interaction between execution of the control algorithm and the time-varying traffic conditions due to the control operations. This mechanism has been programmed to provide three main functions (i.e., Initialization, VSL control, and Termination), which enable the developed optimal VSL module to communicate with CORSIM during every time interval *k*. Figure 5.5.2 illustrates the interaction process among CORSIM, Linear Optimization Program, and the VSL algorithm.

More specifically, with the interactive process shown in Figure 5.5.2, this system continues to simulate the work-zone condition at each unit time interval *k* (i.e., 60 seconds), and feeds back to RTE to generate a set of optimal speed limits for each subsegment *i* during subsequent control intervals. Such interactive procedures will be repeated for the entire simulation time period (e.g., 1 hour).

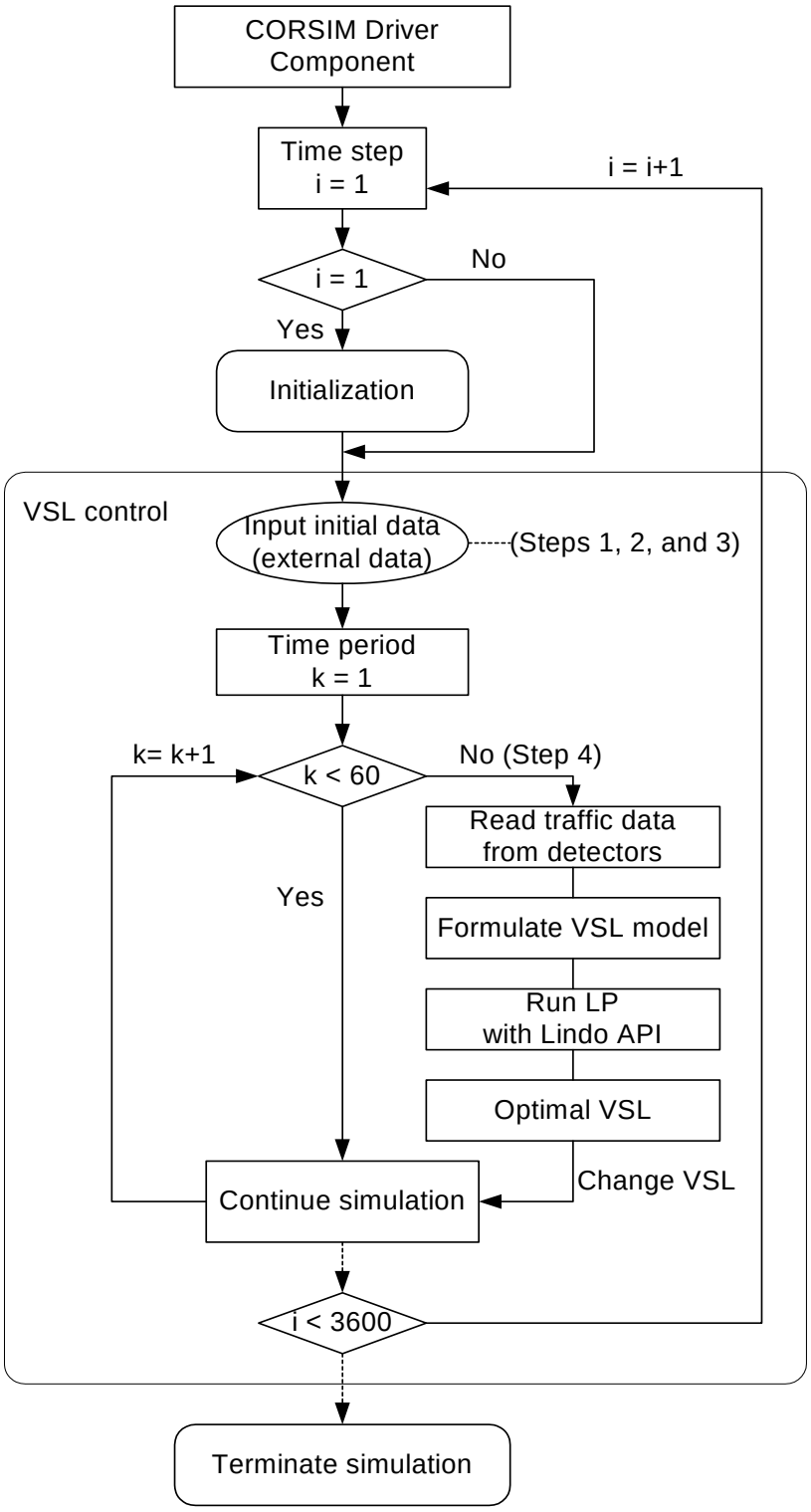

Figure 5.5.2 Interfacing mechanism for executing the VSL algorithm

5.5.3 Trends of optimal VSL

To show how to optimize the set of control speeds based on the proposed VSL model, Figure 5.5.3 shows the examples of optimal VSL speeds displayed on VSL 1 to VSL 5 (i.e., Links 1 to 5) in the 2-1 work-zone type (see Figure 5.5.1), using the proposed on-line control process.

These results show that the VSL displayed speeds are within the reasonable range and with small speed variations. It is notable that as the upstream volume increase to a critical level, the VSL speeds seem to converge to stable values.

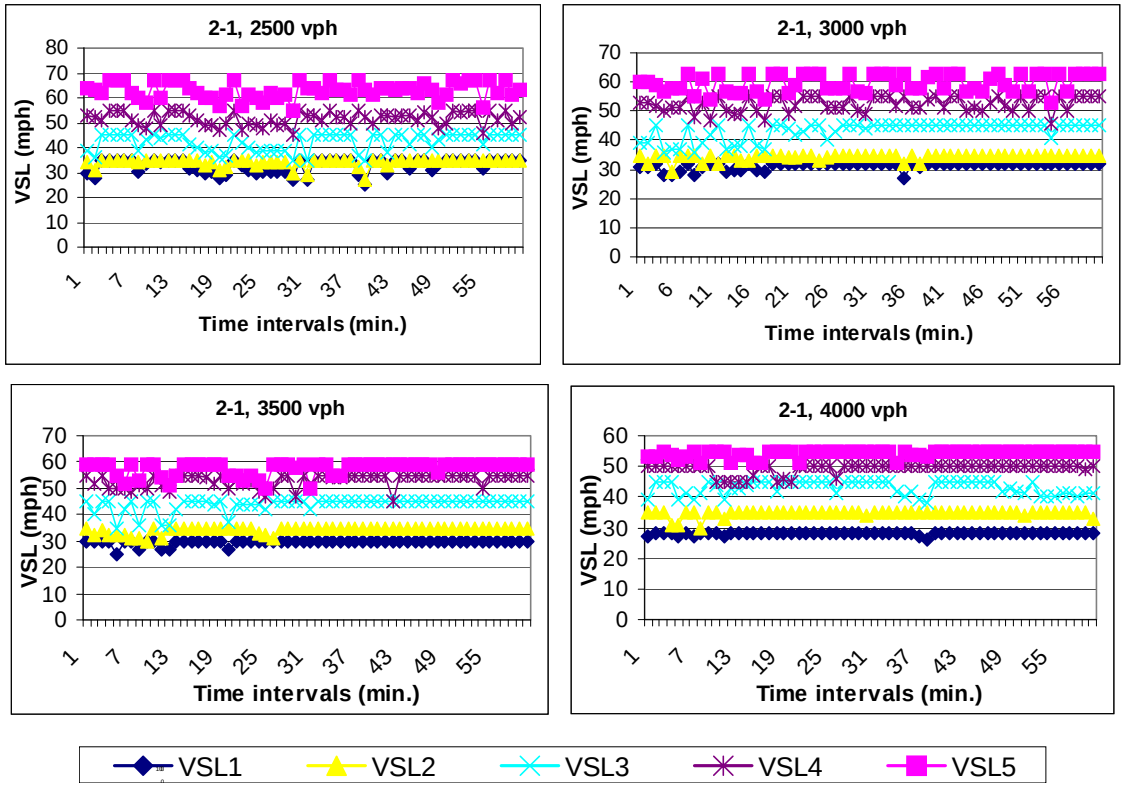

Figure 5.5.3 Trends of the optimal VSL sets

5.5.4 Sensitivity analysis

To assess the effectiveness of the developed VSL with various existing methods for PSL, this study has analyzed the performance of the work zone system under three possible PSL controls. Figure 5.5.4 shows the examples of the detected speed distribution from the 2-1 work-zone type simulation results at the volume level of 2,500 vph, under three PSL controlled speeds of 35 mph, 45 mph, and 55 mph. Although the times for the detected speeds to drop seem to reduce as the posted speed limits increase, it is evident that the speeds under all three PSL controls drop drastically over time, especially for those subsegments near the work-zone area. In contrast, as indicated in Figure 5.5.5, the detected speeds under the VSL control decrease at a smoother rate, compared to those under three PSL controls.

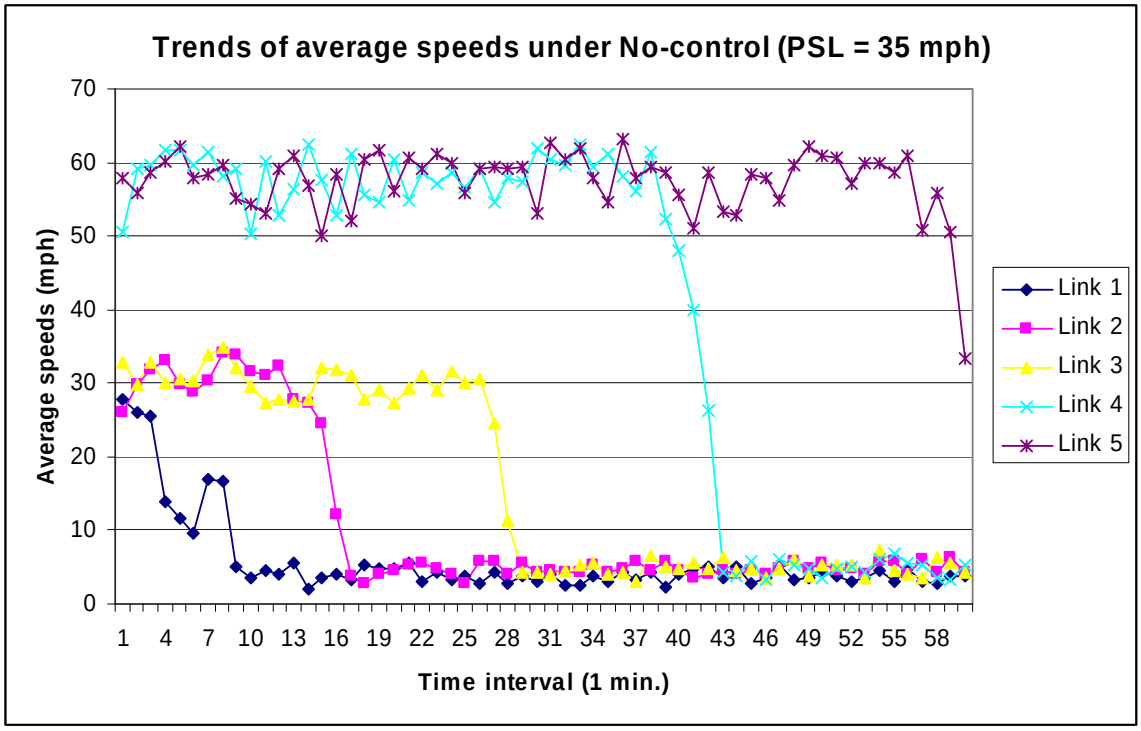
Trends of average speeds under No-control (PSL = 35 mph)
Average speeds (mph)
0
10
20
30
40
50
60
70
1 4 7 10 13 16 19 22 25 28 31 34 37 40 43 46 49 52 55 58
Time interval (1 min.)
Link 1
Link 2
Link 3
Link 4
Link 5

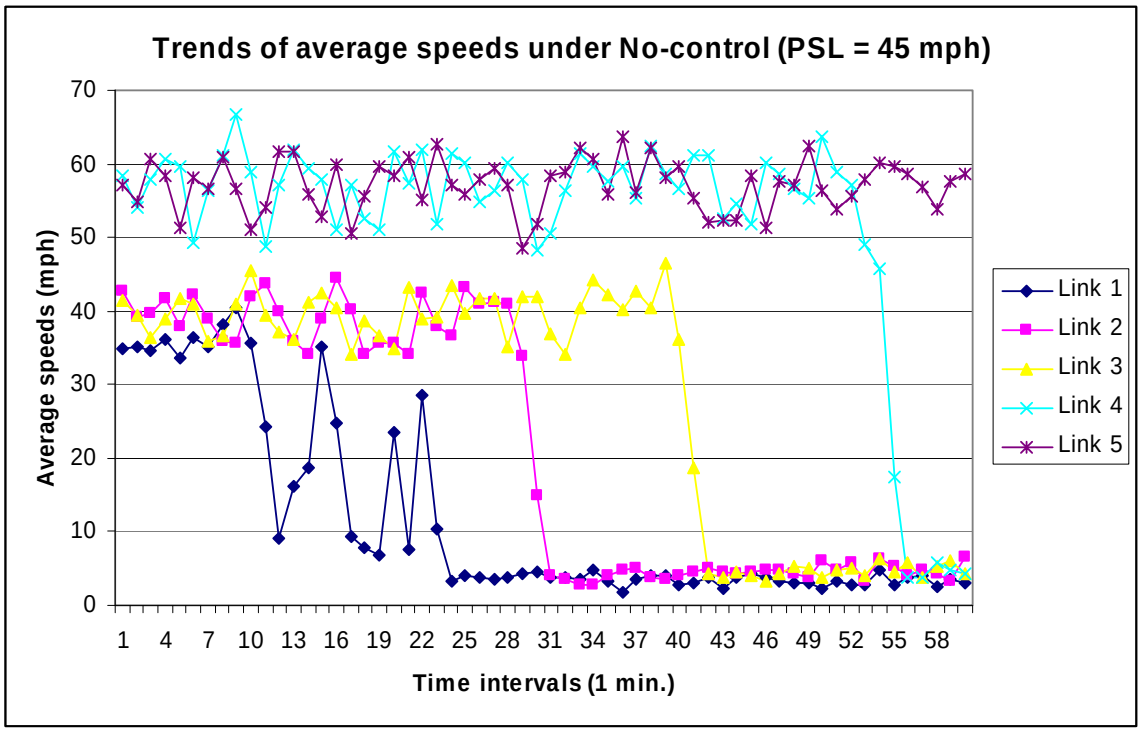
Trends of average speeds under No-control (PSL = 45 mph)
Average speeds (mph)
0
10
20
30
40
50
60
70
1 4 7 10 13 16 19 22 25 28 31 34 37 40 43 46 49 52 55 58
Time intervals (1 min.)
Link 1
Link 2
Link 3
Link 4
Link 5

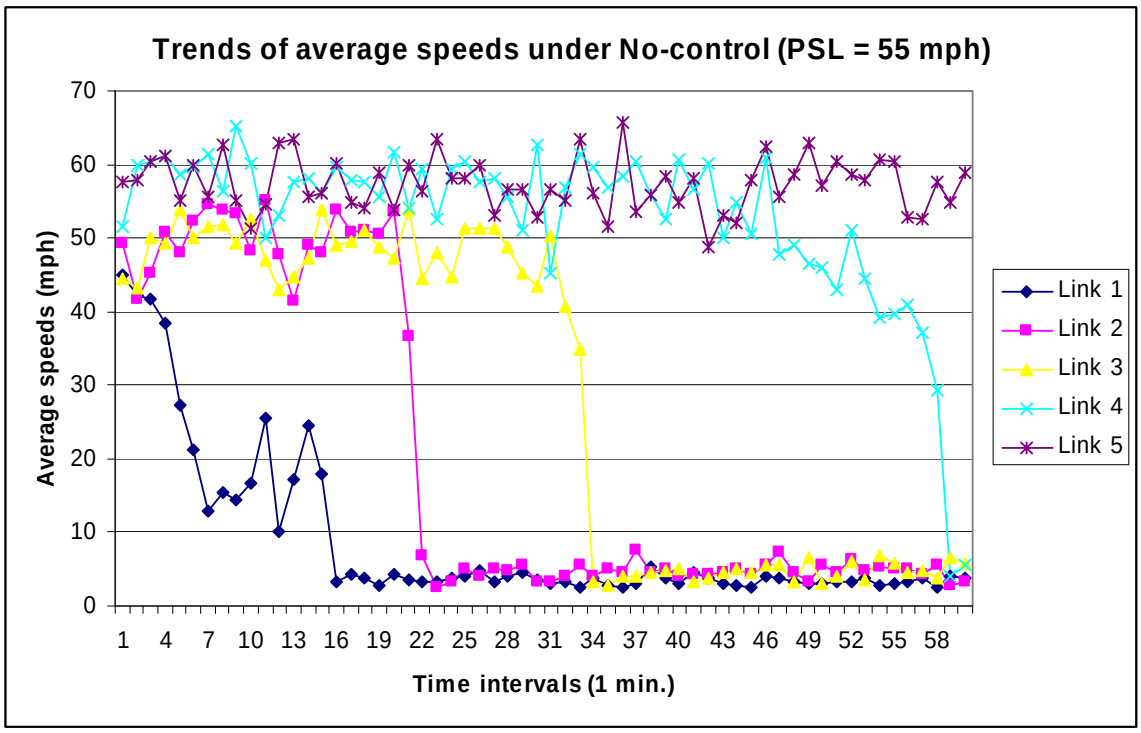

Figure 5.5.4 Distributions of the detected speeds under three PSL controls (No-control)

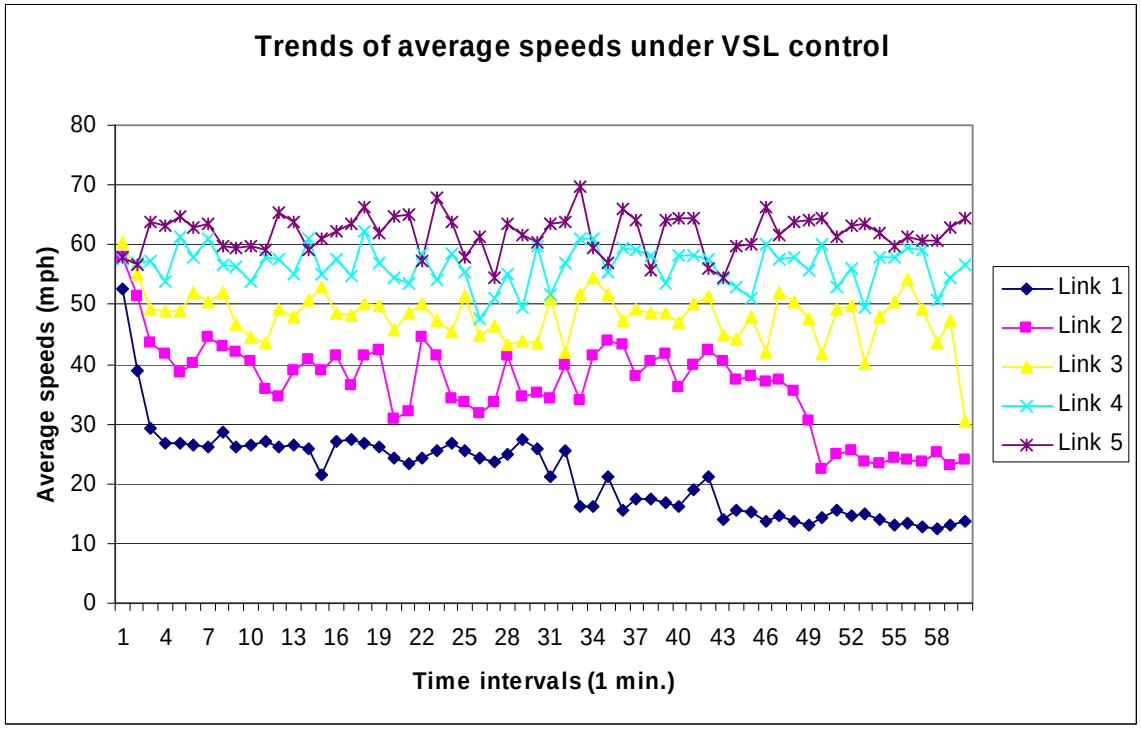

Figure 5.5.5 Distributions of the detected speeds under the VSL control

Table 5.5.2 also shows the comparison of the work zone throughput and speed variation between the VSL and those three PSL controls, where the VSL control seems to clearly outperform all those PSL controls with an increase in the throughput and reduction in the speed variation.

Table 5.5.2 Comparison of the work zone throughput and speed variation

Controls	PSL control			VSL control
Speed limits	35 mph	45 mph	55 mph	Variable speeds
Throughputs	1224 vphpl	1507 vphpl	1322 vphpl	1652
Speed variations	24.0	22.6	24.3	15.5

5.5.5 Evaluation of the VSL control model performance

To evaluate the proposed VSL model, the study employs the work zone maximum throughput, average delay and speed as the critical MOEs (measures of effectiveness). In addition, the variance of speeds over the entire upstream segment of the work zone is used to measure the potential improvement on the driving environment that is often correlated significantly with traffic safety. The total throughput is detected at the middle point of work zone while the average delay and speed are obtained over the pre-specified subsegments (i.e., link 1 to link 5) in advance of the work zone (see Figure 5.5.1).

To investigate the performance of this proposed VSL under different traffic conditions, the simulation experiments have included five types of work zones and various traffic volume levels as shown in Table 5.5.3.

Table 5.5.3 Upstream entry volumes used in experimental scenarios

Work zone types	Upstream entry volumes (vph)		
	Lower bound	Upper bound	Increment
2-1	2500	4500	500
3-1	4000	6500	500
3-2	2500	5000	500
4-1	5500	8000	500
4-2	4000	6500	500

Tables 5.5.4 to 5.5.6 show the comparisons of work zone throughput, average delay, and average speed, respectively, from the simulation results. These results seem to clearly demonstrate the effectiveness of the proposed VSL optimization model.

For example, as shown in Table 5.5.4, the proposed control model can increase approximately 310 vphpl of work zone throughput in the 2-1 type; 260 vphpl in the 3-1 type; 250 vphpl in the 3-2 type; 270 vphpl in the 4-1 type; and by 200 vphpl in the 4-2 type under the normal level of upstream volume. Likewise, Table 5.5.5 indicates that the VSL model can reduce about 560 seconds of the average delay per vehicle for traffic through the work zone in Type 2-1; 230 seconds in Type 3-1; 300 seconds in Type 3-2;

270 seconds in Type 4-1; and 290 seconds in Type 4-2 under the normal level of upstream volume. With respect to the average speed, the results in Table 5.5.6 indicate that the implementation of VSL does not result in a substantial reduction in the average speed under various approaching traffic volumes.

Table 5.5.4 Work-zone throughputs (unit: vphpl) from simulation experiments

Volume levels	Work zone types									
	2-1		3-1		3-2		4-1		4-2	
	No-VSL	VSL	No-VSL	VSL	No-VSL	VSL	No-VSL	VSL	No-VSL	VSL
2500	1477	1430			1497	1430				
3000	1520	1553			1512	1761				
3500	1561	1875			1570	1732				
4000	1582	1820	1436	1371	1469	1538			1297	1250
4500	1476	1489	1443	1419	1410	1424			1304	1318
5000			1444	1694	1388	1368			1387	1461
5500			1579	1729			1547	1528	1323	1526
6000			1571	1682			1608	1593	1444	1521
6500			1395	1383			1558	1824	1392	1449
7000							1596	1840		
7500							1522	1687		
8000							1503	1592		

Table 5.5.5 Average delay (unit: sec/veh) from simulation experiments

Volume levels	Work zone types									
	2-1		3-1		3-2		4-1		4-2	
	No-VSL	VSL	No-VSL	VSL	No-VSL	VSL	No-VSL	VSL	No-VSL	VSL
2500	801.8	875.0			871.2	938.8				
3000	1205.4	1005.0			1282.8	1039.4				
3500	1661.2	1097.0			1535.8	1237.5				
4000	1825.4	1412.2	624.7	648.1	2080.6	1926.5			656.0	810.0
4500	2107.8	2084.1	1025.6	1141.1	2460.6	2383.8			1170.0	1159.2
5000			1362.2	1255.8	2702.5	2686.1			1518.9	1326.0
5500			1631.5	1400.0			489.5	501.6	1639.0	1348.1
6000			1962.0	1683.5			689.2	694.7	1801.2	1550.0
6500			2150.5	2272.0			1040.8	812.3	2090.4	1941.8
7000							1256.9	987.4		
7500							1529.4	1203.8		
8000							1766.3	1641.1		

Table 5.5.6 Average speed (unit: mph) from simulation experiments

Volume levels	Work zone types									
	2-1		3-1		3-2		4-1		4-2	
	No-VSL	VSL	No-VSL	VSL	No-VSL	VSL	No-VSL	VSL	No-VSL	VSL
2500	37.8	34.7			43.3	37.8				
3000	27.0	27.1			35.4	36.7				
3500	20.0	25.1			30.7	31.4				
4000	16.5	19.7	40.1	37.6	23.2	22.8			39.6	35.2
4500	14.2	13.9	33.4	31.3	19.0	18.6			31.4	32.0
5000			26.7	27.2	15.8	15.6			25.4	24.1
5500			21.2	20.9			46.3	43.8	20.9	20.0
6000			17.0	16.5			41.4	40.2	18.1	17.9
6500			13.4	12.7			35.4	34.6	15.7	14.9
7000							29.7	29.0		
7500							25.6	24.9		
8000							20.1	19.8		

However, it should be noted that as the upstream traffic volume increases, the improvement in each MOE with VSL (e.g., work zone throughput and average delay) first increases and then decreases. This implies that the proposed VSL algorithm should again be reset based on Steps 1 to 3 because the actual queue length has exceeded the initially estimated maximum queue length (see Figure 5.4.1). It should also be noted that the benefits of implementing VSL control seem to diminish from moderate congested to heavy traffic conditions. Thus, it is expected that under oversaturated jam traffic conditions, the benefits of implementing VSL may not justify its operating costs.

For convenience of illustration, Figures 5.5.6 to 5.5.8 present the differences in MOEs (e.g., work zone throughput, average delay, and average speed, respectively) under the VSL control in the 2-1 work-zone type.

As reflected in those graphical results, under the normal level of the upstream volume (e.g., 3500 vph), the presented VSL optimization model can increase the throughput by 310 vphpl, and reduce an average delay per vehicle by 560 seconds for traversing over the work-zone area (see Figures 5.5.6 and 5.5.7). As mentioned previously, Figure 5.5.8 proves that the speed differences between No-VSL and VSL controls are not significant. This indicates that the VSL control strategy does not slow down the average flow speed despite the speed limitation.

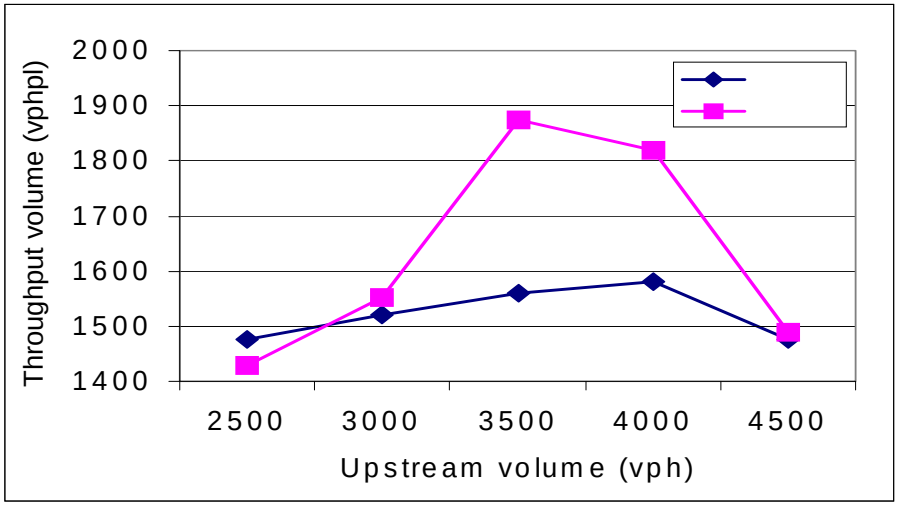

Figure 5.5.6 Work-zone throughput volume for Type 2-1

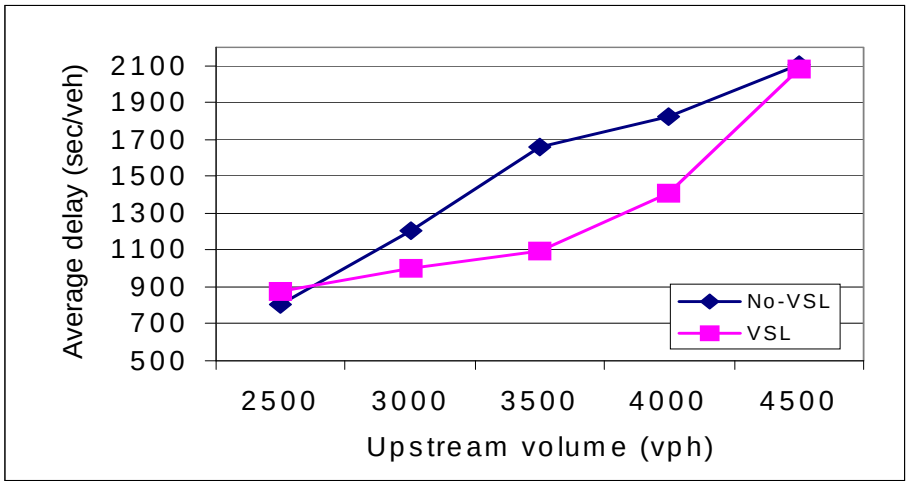

Figure 5.5.7 Average delay over subsegments for Type 2-1

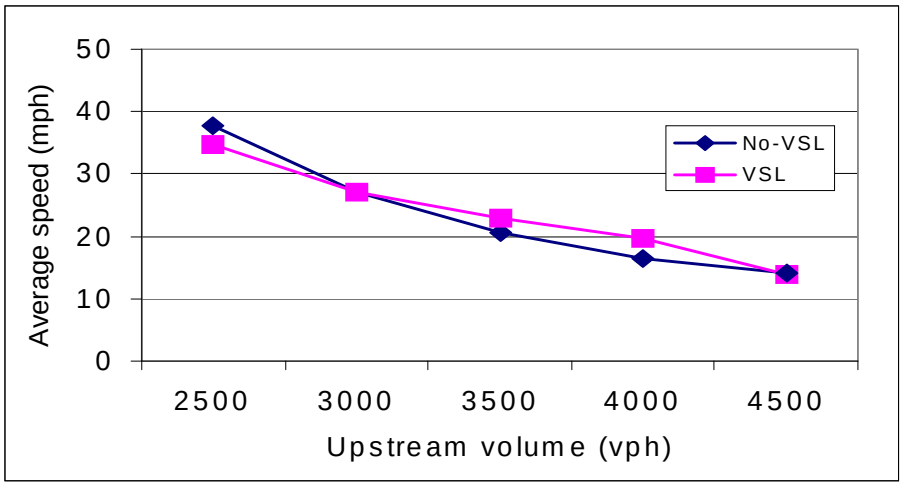

Figure 5.5.8 Average speed over subsegments for Type 2-1

Although one can evaluate the operational efficiency based on those three MOEs, it is actually difficult to evaluate the improvement on safety because accidents data cannot be realistically captured with simulation. Instead, as mentioned previously, this study has used the speed variance over each subsegment as an indicator for reflecting the traffic safety related environment.

Table 5.5.7 reports the comparison results of speed variances over three links (i.e., links 1 to 3) in advance of the work zone, where the average speed data was obtained over each time interval from the detectors. It is notable that most speed variances under the VSL control are lower than those under the No-VSL situation at four levels of traffic volume. The low speed variance along with an increased throughput seems to indicate that the proposed VSL algorithm can help drivers pass the work zone safely and efficiently.

Table 5.5.7 Comparisons of speed variances (standard deviations) from simulation experiments

Volume levels	Work zone types									
	2-1		3-1		3-2		4-1		4-2	
	No-VSL	VSL	No-VSL	VSL	No-VSL	VSL	No-VSL	VSL	No-VSL	VSL
2500	25.2	19.0			27.1	20.2				
3000	19.1	15.7			25.0	19.1				
3500	16.9	16.0			22.7	18.0				
4000	15.1	14.0	29.6	23.8	19.3	15.3			32.0	27.4
4500	17.4	14.4	26.5	22.8	17.0	13.6			29.3	25.9
5000			23.7	19.0	14.8	12.1			22.5	19.8
5500			20.7	17.6			34.9	29.7	18.8	15.5
6000			18.8	14.2			32.0	27.4	16.3	13.6
6500			15.7	13.2			29.9	26.0	11.6	8.8
7000							25.4	22.7		
7500							20.9	17.7		
8000							12.0	9.0		

5.6 Summary

This chapter has presented a dynamic model for optimizing variable speed limits and its algorithm for highway work zone operations, based on the evolution of detected dynamic traffic states and macroscopic traffic characteristics. For on-line applications, some non-linear traffic flow relations have been approximated with linear functions but updated continuously from on-line detector data. To reflect the need of improving traffic safety, a set of speed boundaries has been given as model constraints. Moreover, the normal deceleration rate has been used in determining the length of each subsegment, which is to ensure that drivers can reduce their speeds at an acceptable braking rate in response to those displayed VSL signs.

The proposed model with a proper set of parameters has demonstrated that under normal traffic conditions, it can increase the throughput over the work zone and reduce the average delay over upstream segments of the lane-closure location. The simulation results have also indicated that although the average speeds under the VSL control do not vary significantly for those under No-VSL control, the resulting speed variance among those vehicles traveling over the work zone is substantially lower than that under no-control scenarios.

In brief, the proposed VSL control seems to offer a promising alternative for contending with congestion and safety related issues. Further studies along this line will be focused on developing the optimal control algorithm for each type of work-zone operations, and collecting extensive field data for further model testing as well as enhancements.

CHAPTER 6 . INTEGRATED CONTROL ALGORITHM OF THE DLM AND VSL CONTROL STRATEGIES

6.1 Introduction

Based on the numerical results presented in previous chapters, it is clear that how to best operate the DLM and VSL controls under various congested work-zone conditions so as to maximize their compound effectiveness remains an imperative issue. Thus, this chapter focuses on exploring the potential of integrating those two control strategies in work-zone operations and comparing its effectiveness with that under each individual control. The core logic of an integrated control is to facilitate the merging maneuvers and minimize potential collisions with the VSL during the DLM operation period, and to coordinate the sequence of VMS messages generated from both control algorithms.

To ensure the proper integration, this chapter first presents some potential issues, and then proposes the set of procedures for integrated operations in Sections 2 and 3, respectively. Numerical experiments for performance evaluation of such an integrated control are reported in Section 4. Finally, research results and on-going studies are summarized in last section.

6.2 Critical issues for integration

To best integrate DLM and VSL, one needs to examine their compatibility and implementation priority especially with respect to the operational efficiency and traffic safety. For example,

- Are the control objectives of both systems compatible or not? Since the objective function of both proposed control systems is to maximize the total throughputs over the upstream subsegments, it is undoubted that one can operate both systems in a compatible format.
- Has any conflict factor embedded in those two control processes that may degrade their integrated performance? Note that the proposed DLM control is designed to guide drivers' merging actions between the open and closed lanes, while the VSL strategy is to control their approaching speeds to both lanes, regardless of the merging maneuvers. Thus, their model structures do not have any conflict components to prevent their integrated operations.
- How to determine the implementation priority between DLM and VSL? Since the foremost objective of the work zone control is to guide drivers over the lane-closure segments with proper merging maneuvers, one shall view DLM as the direct and the first level control. The VSL, designed for the speed control, can be viewed as a supplementary strategy for improving the safety and the efficiency during merging operations.

6.3 Development of the integrated algorithm

As mentioned previously, the purpose of an integrated DLM/VSL operation is to dynamically control drivers' merging activities and speeds, with the optimal merging control thresholds and speed limits based on detected traffic conditions. Since there is no compatibility and implementation issues between those two algorithms, this study has proposed the following procedures for their integrated operations.

Step-1: Compute the potential maximum queue length

The purpose of this step is to approximate the maximum queue length, based on the difference in maximum flow rates between the upstream segment and the work zone, as the computed queue length will be used as the target control segment for the DLM and VSL operations. If the actual traffic queue caused by the work zone operations exceeds the target segment, then one should extend the target control boundaries to cover the entire roadway segment potentially impacted by the work zone traffic queue.

Step-2: Set the initial speed boundaries for the VSL control

This step is designed to set an initial speed boundary that reflects the free flow speed for each subsegment *i*. This boundary is designed to prevent the optimal speed limit of subsegment *i* from exceeding the boundary of its upstream subsegment (*i+1*). Thus, a set of optimal VSL, based on these speed boundaries, will enable drivers to smoothly adjust their speed when approaching the work zone. Such speed boundaries will be revised dynamically by the central control unit, based on the detected speed data.

Step-3: Locate the DLM and VSL trailers

The locations of DLM and VSL trailer set should be determined on the basis of the average decelerating rate of drivers when they perceive each displayed VSL or DLM sign. By using a normal deceleration rate (e.g., a=3.3mph/sec), one can divide the target segment into *n* subsegments. This is to ensure that when perceiving the DLM and VSL signs, drivers need not to experience an uncomfortable and unsafe deceleration rate.

Step-4: Initialize all PCMS and VSL systems

The integration system is initialized by setting VSL with a set of initial speed boundaries and DLM to be at the Early Merge (or conventional static merge) state. Such an initialization can be done only when the lane-closure operations are started under the free flow traffic condition. Each sensor should also be activated for measuring the traffic data (e.g., volume and speed) at this initialization stage.

Step-5: Execute Dynamic Late Merge control

The proposed DLM control can be executed by identifying the detected traffic states (e.g., moderate, congested, and heavily congested traffic conditions), and then followed by displaying the optimal merging directions on PCMS (Portable Changeable Message Sign) or VMS (Variable Message Sign).

Step-6: Update the speed boundaries

One can also employ the measured traffic data (i.e., speeds) for the DLM control to update the speed boundaries (see Step-2).

Step-7: Execute the optimal VSL control model

The final step is to optimize a set of speed limits over all subsegments during each control time interval (e.g., 1min.). As mentioned in Step-1, if the actual queue length is longer than the projected maximum queue length, then go to Step-1. Otherwise, the system shall repeat Steps 5, 6, and 7 with the data detected from the sensors.

Figure 6.3.1 presents the principal steps for integrated operations of the DLM and VSL controls, including the interactions between sensors, DLM, VSL, and the feedback process. The entire process is designed to ensure that the VSL can always reflect the traffic states controlled by DLM and take into account the embedded safety constraints (e.g., speed boundary and sign locations).

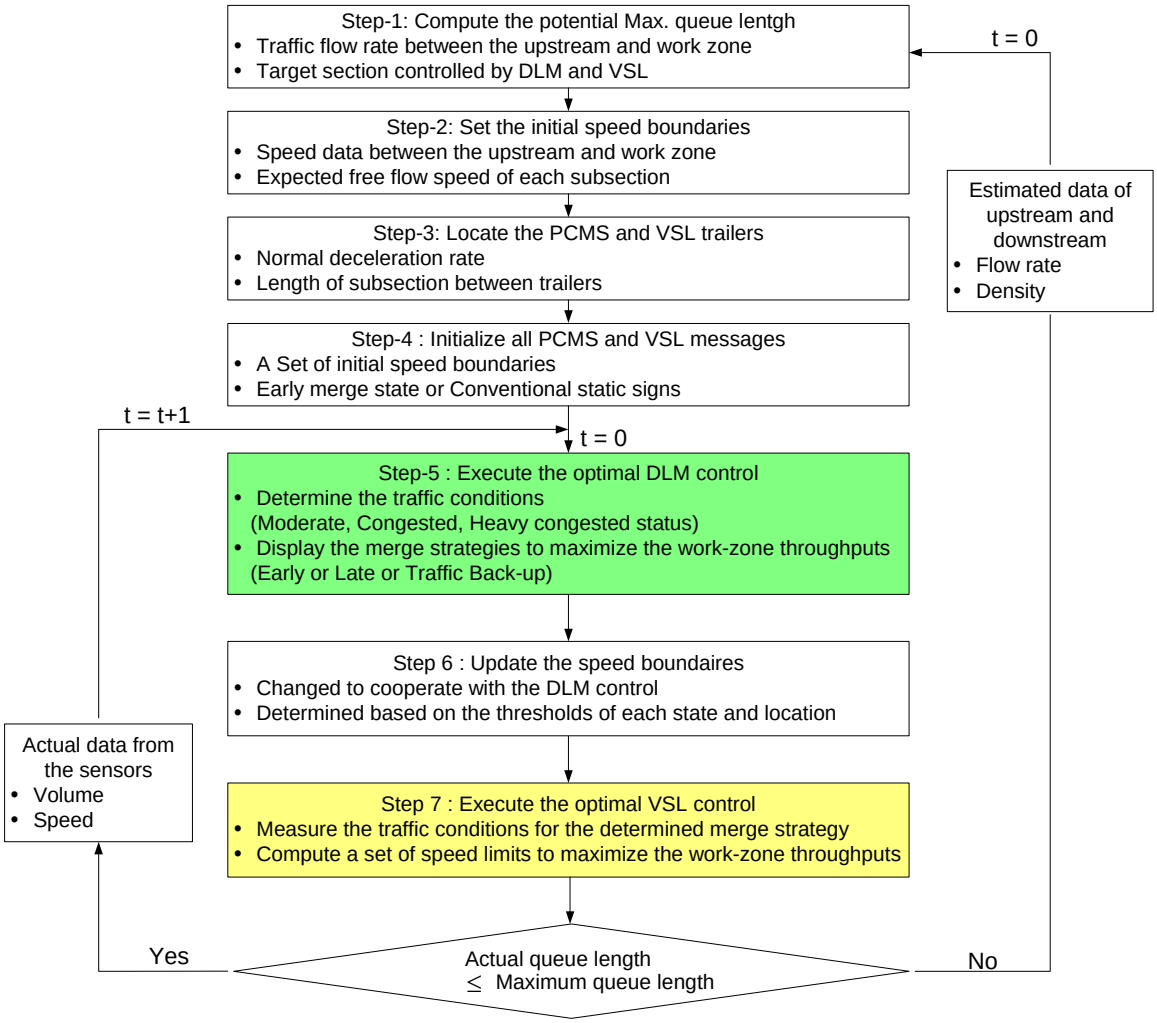

Figure 6.3.1 An Integrated algorithm of DLM and VSL controls

6.4 Evaluation of the integrated control

6.4.1 Design of experiments

To simulate the on-line work-zone control with the proposed integrated operations (see Figure 6.3.1), this study has designed the experimental scenarios with CORSIM-RTE (CORridor SIMulation – Rune Time Extension), a program designed to capture the interactions between the simulated vehicles and the execution of the integrated DLM/VSL control under the time-varying traffic conditions. Figure 6.4.1 illustrates an example work-zone system for simulation experiments, in which one left lane was closed on a two-lane highway segment, and drivers are all assumed to cooperate with the displayed messages.

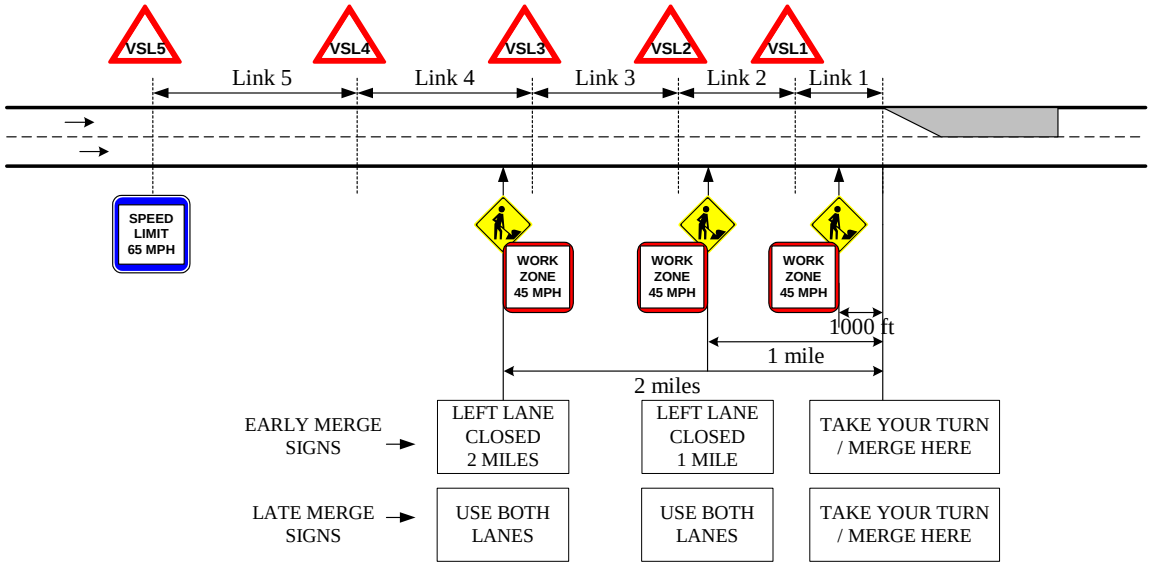

Figure 6.4.1 Configuration of the integrated control system

6.4.2 Performance evaluation

The evaluation task is focused on comparing the integrated control (called DLM/VSL) with the DLM control (called DLM) and the DLM control by Mn/DOT (called Mn-DLM) same as those conduced in Chapter 4. The performance evaluation includes both the operational efficiency and traffic safety. The experimental results on those two regards are summarized below.

i. Operational efficiency

The operational efficiency of the target work zone system (see Figure 6.4.1) is evaluated with two measures of effectiveness (MOE), the work zone throughput and average speed.

- Figure 6.4.2 compares the work zone throughputs between those three control strategies under the time-varying traffic conditions. The DLM/VSL and DLM controls produced 1750 vphpl and 1670 vphpl throughputs, respectively under the

average volume of 2000 vph (see Figure 6.4.2a); and 1870 vphpl and 1720 vphpl, respectively under the average volume of 2400 vph (see Figure 6.4.2b). These results indicate that with the complemental VSL control, the DLM operations can indeed yield a higher throughput than that when it works alone.

- Figure 6.4.3 represents the average speeds detected from the upstream subsegments (e.g., Links 1 to 5, see Figure 6.4.1). Overall, there exists no significant difference in the average speeds between the DLM/VSL and DLM controls. It seems that the implementation of VSL does not contribute to any reduction in the average flow speed, which instead may actually improve the average flow speed on the upstream subsegments (e.g., Links 1 to 3 at Figure 6.4.3a, and Links 1 and 4 at Figure 6.4.3b).

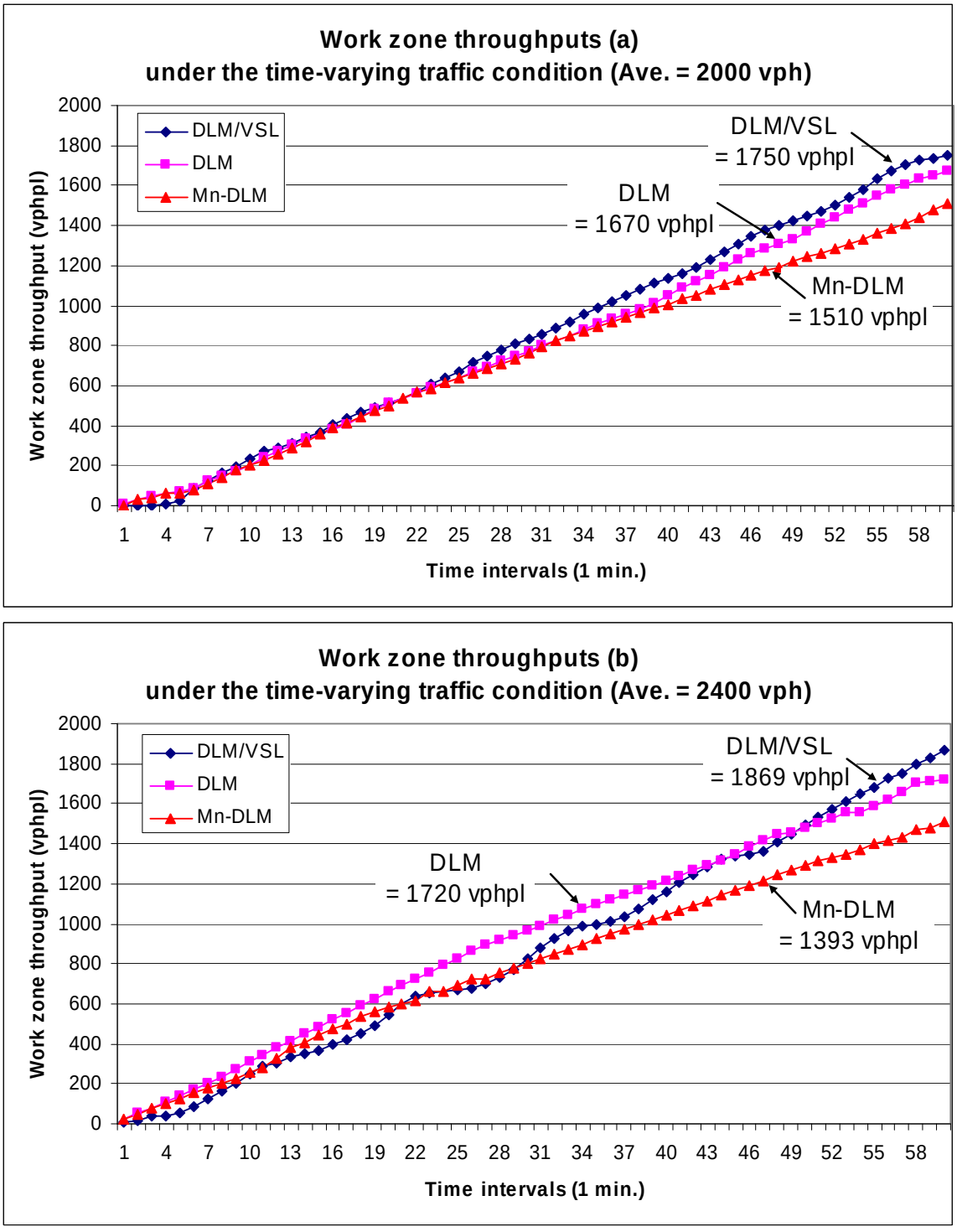

Figure 6.4.2 Comparison of work-zone throughputs under time-varying and congested traffic conditions

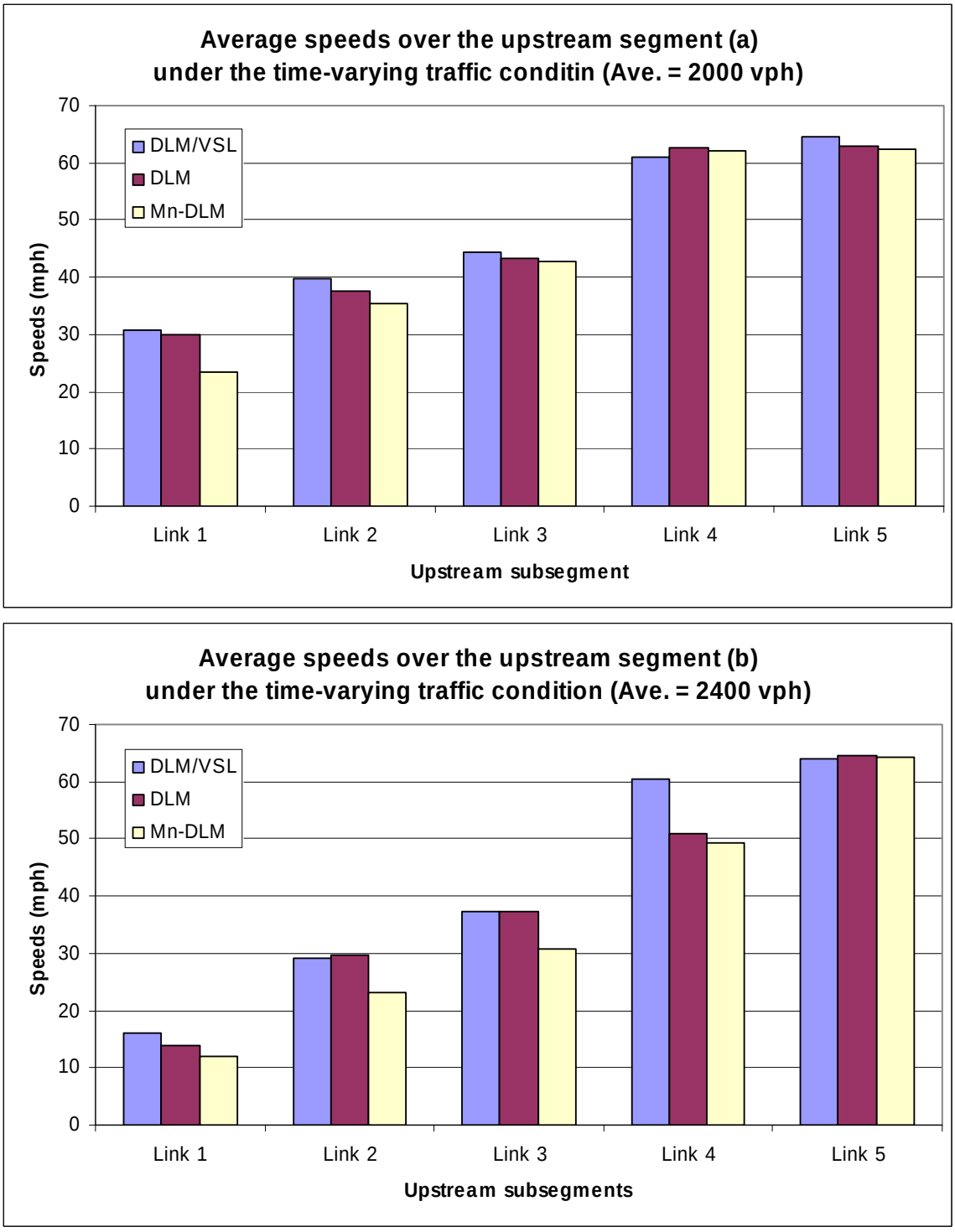

Figure 6.4.3 Comparisons of average speeds under time-varying and congested traffic conditions

ii. Traffic safety

Traffic safety is one of the most important issues during work-zone operations, especially under the congested and fluctuating traffic conditions. Under the integrated operations, the VSL control is expected to help drivers properly adjust their speeds on their merging and lane-changing maneuvers so as to increase the performance of the DLM control. The simulation results with respect to traffic safety are summarized below.

- Figure 6.4.4 compares the patterns of speed changes detected over the upstream subsegments (e.g., Links 1 to 3, see Figure 4) under the time-varying traffic conditions of average volume equal to 2000 vph. As highlighted in Figure 6.4.4a, the average speed drops or changes drastically and inconsistently under the DLM control. In contrast, Figure 6.4.4b shows that under the DLM/VSL control, the speeds on those links at a relatively smooth and consistent rate, despite the fluctuating traffic conditions. During the example operational period, their numerical comparison of speed changes between the initial and latter time intervals is reported in Table 6.4.1.
- Under the other time-varying traffic conditions of average volume equal to 2400 vph, Figure 6.4.5 compares the patterns of speed changes detected over three upstream subsegments (i.e., Links 1 to 3) during the specified time intervals (e.g., highlighted circles). Figure 6.4.5a shows the fluctuating and inconsistent pattern of speed changes under the DLM control. Under the DLM/VSL control, however, Figure 6.4.5b indicates that their average speeds are maintained smoothly and consistently, with corresponding to the time-varying traffic condition. Likewise, the numerical example of speed changes during the specified time intervals is also compared in Table 6.4.1.

Table 6.4.1 Comparison of speed changes (unit: mph) between DLM and DLM/VSL

Upstream subsegments	Figure 7 (operational period)		Figure 8 (specified time intervals)	
	DLM Initial / Latter	DLM/VSL Initial / Latter	DLM From / To	DLM/VSL From / To
Link 1	15.0 / 6.0	22.0 / 13.0	5.0 / 9.3	10.0 / 11.0
Link 2	41.0 / 12.0	42.0 / 30.0	48.0 / 6.0	30.0 / 35.0
Link 3	27.0 / 29.0	51.0 / 37.0	41.0 / 42.0	38.0 / 40.0

- As compared in Figures 6.4.5(a) and (b), particularly, it should be noted that as the simulation time interval increases, the DLM/VSL still maintains higher speeds (approx. 10.0 mph) around the merge point (i.e., Link 1) than those (approx. 5.0 mph) under the DLM control. This indicates that the integrated control retards the impacts of traffic congestion and merging conflict on the merge point by the effective speed control of VSL, during the work zone operation period.
- Consequently, the integrated control is expected to help drivers pass the upstream segment of the work zone area with smooth speed changes. This is supported by the results shown in Figure 6.4.6, where the speed variations over the upstream subsegments (i.e., Links 1 to 5, see Figure 6.4.1) are overall lower under the

DLM/VSL control than under the DLM control. This result means that the integrated control can mitigate the impacts of the frequently changed merge strategies by DLM on the speed variations, and enhance the performance of the DLM control with the help of VSL.

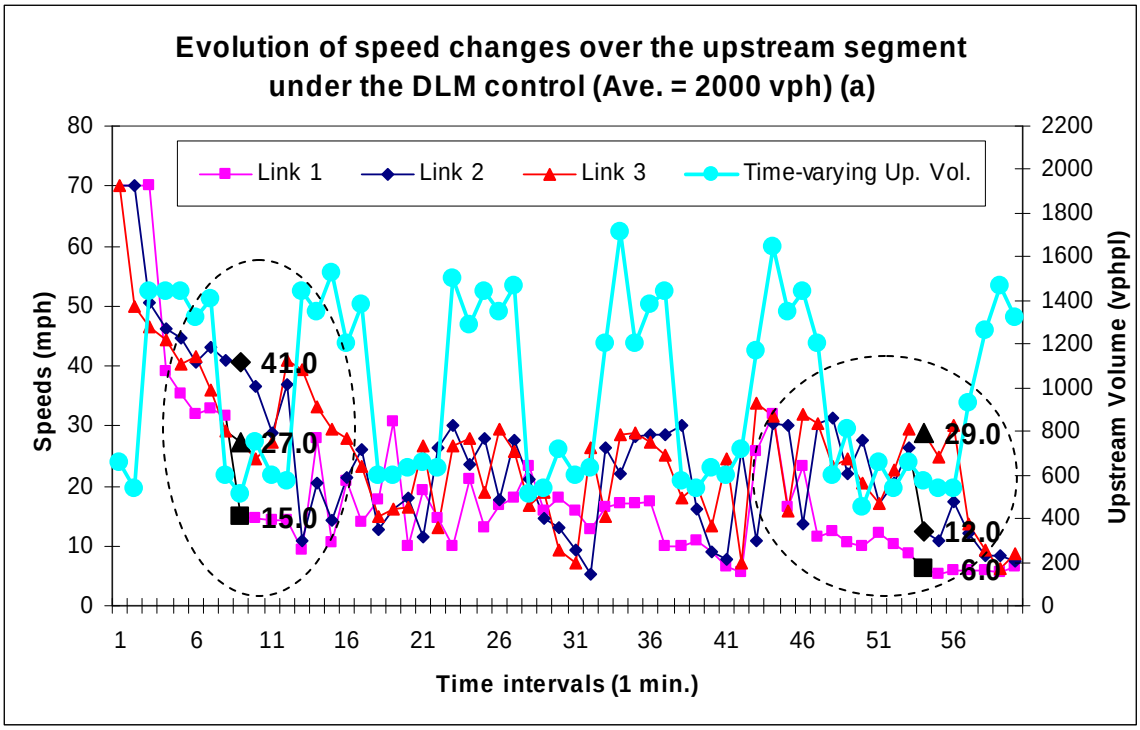

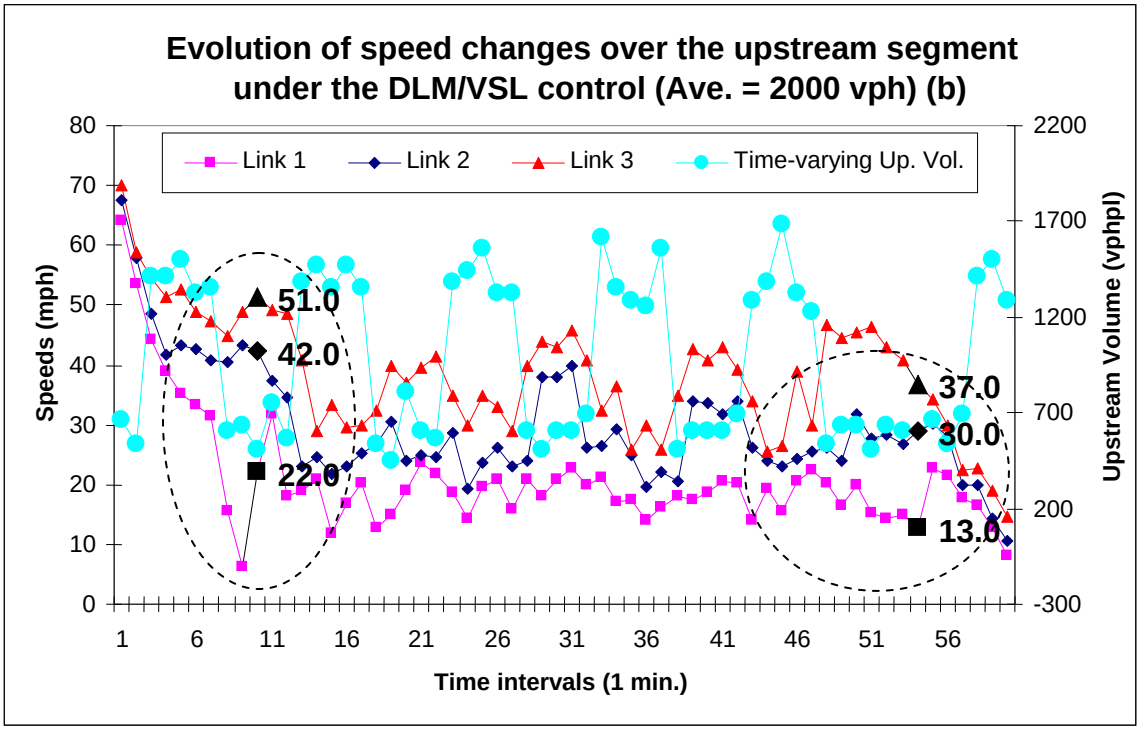

Figure 6.4.4 Comparison of speed changes over the upstream segment (Ave. = 2000 vph)

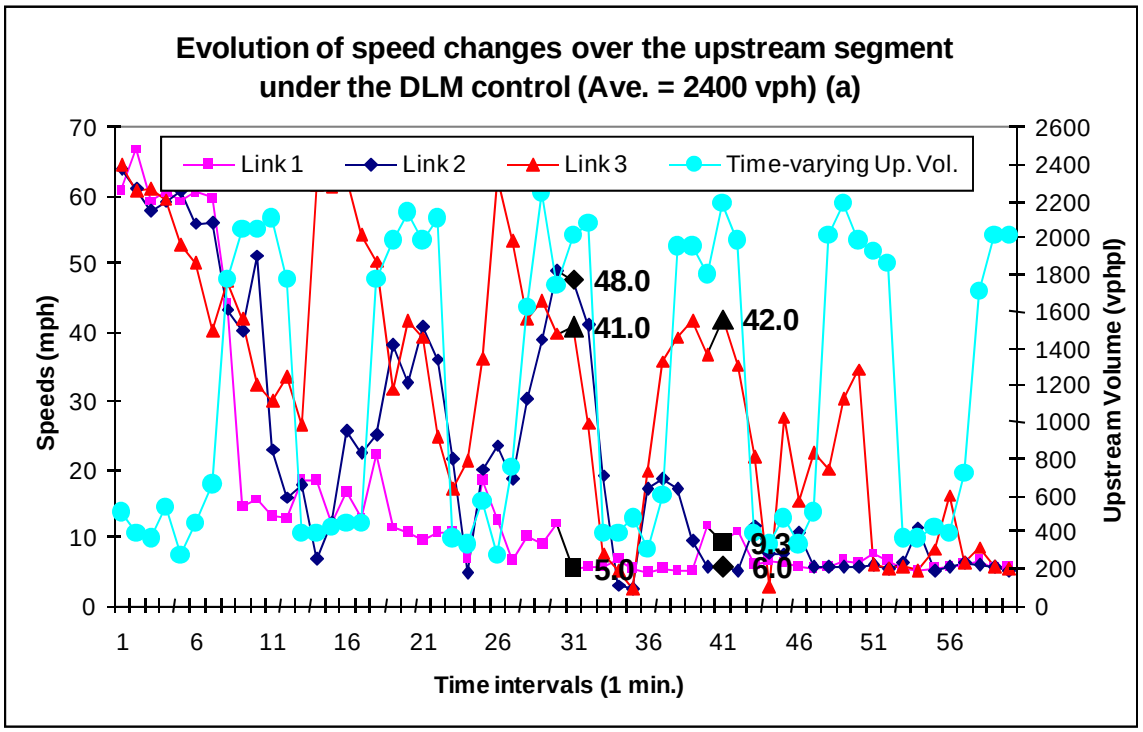

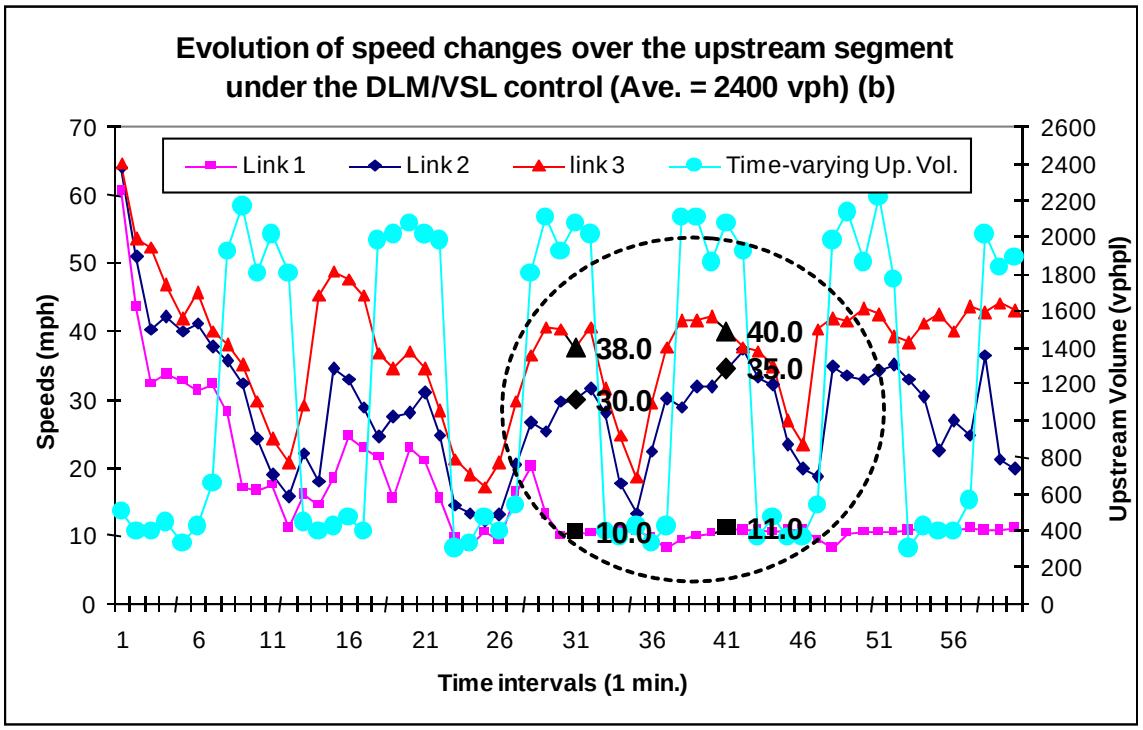

Figure 6.4.5 Comparison of speed changes over the upstream segment (Ave. = 2400 vph)

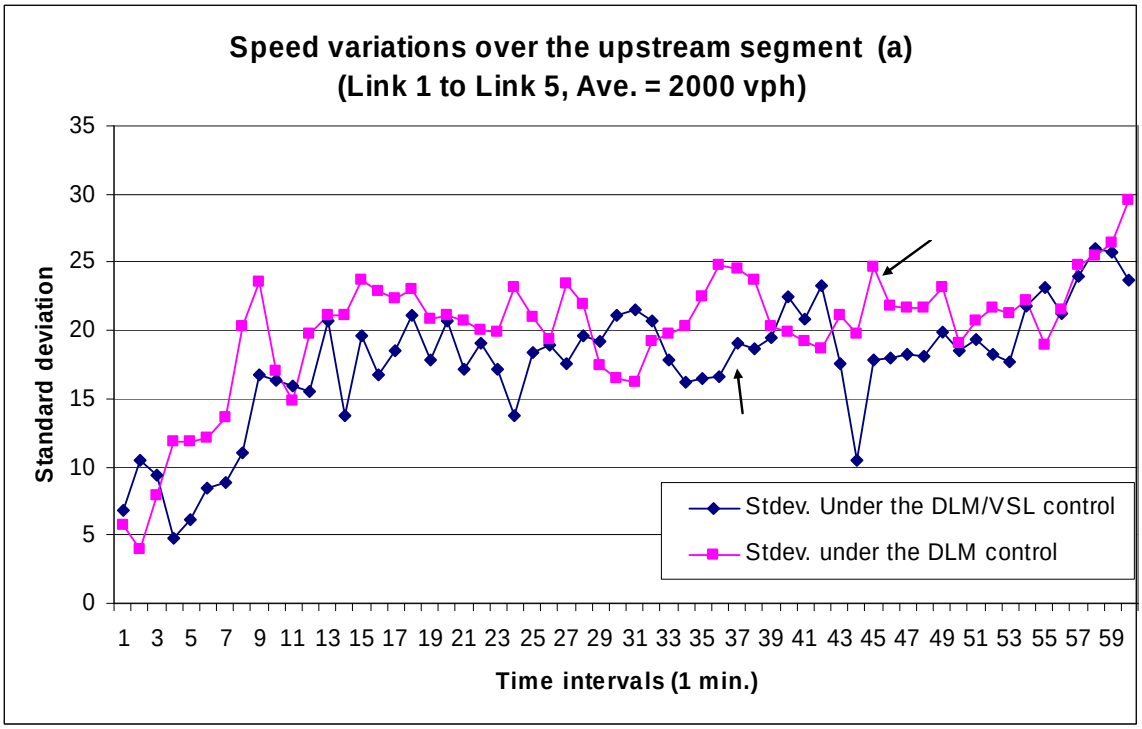

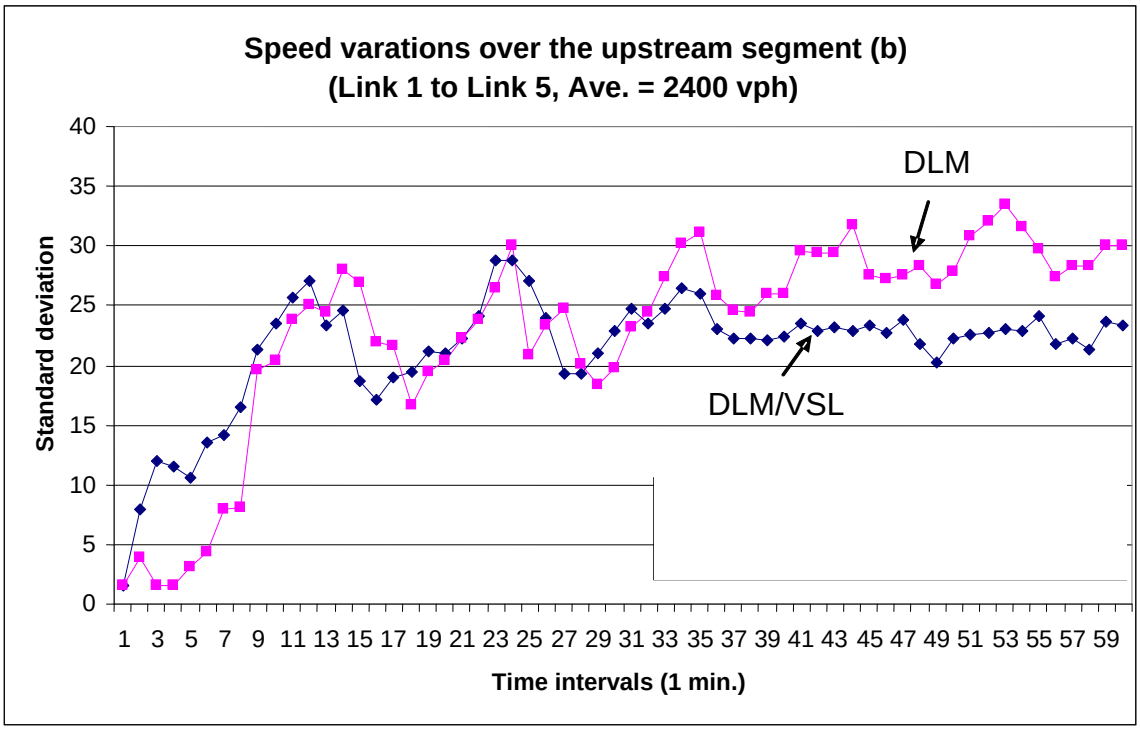

Figure 6.4.6 Comparison of speed variations over the upstream segment under time-varying and congested traffic conditions

6.5 Summary

To facilitate the merging maneuvers and minimize potential collisions during the DLM operations, this study has developed a system control process that can integrate the VSL with the DLM so as to maximize the total effectiveness. The proposed integrated control process has used the optimal VSL control model as a supplementary strategy of the entire DLM operations, and coordinated the sequence of VMS messages generated from the DLM and VSL algorithms.

From the simulation experiment, the integrated algorithm of the DLM and VSL controls has shown to respond well to time-varying traffic conditions and yielded more work-zone throughputs than the DLM control without VSL. It has also demonstrated that the integrated control results in an increase in the average speed and a decrease in the speed variation. In particular, the VSL effect is evident as a supplementary role for the dynamic merge control.

However, it should be mentioned that this type of advanced control systems cannot guarantee the performance in field applications unless a sufficient number of sensors required for the DLM and VSL control models function properly with respect to their accuracy and reliability. Thus, a further study is to consider the limitations caused by the sensor system in field applications, based on the actual traffic flow data and the lessons observed from the previously tested DLM systems. One also needs to properly identify the locations of VMS and the displayed messages so as to increase the compliance rate of drivers.

CHAPTER 7 . CONCLUSIONS AND RECOMMENDATIONS

7.1 Summary of Research Accomplishments

To improve traffic mobility and safety in highway work zones, this study has focused mainly on developing advanced merge and speed control strategies, including both their individual and integrated control algorithms. Based on the deficiencies and limitations of existing work zone control operations, this research has made contributions mainly on the following four regards:

- Understanding traffic flow characteristics under work zone traffic conditions with empirical data and identifying the fact that the interrelations between parameters for key traffic flow properties vary with the distance to the merge location;
- Developing an operational model for computing the optimal set of thresholds for DLM and its implementation algorithm, where the set of optimal control thresholds is employed to dynamically select the merge control strategy, based on the detected traffic conditions;
- Proposing an optimal speed limit control model that can maximize the throughput of a lane-closure highway segment with a set of dynamically adjusted speed limits; and
- Constructing an integrated operational algorithm to take the advantage of the strengths of DLM and VSL controls.

A brief summary of research finding on those regards is presented below.

Capturing Work-zone Traffic Flow Properties with Empirical Statistical Models

Since only a few studies and limited field observation have been conducted on work zone traffic conditions, it is difficult to analyze the impacts of work zone activities on traffic flow characteristics. Chapter 3 has proposed a set of statistical models based on both empirical and simulation results for the flow-density relation, which serves as a tool for analyzing the traffic flow properties under the work-zone operations. The results of this task indicate that any operational strategy for highway work-zone control should realistically capture the complex interactions between evolution of traffic queues, the approaching flow rates, merging activities between lanes, and the capacity reduction due to lane-closure operations.

Developing an Advanced Dynamical Late Merge Control Model and Algorithm based on the Optimal Control Thresholds

Since state-of-the-art dynamic merge models with their static control thresholds cannot optimize the work-zone efficiency under fluctuating traffic conditions, Chapter 4 has developed an advanced DLM control and its operational algorithm for highway work-zone operations, based on the optimal merge control threshold. The focus is on selection of the control variables and on determining their thresholds in response to traffic flow dynamics, since each type of merge control can be most effective only under its applicable range of traffic conditions.

Under the simulated environments, the optimal control threshold, based on the proposed model, has shown to effectively respond to time-varying traffic conditions, and yielded higher work-zone throughput than existing DLM controls based on static thresholds. The experimental results have also demonstrated that the proposed DLM control results in an increase in the average speed and a decrease in speed variance.

Formulating a Variable Speed Control Model and Algorithm

Most existing VSL systems are developed mainly in response to traffic safety concerns, and their control algorithms cannot minimize traffic congestion by dynamically setting the optimal speed limits and coordinating them based on their spatial relations. Chapter 5 has presented an optimal VSL control model and its operational algorithm for highway work zone operations, based on the evolution of dynamic traffic states and macroscopic traffic characteristics. For on-line applications, the proposed model has approximated some non-linear traffic flow relations with linear functions but updated continuously with on-line detector data. To reflect traffic safety concern, the proposed model employs a set of speed boundaries as its safety constraints, and adopts the normal deceleration rate in determining the length of each subsegment between the VSL signs so as to ensure that drivers can reduce their speeds at an acceptable braking rate in response to their displayed speed limits.

The proposed model with a well-calibrated set of parameters has demonstrated that it can increase the throughput over the work zone and reduce the average delay over upstream segments of the lane-closure location. The simulation results have also revealed that although the average speed under the VSL control does not vary significantly from those under No-VSL control, the resulting speed variance among those vehicles traveling over the work zone is substantially lower than that under the no-control scenarios.

Development of the Integrated Control Algorithm of the DLM and VSL Controls

To best integrate the strengths of both controls, Chapter 6 has proposed an integrated operational algorithm for the DLM and VSL control strategies developed in Chapters 4 and 5, respectively. The core logic is to facilitate the merging maneuvers and minimize potential collisions during the DLM operation with the support of VSL so as to maximize their compound effectiveness. From the simulation experiment, the integrated algorithm of the DLM and VSL controls has shown to effectively respond to time-varying traffic conditions and yielded higher work-zone throughputs than the DLM control without VSL. It has also demonstrated that the integrated operation results in an increase in the average speed and a decrease in the speed variation.

7.2 Conclusions and Recommendations

To improve traffic mobility and safety on highway segments plagued by work zone activities, this study has focused on developing the advanced dynamic merge and variable speed limit controls for work zone applications, including an integration of both controls for best use of their strengths in maximizing throughputs and minimizing speed variance in traffic

flows. The simulation results have demonstrated that the developed DLM and VSL controls have better performance in terms of traffic mobility and safety than their existing controls based on static approaches, and also shown that the proposed integrated control of the DLM and VSL control has more promising properties than each individual control.

However, although the DLM and VSL controls and their integrated control algorithm proposed in this study offer the potential for improving traffic mobility and safety in highway work zone operations, much remains to be done for effectively contending with work zone related congestion. Examples of some critical studying issues are summarized below.

- DLM and VSL Operations without Sufficient Traffic Sensors

Note that the DLM and VSL models accomplished so far in this research are grounded on the assumption that all needed sensors are available and function properly. Such ideal conditions, however, may not always exist, especially for relatively long-term work-zone operations. In practice, it is most likely to have an inadequate number of traffic sensors due to cost concerns and some malfunction detectors caused by unexpected communication or operation issues. Both the hardware and communication costs for such operations could be quite high for a long period of work-zone projects.

Hence, one shall develop optimal time-of-day merge and speed control methods, which can recognize the time-varying nature of traffic volume in the work zones, and divide the entire day of operations into a number of control periods. During each control period, they may employ pre-calibrated traffic flow models to estimate the key traffic condition data or to produce the approximation with historical data. The estimated traffic characteristics can subsequently be used in computing a set of the robust merge control thresholds and speed limits for each control period.

- Lane-based Signal Merge Control

Note that the optimal control strategies proposed in this study are grounded on the assumption that most drivers are willing to cooperate with the merge messages and speed limit signs. Under the congested traffic conditions, however, the compliance rates of drivers are likely to be low, and thus degrade the performance of either DLM and/or VSL systems. Thus, how to concurrently improve traffic safety and traffic mobility remains a critical issue. Using a specially designed signal system to regulate the traffic flow on each lane can be a potentially effective control strategy, especially on a multi-lane highway work zone segments. Certainly, how to properly set such a signal system, considering both the safety and operational needs, is a challenging task.

REFERENCES

Adeli, H. and Ghosh-Dastidar, S. Mesoscopic-Wavelet Freeway Work Zone Flow and Congestion Feature Extraction Model, Journal of Transportation Engineering, ASCE, Vol. 130(1), January 2004, pp. 94-103.

Banks, J. H. Investigation of Some Characteristics of Congested Flow, In Transportation Research Record 1678, TRB, National Research Council, Washington, D.C., 1999, pp. 128-134.

Banks, J. H. Freeway Speed-Flow-Concentration Relationships: More Evidence and Interpretation, In Transportation Research Record 1225, TRB, National Research Council, Washington, D.C., 1989, pp. 53-60.

Beacher, A. G., Fontaine, M. D., and Garber, N. J. Field Evaluation of the Late Merge Work Zone Traffic Control, TRB 84th Annual Meeting, CD-ROM, 2005.

Beacher, A. G., Fontaine, M. D., and Garber, N. J. Guidelines for Using Late Merge Work Zone Traffic Control: Results of a Simulation-based Study, TRB 84th Annual Meeting, CD-ROM, 2005.

Berg, P., Mason, A., and Woods, A. 2000. Continuum approach to car-following models, Physical Review E, 61(2), pp. 1056-1066.

Berg, P. and Woods, A. 1999. Relating car-following and continuum models of road traffic, Traffic and Granular Flow, edited by Helbing, D., Hermann, H. J., Schreckenberg, M., and Wolf, D. E., Springer, New York, pp. 389-394.

Berg, P. and Woods, A. in press, Physical Review E, 1999.

Bando, M., Hasebe, K., Nakayama, A., Shibata, A., and Sugiyama, Y. 1995. "Dynamic Model of Traffic Congestion and Numerical Simulation", Physical Review E, 51(2), pp. 1035-1051.

Bowie, J., Saito, M., and Burns, S. Efficacy of Speed Monitoring Displays in Highway Work Zones. TRB 83rd Annual Meeting, CD-ROM, 2004.

Chang, G. L. and Kang, K. P., *Evaluation of Intelligent Transportation System Deployments for Work Zone Operations.* Report MD-05-SP, Department of Civil Engineering, University of Maryland (UMCP), Sponsored by Maryland State Highway Administration, August 2005.

Chang, G. L., Wu, J., and Lieu, H., Real-Time Incident-Responsive System for Corridor Control: Modeling Framework and Preliminary Results. In Transportation Research Record 1452, TRB, National Research Council, Washington, D.C., 1995, pp.42-51.

Coleman, J. A. et al., FHWA Study Tour for Speed Management and Enforcement Technology. FHWA-PL-96-006. Federal Highway Administration, U.S. Department of Transportation, February 1996.

Cremer, M. and Schoof, S., On Control Strategies for Urban Traffic Corridors. International Federation of Automatic Control, 1989, pp. 213-219.

Datta, T., Schattler, K., Kar P., and Guha, A., Development and Evaluation of an advanced dynamic lane merge traffic control system for 3 to 2 lane transition areas in work zones, Report RC-1451, Transportation Research Group, Department of Civil & Environmental Engineering, Sponsored by Michigan Department of Transportation, January 2004.

Dixon, K. K., Hummer J. E., and Lorscheider, A. R., Capacity for North Carolina Freeway Work Zones. In Transportation Research Record 1529, TRB, National Research Council, Washington, D.C., 1996, pp. 27-34.

Dudek, C. L. and Richards, S. H., *Traffic Capacity Through Work Zones on Urban Freeways*. Report FHWA/TX-81/28+228-6. Texas Department of Transportation, Austin, 1981.

Erick van den Hoogen and Stef Smulders, Control by Variable Speed Signs : Results of the Dutch Experiment. 7th International Conference on Road Traffic Monitoring and Control. 1996.

Federal Highway Administration (FHWA), Intelligent Transportation Systems, *Intelligent Transportation Systems in Work Zones: A Case Study – Dynamic Lane Merge System,* U.S. Department of Transportation, October 2004.

Federal Highway Administration (FHWA), *Work Zone Safety Findings: Statement of the Problem*, National Conference on Work Zone Safety, 1994, p 19.

Federal Highway Administration (FHWA), *Part IV of Manual on Uniform Traffic Control Devices (MUTCD)*, Revision 4, Department of Transportation. U.S. January 1995.

Gazis, D. Application of Kalman Filtering for Density Estimation in Traffic Networks, Traffic Theory, 2002, Kluwer Academic Publisher, Massachusetts.

Gazis, D. and Liu, C. Kalman filtering estimation of traffic counts for two network links in tandem, Transportation Research Part B, 2003, pp. 737-745.

Greene, W. H. Economic Analysis (4th ed), 2000. Prentice Hall, pp 349-353.

Hall, F. L. and Hall, L. M. Capacity and Speed-Flow Analysis of the Queen Elizabeth Way in Ontario, In Transportation Research Record 1287, TRB, National Research Council, Washington, D.C., 1990, pp. 108-118.

Hall, F. L., Hurdle, V. F. and Banks, J. H. Synthesis of Recent Work on the Nature of Speed-Flow and Flow-Occupancy (or Density) Relationships on Freeways, In Transportation Research Record 1365, TRB, National Research Council, Washington, D.C., 1992, pp. 12-18.

Hall, F. L., Pushkar, A., and Shi, Y. Some Observations on Speed-Flow and Flow-Occupancy Relationships Under Congested Conditions, In Transportation

Research Record 1398, TRB, National Research Council, Washington, D.C., 1993, pp. 24-30.

Hall, J. and Wrage, E. *Controlling Vehicle Speeds in Highway Construction Zones*, NMSHTD-97-07. Department of Civil Engineering, University of New Mexico, sponsored by New Mexico State Highway and Transportation Department. December 1997.

International Road Dynamic (IRD) Inc., *Operator Manual: Late Merger Safety System*. September 2003.

Institute of Transportation Engineers. *Transportation and Traffic Engineering Handbook*, Second edition. 1982, pp. 168-169.

ITT Industries, Inc., Systems Division, ATMS R&D and Systems Engineering Program Team, *CORSIM Run-Time Extension (RTE) Developer's Guide*, FHWA, 2003.

Jain, R. and Smith, J. M., Modeling Vehicular Traffic Flow Using M/G/C/C State Dependent Queueing Models. Transportation Science, Vol. 31(4), 1997, pp. 323-336.

Jiang, Y., Traffic Capacity, Speed, and Queue-Discharge Rate of Indiana's Four-Lane Freeway Work Zones. In Transportation Research Record 1657, TRB, National Research Council, Washington, D.C., 1999, pp. 10-17.

Kang, K. P., Chang, G. L., and Zou, N., Optimal Dynamic Speed Limit Control for Highway Work-Zone Operations, In Transportation Research Record 1877, TRB, National Research Council, Washington, D.C., 2004, pp. 77-84.

Kang, K. P., Chang, G. L., and Zou, N. Optimal Variable Speed Limit Model, Proceedings of the 10th International Federation of Automatic Control (IFAC) on Control of Transportation Systems, May, 2004.

Kermode, R. H. and Myyra, W. A., *Freeway Lane Closure*. Traffic Engineering, Vol. 40, No. 5, 1970.

Kerner, B. S. and Rehborn, H. Experimental Properties of Phase Transitions in Traffic Flow, Physical Review Letters, Vol. 79, pp 4030-4033, 1997.

Kerner, B. S. and Rehborn, H. Experimental properties of complexity in traffic flow, Physical Review E, Vol. 53, pp R4274-R4278, 1996.

Kim, T. H., Lovell, D. J., and Paracha, J., A New Methodology to Estimate Capacity for Freeway Work Zones. 2001 Transportation Research Board Annual Meeting (CD-ROM), Washington, D.C., 2001.

Kraemer, Lagenbach-Belz, Approximate formulae for the delay in the queueing system GI/GI/1. Conference book. Melbourne, 8th International Teletraffic Congress, pp. 235-1/8, 1976.

Krammes, R. A. and Lopez, G. O., *Updated Short-Term Freeway Work Zone Lane Closure Capacity Values*. Report FHWA/TX-92/1108-5. Federal Highway

Administration, U.S. Department of Transportation and Texas Department of Transportation, Austin, 1992.

Lee, C., Hellinga, B, and Saccomanno, F., Assessing Safety Benefits of Variable Speed Limits, Transportation Research Board Annual Meeting (CD-ROM), Washington, D.C., 2004.

Lin, P. W., Kang, K. P. Kang, and Chang, G. L., "Exploring the Effectiveness of Variable Speed Limit Controls on Highway Work-Zone Operations" In Journal of Intelligent Transportation Systems, Vol. 8 (3), pp 155-168, July 2004.

Lyles, R. W., Taylor, W. C., Lavansiri, D., and Grossklaus, J., A Field Test and Evaluation of Variable Speed Limits in Work Zones, Transportation Research Board Annual Meeting (CD-ROM), Washington, D.C., 2004.

Loerger, T. R., Meeks, J. H., and Nelson, P. Investigation of Density and Flow Relationships in Congested Traffic with Videogrammetric Data, In Transportation Research Record 1776, TRB, National Research Council, Washington, D.C., 2001, pp. 167-177.

McCoy, P. T., Bonneson, J. A., and Kollbaum, J. A. Speed Reducing Effects of Speed Monitoring Displays with Radar in Work Zones on Interstate Highways. In Transportation Research Record 1509, TRB, National Research Council, Washington, D.C., 1995, pp. 65-72.

McCoy, P. T., Pesti, G., and Byrd, P. S., ALTERNATIVE DRIVER INFORMATION TO ALLEVIATE WORK-ZONE-RELATED DELAYS, Research Project SPR-PL-1(35)P513. Department of Civil Engineering College of Engineering and Technology, sponsored by Nebraska Department of Roads, February 1999.

McCoy, P. T. and Pesti, G. Dynamic Late Merge-Control Concept for Work Zones on Rural Interstate Highways, In Transportation Research Record 1745, TRB, National Research Council, Washington, D.C., 2001, pp. 20-26

Migletz, J., Graham, J. L., Anderson, I. B., Harwood, D. W., and Bauer, K. M. Work Zone Speed Limit Procedure. In Transportation Research Record 1657, TRB, National Research Council, Washington, D.C., 1999, pp. 24-30.

Meyer, E. Project Year 2002 Evaluations: Construction Area Late Merge (CALM) System. Federal Highway Administration (FHWA) Pooled Fund Study, University of Kansas, 2004.

National Cooperative Highway Research Program (NCHRP), *Procedure for Determining Work Zone Speed Limits,* Research Results Digest, No. 192, 1999. Washington, D.C.

Park, Byungkyu and Yadlapati, S. S., Development and Testing of Variable Speed Limit Logics at Work Zones Using Simulations, Transportation Research Board Annual Meeting (CD-ROM), Washington, D.C., 2003.

Persaud, B. N. and Hurdle, V. F. Some New Data That Challenge Some Old Ideas About Speed-Flow Relationships, In Transportation Research Record 1194, TRB, National Research Council, Washington, D.C., 1988, pp. 191-198.

Pesti, G. Alternative Way of Using Speed Trailers: Evaluation of the D-25 Speed Advisory Sign System, TRB 84th Annual Meeting, CD-ROM, 2005.

Pesti, G., Jessen, D. R., Byrd, P. S., and McCoy, P. T., Traffic Flow Characteristics of the Late Merge Work Zone Control Strategy. In Transportation Research record 1657, TRB, National Research Council, Washington, D.C., 1999, pp. 1-9.

Pesti, G. and McCoy, P. T. Long-Term Effectiveness of Speed Monitoring Displays in Work Zones on Rural Interstate Highways. In Transportation Research Record 1754, TRB, National Research Council, Washington, D.C., 2001, pp. 21-30.

Pili-Sihvola, Y., and Taskula, K., Mustaa Jaata and Finland's Weather-Controlled Road. In Traffic Technology International '96, UK & International Press, Surrey, United Kingdom, pp. 204-206. 1996.

Smulders, S., Control by Variable Speed Signs: Results of the Dutch Experiment. 6th International Conference on Road Traffic Monitoring and Control. 1992.

Steinke, D. P., et al. *Methods and Procedures to Reduce Motorist Delays in Europe Work Zones*, Office of International Programs and Office of Policy, FHWA, U.S. Department of Transportation, FHWA-PL-00-001, October, 2000.

Stidger, RW. *HOW MNDOT SETS SPEED LIMITS FOR SAFETY*, Better Roads Vol. 73(11), pp. 74-81. November 2003.

Sumner, R. L., and Andrew, C. M., Variable Speed Limit System. Report FHWA-RD-89-001. Federal Highway Administration, U.S. Department of Transportation, March 1990.

Taavola, D., Jackels, J., and Swenson, T., *Dynamic Late Merge System Evaluation: Initial Deployment on US-10*, Summer 2003, Minnesota Department of Transportation, 2004.

Tarko, A. and Venugopal, S., Safety and Capacity Evaluation of the Indiana Lane Merge System, FHWA/IN/JTRP-2000/19. Joint Transportation Research Program, Purdue University, sponsored by Indiana Department of Transportation, February 2001.

Tarko, A., Kanipakapatnam, S., and Wasson, J., Modeling and Optimization of the Indiana Lane Merge Control System on Approaches to Freeway Work Zones, FHWA/IN/JTRP-97/12. Joint Transportation Research Program, Purdue University, sponsored by Indiana Department of Transportation. May 1998.

Transportation Research Board (TRB), Committee for Guidance on Setting and Enforcing Speed Limits. Managing speed, National Research Council, Special Report 254, 1998.

Vandaele, N., Woensel, T. V., and Verbruggen, A. A queueing based traffic flow model, Transportation Research Part D, Vol. 5 pp. 121-135, 2000.

Walters, C. H. and Cooner, S. A. *Understanding Road Rage: Evaluation of Promising Mitigation Measures.* Texas Transportation Institutes, College Station, 2001.

Walters, C. H., Pezoldt, V. J., Womack, K. N., Cooner, S. A., and Kuhn, B. T., UNDERSTANDING ROAD RAGE: SUMMARY OF FIRST-YEAR PROJECT ACTIVITIES, TX-01/4945-1. Texas Transportation Institute, sponsored by Texas Department of Transportation Construction Division. November 2000.

Wilkie, J. K., Using Variable Speed Limit Signs To Mitigate Speed Differentials Upstream of Reduced Flow Locations. In Compendium of Graduate Student Papers on Advanced Surface Transportation System; Texas Transportation Institute Report SWUTC/97/72840-00003-2. August 1997.

Wu, J. and Chang, G. L., Heuristic Method for Optimal Diversion Control in Freeway Corridors. In Transportation Research Record 1667, TRB, National Research Council, Washington, D.C., 1999, pp. 8-15.

Wu, N. A new approach for modeling of Fundamental Diagrams, Transportation Research Part A, Vol. 36 pp. 867-884, 2002.